REPUBLIC OF BENIN

------000------

MINISTRY OF HIGHER EDUCATION AND SCIENTIFIC RESEARCH

------000------

UNIVERSITY OF ABOMEY - CALAVI

------000------

DOCTORAL SCHOOL OF LIFE AND EARTH SCIENCES

------000------

Registered under N°: ***487***

A DISSERTATION

Submitted

In partial fulfillment of the requirements for the degree of

DOCTOR of Philosophy (PhD) of the University of Abomey-Calavi

In the framework of the

Graduate Research Program on Climate Change and Water Resources (GRP-CCWR)

By

Orou Moctar GANNI MAMPO

Public defense on: 11/28/2025

Subject: Hydrology
Speciality: Climate Change and Water Resources

======

HYDRO-METEOROLOGICAL DROUGHT UNDERSTANDING AND PREDICTABILITY ACROSS THE BENINESE PART OF NIGER RIVER BASIN, WEST AFRICA

======

Supervisors:		
Kossi François GUEDJE	Associate Professor	University of Abomey-Calavi, Bénin
Adechina Eric ALAMOU	Full Professor	UNSTIM, Benin
Reviewers:		
Sounmaïla MOUMOUNI	Full Professor	UNSTIM, Benin
Arona DIEDHIOU	Director of Research	IRD (HDR), France
Kwaku Amaning ADJEI	Full Professor	KNUST, Ghana

JURY

Agnidé Emmanuel LAWIN	Full Professor, University of Abomey Calavi, Benin	President
Sounmaïla MOUMOUNI	Full Professor, UNSTIM, Benin	Reviewer
Arona DIEDHIOU	Director of Research, IRD (HDR), France	Reviewer
Kwaku Amaning ADJEI	Full Professor, KNUST, Ghana	Reviewer
Eliezer BIAOU	Associate Professor, UNSTIM, Benin	Examiner
Kossi François GUEDJE	Associate Professor, University of Abomey Calavi, Benin	Supervisor
Adechina Eric ALAMOU	Full Professor, UNSTIM, Benin	Co-Supervisor

WASCAL West African Science Service Centre on Climate Change and Adapted Land Use

With funding from the: Federal Ministry of Research, Technology and Space

REPUBLIQUE DU BENIN

------000------

MINISTERE DE L'ENSEIGNEMENT SUPERIEUR ET DE LA RECHERCHE SCIENTIFIQUE

------000------

UNIVERSITE D'ABOMEY - CALAVI

------000------

ECOLE DOCTORALE SCIENCES DE LA VIE ET DE LA TERRE

------000------

Enregistrée sous N°: ***487***

THESE

Soumise pour obtenir le grade de

DOCTEUR de l'Université d'Abomey-Calavi

Dans la Spécialité:

Changement climatique et Ressources en Eau

Par

Orou Moctar GANNI MAMPO

Soutenue publiquement le : 28/11/2025

Discipline: Hydrologie
Spécialité: Changements Climatiques et Ressources en Eau

======

COMPRÉHENSION ET PRÉVISIBILITÉ DE LA SÉCHERESSE HYDROMÉTÉOROLOGIQUE DANS LA PARTIE BÉNINOISE DU BASSIN DU FLEUVE NIGER, AFRIQUE DE L'OUEST

======

Directeurs de thèse:

Kossi François GUEDJE	Maître de Conférences	Université d'Abomey-Calavi, Bénin
Adechina Eric ALAMOU	Professeur Titulaire	UNSTIM, Benin

Rapporteurs:

Sounmaïla MOUMOUNI	Professeur Titulaire	UNSTIM, Benin
Arona DIEDHIOU	Directeur de Recherche	IRD (HDR), France
Kwaku Amaning ADJEI	Professeur Titulaire	KNUST, Ghana

JURY

Agnidé Emmanuel LAWIN	Professeur Titulaire, Université d'Abomey Calavi, Benin	President
Sounmaïla MOUMOUNI	Professeur Titulaire, UNSTIM, Benin	Rapporteur
Arona DIEDHIOU	Directeur de Recherche, IRD (HDR), France	Rapporteur
Kwaku Amaning ADJEI	Professeur Titulaire, KNUST, Ghana	Rapporteur
Eliezer BIAOU	Maître de Conférences, UNSTIM, Benin	Examinateur
Kossi François GUEDJE	Maître de Conférences, Université d'Abomey Calavi, Benin	Superviseur
Adechina Eric ALAMOU	Professeur Titulaire, UNSTIM, Benin	Co-Superviseur

WASCAL West African Science Service Centre on Climate Change and Adapted Land Use
With funding from the: Federal Ministry of Research, Technology and Space

Dedication

With heartfelt gratitude to Almighty God, this thesis is lovingly dedicated to my supportive father, Zacharie GANNI MAMPO; devoted mother, Aîssatou OSSENI; amazing wife, Wassilatou OROU DADAGUI; treasured son, Riyad, and precious daughter, Rihanath.

Acknowledgment

This PhD research is realized in the framework of the West African Science Service Center on Climate Change and Adapted Land Use (WASCAL) and funded by the German Ministry of Education and Research (BMBF) in collaboration with the Benin Ministry of Higher Education and Scientific Research (MESRS).

My special gratitude goes to the German Federal Ministry of Education and Research (BMBF) for generously funding this research through the West African Science Service Centre on Climate Change and Adapted Land Use (WASCAL).

I would like to express my deep gratitude to my main supervisor **Prof. Kossi François Guedje,** for his insightful guidance, suggestions, and unwavering encouragement throughout this journey.

I would like to express my deep gratitude to my Co-supervisor **Prof. Adechina Eric Alamou**, Director of the National School of Civil Engineering, for his insightful guidance, suggestions, and unwavering encouragement throughout this journey.

I would like to express my deep gratitude to my Advisor, **Prof. Bruno Merz**, Head of the Hydrology section at Helmholtz Centre GFZ Potsdam and Full Professor at the University of Potsdam, Germany, for his insightful guidance, suggestions, and unwavering encouragement throughout this journey. I am deeply thankful to his family, his wife **Petra**, daughters **Lea**, **Emma**, and **Sara**, his son **Marius**, and his son-in-law **Richard** for their warm hospitality and for making my six-month stay in Potsdam both enriching and memorable. I would also like to acknowledge my colleagues and friends at GFZ for their invaluable support.

I would like to express my sincere gratitude to the members of the jury for their valuable contribution and thoughtful insights, which have enhanced the scientific quality of this work.

Special thanks to **Prof. Julien Adounkpe**, Director of the Graduate Research Program on Climate Change and Water Resources at the University of Abomey-Calavi (Benin), along with the Deputy Director, **Prof. Agnidé Emmanuel Lawin**, the Scientific

Coordinator, **Dr. Jean Hounkpe**, and the secretary, **Mrs. Djagoun Imelda,** for their invaluable support and guidance.

My deep gratitude to my seniors, **Dr Ravi Kumar Guntu**, **Dr Ezechiel Obada** and **Dr Halissou Yarou** for their insightful support and advice.

My heartfelt appreciation also goes to my colleagues in the WASCAL program for their unwavering support and collaboration throughout this journey.

I extend my heartfelt gratitude to my two cherished grandparents, late **El Hadj Osseni Bani** and **Baké Doué**, for their boundless love and blessings. May you both enjoy long and healthy lives. I also wish to express my sincere appreciation to my grand-uncle, **He Bio Gounou Idrissou Sina**, and his wife, **Mariam Bori**, for their unwavering support.

I am deeply grateful to all those who contributed, whether near or far, to the achievement of this thesis.

Abstract

Understanding hydroclimatic variability and climate teleconnections in a warming world is crucial for drought-prone regions like West Africa, where economies heavily depend on rain-fed agriculture. This study improves meteorological and hydrological drought prediction in the Benin Part of the Niger River Basin by enhancing the understanding of hydroclimatic variability, its links to climate teleconnections and farmers' perception in the Beninese Part of the Niger River Basin (BPNRB). Using the Standardized Precipitation Index (SPI), the Standardized Precipitation Evapotranspiration Index (SPEI), the Consecutive Dry Days Index (CDD), and the Streamflow Drought Index (SDI), the study assessed drought variability on 3- and 12-month timescales. Statistical and wavelet coherence analyses were employed to explore the connections between drought patterns and global climate drivers. Using a questionnaire administered to 509 households across 96 villages in eight municipalities, we collected and analyzed qualitative and quantitative data through statistical and machine-learning methods. The findings of hydroclimatic variability confirmed the recovery phase in the 1990s following severe droughts in the 1970s and 1980s. Significant trends include increased CDD values during the rainy season, with an average of 18 dry spell days, and a pronounced upward trend in SDI, indicating intensifying hydrological droughts. The application of wavelet transform coherence reveals that rainfall and streamflow variability are modulated by the climate teleconnections El Niño-Southern Oscillation (ENSO), Atlantic Multidecadal Oscillation (AMO), and Dipole Mode Index (DMI). In relation to rainfall, we find a tendency of a shift from lower-frequency coherence (around 4–10 years) in earlier decades to higher-frequency coherence (1–3 years) in recent decades. These patterns are less pronounced for streamflow, which is more indirectly influenced by climate teleconnections. The analysis highlights the crucial role of oceanic teleconnections in improving the predictability of seasonal rainfall anomalies, with performance steadily increasing from R^2 = 0.58 in June to R^2 = 0.70 in September, and effective predictors such as the Niño indices, TASI, SAT, and SWIO contributing to this variability detection, while monthly mean squared errors (MSE) ranged from 0.150 in June to 0.129 in September. The survey results reveal that although 71% of farmers demonstrate a good understanding of local hydroclimatic variability, only 9% attribute its underlying causes, particularly rising temperatures, to global climate change. Key factors influencing knowledge levels include age and farming experience, with older and more experienced farmers demonstrating better understanding, whereas formal education showed a weak effect. These insights support policymakers in designing more effective climate adaptation policies; drought monitoring in Northern Benin, and inform policies on agriculture and water management.

Keywords: Niger River Basin; West Africa; rainfall; streamflow; teleconnection; drought

Synthèse de la Thèse

Résumé

La compréhension de la variabilité hydroclimatique et des téléconnexions climatiques est cruciale pour les régions sujettes à la sécheresse comme l'Afrique de l'Ouest, où l'agriculture pluviale domine. Cette étude renforce la prévisibilité des sécheresses météorologique et hydrologique en approfondissant la compréhension de la variabilité hydroclimatique, de ses liens avec les téléconnexions climatiques et de la perception des agriculteurs dans la partie béninoise du bassin du Niger (BPNRB). En utilisant des indices tels que le SPI, le SPEI, le CDD et le SDI, la variabilité de la sécheresse a été analysée sur des échelles de 3 et 12 mois. Des analyses statistiques et des ondelettes ont exploré les liens entre les sécheresses et des facteurs climatiques globaux, notamment l'ENSO, l'AMO et le DMI. Une enquête auprès de 509 ménages dans 96 villages a permis de collecter des données qualitatives et quantitatives, analysées via des méthodes statistiques et d'apprentissage automatique. Les résultats montrent une phase de récupération dans les années 1990 après les graves sécheresses des années 1970-1980. Les durées CDD augmentent pendant la saison des pluies, atteignant en moyenne 18 jours de sécheresse. Une hausse marquée du SPI indique une intensification des sécheresses hydrologiques. L'analyse par ondelettes révèle que la variabilité des précipitations et des débits est modulée par les téléconnexions climatiques. Une transition de cohérences à basse fréquence (4-10 ans) à haute fréquence (1-3 ans) est observée dans les précipitations, tandis que les débits des cours d'eau restent modérément influencés. L'analyse met en évidence le rôle crucial des téléconnexions océaniques dans l'amélioration de la prévisibilité des anomalies pluviométriques saisonnières, avec une performance qui augmente régulièrement de $R^2 = 0.58$ en juin à $R^2 = 0.70$ en septembre, et des prédicteurs efficaces tels que les indices Niño, TASI, SAT, et SWIO contribuant à la détection de la variabilité, tandis que les erreurs quadratiques moyennes mensuelles (MSE) ont varié de 0.150 en juin à 0.129 en septembre. L'enquête révèle que, bien que 71% des agriculteurs aient une bonne compréhension de la variabilité hydroclimatique locale, seuls 9 % attribuent les causes, notamment la hausse des températures, au changement climatique global. Les résultats indiquent que l'âge et l'expérience agricole jouent un rôle déterminant dans le niveau de connaissance, contrairement à l'éducation formelle, dont l'impact reste limité. Ces résultats contribuent à l'orientation des politiques d'adaptation au climat, la gestion de l'eau et l'agriculture dans le nord du Bénin, tout en renforçant les systèmes de surveillance des sécheresses.

Mots-clés : Bassin du fleuve Niger ; Afrique de l'Ouest ; précipitations ; débit ; téléconnexion ; sécheresse

1. Introduction

Les précipitations sont essentielles pour de nombreux aspects de la vie en Afrique de l'Ouest, particulièrement en raison de la dépendance de la région à l'agriculture pluviale comme principale source de subsistance (Diatta et al., 2020; Thompson et al., 2010). Cependant, cette région est fortement vulnérable au changement climatique en raison de sa grande variabilité climatique, de ses capacités économiques limitées et de son exposition élevée aux sécheresses, notamment dans ses zones arides et semi-arides (Ndehedehe et al., 2020).

Les sécheresses constituent également une préoccupation majeure pour le Bénin. Selon l'Agence nationale pour la protection civile, environ 18 % de la population total au Benin, est exposée au risque de sécheresse, (MCVDD, 2019). Les sécheresses des années 1970 et 1980 ont entraîné des pertes économiques importantes, notamment en termes de production agricole, de perte de bétail et d'énergie hydroélectrique (Katz & Brown, 1992 ; Obada et al., 2021). Une analyse des données hydrométriques révèle également une diminution des débits fluviaux et de la recharge des nappes phréatiques après cette période (MCVDD, 2019).

Cependant, les changements dans la variabilité des précipitations et des débits des cours d'eau, en lien avec le réchauffement climatique, sont encore mal compris (Akinsanola et al., 2020; Biasutti, 2019a; Pendergrass et al., 2017). Certaines études prévoient une augmentation de la variabilité des précipitations de la mousson d'été en Afrique de l'Ouest, estimée entre 10 et 28 % (Akinsanola et al., 2020), tandis que d'autres suggèrent peu de changements significatifs (Hawkins & Sutton, 2011 ; Thompson et al., 2015).

Les téléconnexions climatiques jouent un rôle crucial dans la variabilité spatio-temporelle des précipitations à travers le monde. Parmi elles, le phénomène El Niño–Southern Oscillation (ENSO) est l'un des plus influents. L'ENSO désigne une interaction océan-atmosphère dans le Pacifique tropical, caractérisée par des phases alternantes : El Niño (réchauffement anormal des eaux de surface dans le Pacifique central et oriental) et La Niña (refroidissement de ces mêmes eaux), accompagnées de modifications de la circulation atmosphérique. Ce phénomène exerce une influence significative sur la variabilité interannuelle et même décennale des précipitations dans plusieurs régions du

globe, notamment en Afrique de l'Ouest, où il peut moduler l'intensité et la distribution des saisons des pluies. Fontaine & Bigot (1993) ; Fontaine & Janicot, (1996) ; Giannini, (2010) ; Losada et al., (2012) ; Pomposi et al., (2016). D'autres facteurs, comme l'Oscillation Multidécadale Atlantique (AMO) et le Indice de Mode Dipolaire (DMI), influencent également les précipitations à différentes échelles temporelles (Fontaine & Bigot, 1993 ; Giannini et al., 2003 ; Nicholson & Selato, 2000 ; Pomposi et al., 2016).

Les connaissances locales, souvent négligées, offrent des perspectives précieuses en matière d'adaptation. Les communautés locales utilisent des stratégies telles que la collecte d'eau, l'irrigation et la plantation de cultures résistantes à la sécheresse pour répondre aux changements climatiques (Jellason et al., 2021). Ces connaissances traditionnelles sont particulièrement précieuses en l'absence de données climatiques locales fiables et montrent parfois une concordance forte avec les observations scientifiques (Oyerinde et al., 2015 ; Tambo & Abdoulaye, 2013 ; Thomas et al., 2007 ; West et al., 2008). Compte tenu de la vulnérabilité du Bénin à la variabilité climatique, il est crucial de mieux comprendre et prévoir les caractéristiques des sécheresses et leur lien avec les téléconnexions climatiques.

2. Zone d'étude

La zone d'étude est la partie béninoise du bassin du fleuve Niger au nord du Bénin. Située entre 1°32' et 3°50' Est et 10° et 12°30' Nord, elle couvre une superficie d'environ 48 000 km², soit 42% de la superficie totale du Bénin (Halissou et al., 2021). Elle est partagée entre 17 communes et comprend les trois bassins versants de la Sota (13 449 km^2), de l'Alibori (13 684 km^2) et de la Mekrou (10 552 km^2) (Fig. 1). La zone d'étude est la plus grande zone de production de coton, de légumes et d'élevage au Bénin. Elle abrite également le Parc du W, qui est l'un des plus importants parcs animaliers d'Afrique de l'Ouest.

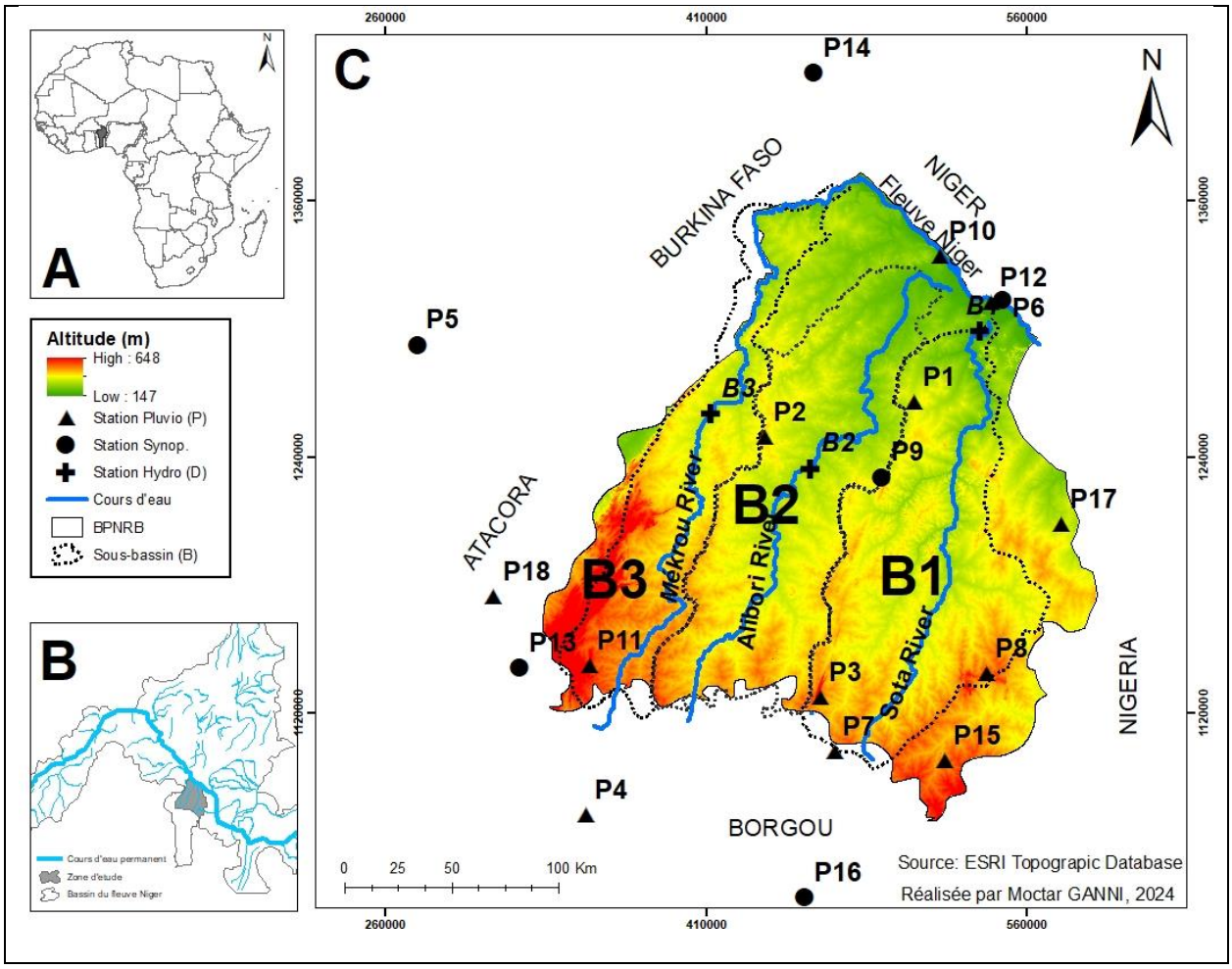

Figure 1: Zone d'étude Partie béninoise du bassin du fleuve Niger (BPNRB). (A) Localisation du Bénin en Afrique de l'Ouest. (B) Bassin du fleuve Niger incluant la zone d'étude. (C) Zone d'étude BPNRB : topographie, localisation des stations climatiques et de débit, et les trois bassins versants (fleuve Sota, B1 ; fleuve Alibori, B2 ; fleuve Mekrou, B3).

La zone d'étude connaît deux saisons distinctes. La saison des pluies s'étend d'avril à octobre, avec un maximum de précipitations généralement en août, tandis que la saison sèche s'étend de novembre à mars (Badou et al., 2021). Les précipitations annuelles varient de 780 à 1 200 mm pour la période 1970-2020. L'évapotranspiration potentielle (ETP) journalière varie entre 1,6 et 10 mm, et la moyenne annuelle de la température maximale journalière est de 33,8°C sur la même période. La moyenne mensuelle de la température maximale journalière peut atteindre environ 40°C. Les trois rivières présentent d'importantes variations saisonnières. La Sota a un régime d'écoulement pérenne avec un faible débit d'environ 3,6 m^3/s pendant la saison sèche ; les rivières Alibori et Mekrou sont à sec pendant la saison sèche (Vissin, 2007).

3. Matériel et méthodes

L'étude adopte une approche multidimensionnelle en combinant des matériaux et des outils à la fois rigides et flexibles. Les principaux outils utilisés comprennent:

- **RStudio version 2022.12.0.353** a été utilisé pour préparer et analyser efficacement des ensembles de données pour diverses tâches de traitement des données, y compris le nettoyage des données, la transformation, l'analyse statistique et la visualisation.
- **Climate Data Operator version 2.5.0** a été utilisé dans l'environnement Ubuntu pour extraire les données Sea Surface Temperature (SST) et (CHIRPS) maillées et préparer les données avant l'analyse de corrélation entre le prédictand et les prédicteurs.
- **MATLAB R2018a version 9.4.0** a été utilisé pour l'analyse avancée des données, la modélisation mathématique et la visualisation, facilitant les calculs complexes, le développement d'algorithmes et la représentation graphique des résultats.
- **KoboToolbox version 2.023.21** est un outil puissant de conception, de déploiement et de gestion des formulaires de collecte de données. Dans cette étude, les données ont été collectées à l'aide de questionnaires, codés et déployés sur Kobotoolbox.

❖ Approche méthodologique pour l'étude des caractéristiques historiques des sécheresses hydrométéorologiques dans l'espace et dans le temps

Pour analyser les sécheresses, quatre indicateurs clés ont été utilisés : l'indice standardisé des précipitations (SPI), l'indice standardisé d'évapotranspiration des précipitations (SPEI), l'indice de sécheresse du débit des cours d'eau (SDI) et l'indice des jours secs consécutifs (CDD). En outre, la durée et l'intensité de la sécheresse ont été calculées pour saisir les variations spatiales et temporelles des sécheresses dans la zone d'étude.

Des mesures statistiques de base, telles que le coefficient de variation (CV) et le coefficient de corrélation de Spearman, ont été appliquées pour évaluer la variabilité et les interdépendances des précipitations et du débit. Pour l'analyse des tendances, le test non paramétrique de Mann-Kendall modifié (MMK) a été utilisé.

- **Approche méthodologique pour l'évaluation des capacités de prévision et la prévisibilité de la sécheresse**

Cette étude se concentre sur l'amélioration de la prévisibilité saisonnière des précipitations, en visant des prévisions d'au moins deux mois à l'avance. Pour ce faire, nous avons utilisé des données de température de surface de la mer (SST) moyennes sur trois mois pour des périodes qui se chevauchent : OND (octobre-novembre-décembre), NDJ (novembre-décembre-janvier), DJF (décembre-janvier-février), JFM (janvier-février-mars), FMA (février-mars-avril), MAM (mars-avril-mai) et AMJ (avril-mai-juin). Ces moyennes de SST ont été utilisées pour prévoir les anomalies de précipitations pour les mois de juin, juillet, août et septembre, respectivement.

En intégrant toutes les variables et tous les indicateurs pertinents, un total de 12 prédicteurs potentiels a été identifié. Avant d'utiliser des modèles multivariés, il est essentiel d'affiner cet ensemble complet pour obtenir un sous-ensemble de prédicteurs plus pertinents. Cette étape permet d'optimiser les performances du modèle. Diverses méthodes statistiques et d'apprentissage automatique ont été appliquées pour sélectionner systématiquement les prédicteurs les plus robustes, capables d'expliquer la variabilité des précipitations dans les trois sous-bassins Sota, Alibori et Mekrou.

Les indices climatiques qui ont influencé les précipitations doivent d'abord être connus pour appliquer les modèles de régression linéaire multiple. Nous considérons toutes les combinaisons possibles des 12 prédicteurs pour construire des modèles de régression linéaire multiple. Les mesures de performance, y compris le coefficient de détermination (R^2), l'erreur quadratique moyenne (EQM) et la P-value, ont été calculées pour évaluer la précision prédictive et la signification statistique des modèles.

- **Approche méthodologique pour la proposition d'un cadre de conception pour la gestion des risques de sécheresse dans la zone d'étude**

Pour étudier la compréhension de la variabilité hydroclimatique par les agriculteurs, nous avons sélectionné 14 questions (tableau 8) qui permettent une comparaison claire entre les perceptions des agriculteurs et les données climatiques observées. Chaque répondant a reçu un score de connaissance basé sur la concordance entre ses réponses aux 14 questions et les observations. Les questions étaient binaires ou à quatre options, avec des scores de 0 pour incorrect, 1 pour correct, et des valeurs intermédiaires pour

les réponses nuancées. Le score final de chaque personne correspond à la moyenne des résultats obtenus, allant de 0 (réponses incorrectes) à 1 (réponses correctes).Notre objectif est d'identifier les facteurs qui améliorent la compréhension de la variabilité hydroclimatique, du changement climatique et des mesures d'adaptation appropriées. Les facteurs potentiels qui ont été inclus dans notre enquête sont le sexe (homme, femme), l'âge, l'expérience (nombre d'années de pratiques agricoles), le niveau d'éducation (aucun, primaire, élevé), l'engagement dans un travail secondaire (oui, non), la localisation (municipalités L1 à L8), et l'orientation technologique/scientifique (oui, mixte, non). Ce dernier facteur n'a pas été demandé directement aux personnes interrogées, mais a été déduit de leurs réponses à des questions relatives à leurs pratiques agricoles et à leurs approches pour augmenter leurs rendements agricoles. Les ménages qui utilisent des pesticides et du matériel agricole ont été classés comme favorables à un point de vue axé sur la technologie/science. Les ménages qui s'appuient sur des rites religieux dans leurs activités agricoles ont été classés comme n'étant pas orientés vers la technologie/science. La classe mixte a été attribuée aux agriculteurs qui utilisaient les deux types d'approches, comme l'utilisation de pesticides et de rites religieux.

Pour comprendre si et comment un certain facteur contribue à la compréhension de la variabilité hydroclimatique et du changement climatique par les agriculteurs, représentée par le score de connaissance sur l'ensemble des 14 questions, nous avons appliqué les méthodes Random Forest et Accumulative Local Effects (effets locaux cumulatifs). La Random Forest (forêt aléatoire) est un ensemble d'arbres de décision dans lequel chaque arbre de décision est formé avec un bruit aléatoire spécifique. De façon plus explicite, elle est un algorithme robuste d'apprentissage automatique connu pour sa capacité à traiter de grands ensembles de données et des interactions complexes entre les variables (Breiman, 2001). Pour faire la lumière sur ces influences, nous avons utilisé des diagrammes d'effets locaux cumulés (ALE) (Apley & Zhu, 2020 ; Robette, 2020).

4. Résultats et discussion

❖ Resultats et discussion pour l’étude des caractéristiques historiques des sécheresses hydrométéorologiques dans l'espace et dans le temps

L'évolution temporelle des moyennes spatiales du SPI et du SPEI montre une alternance de cycles secs et humides sur le bassin de 1970 à 2020. Le SPI présente une tendance à la hausse, tandis que le SPEI affiche une tendance à la baisse, bien que les deux indices fluctuent souvent autour de zéro. Les tendances sèches deviennent plus marquées aux échelles temporelles plus longues. Malgré des variations globalement similaires entre les indices, de légères différences apparaissent. Le test de Mann-Kendall modifié révèle des tendances significatives à toutes les échelles, sauf pour le SPI-3 et le SPEI-12.

Les caractéristiques spatiales du CDD au cours de la période 1970-2020 montrent de grandes différences entre la saison des pluies (AMJJAS) et les saisons entières (saisons des pluies et saisons sèches). Pour l'ensemble de la saison sur la BPNRB de 1970 à 2020, le CDD a varié de 80 à 180 jours. Cet indice augmente avec la latitude des stations. Il a montré une tendance chronologique à la hausse de 0,1 jour/an, statistiquement significative dans le centre-ouest. En saison des pluies, le CDD, qui correspond aux périodes sèches, varie de 9 à 18 jours. Son maximum a été enregistré dans la partie nord du bassin.

L'étude des changements passés (1970-2020) dans les précipitations et les débits des bassins versants, ainsi que leur association avec les téléconnexions climatiques, révèle des régimes de précipitations cohérents dans les trois sous-bassins, avec une reprise après les sécheresses des années 1970-1980 qui a commencé dans les années 1990.

Le nombre de jours humides (jours avec des précipitations > 1 mm) au cours de la saison des pluies augmente fortement, passant d'environ 120 à plus de 140 jours. Cela signifie qu'il pleut (quelque part) dans chaque bassin versant deux jours sur trois. Cette augmentation est significative au niveau de 5 % et cohérente entre les bassins versants. Les précipitations totales ont augmenté de manière significative, en raison d'un plus grand nombre de jours de pluie, bien que la quantité de précipitations des jours humides ait diminué. Ces résultats peuvent être résumés comme suit : « augmentation des précipitations totales, mais moins intenses et plus variables dans l'espace ». Malgré une hausse des précipitations, la sécheresse persiste, en raison d’une forte variabilité interannuelle et décennale.

La variabilité du débit journalier, représentée par l'écart-type et le coefficient de variation, montre un comportement mitigé dans les trois sous-bassins. L'analyse du débit montre que certains champs de variabilité des précipitations se traduisent par de similaires schémas dans le débit. Nous constatons des fluctuations à court terme (zigzag) et décennales similaires dans les précipitations et les débits. Le comportement moins cohérent du débit dans les trois bassins versants peut s'expliquer par les effets supplémentaires que les processus du bassin versant et les activités humaines, tels que l'évapotranspiration, le changement d'utilisation des terres et le captage d'eau, ont sur le débit.

- **Resultats et discussion pour l'évaluation des capacités de prévision et la prévisibilité de la sécheresse**

Nous étudions dans quelle mesure la variabilité des précipitations et des débits dans les trois bassins versants est modulée par les téléconnexions climatiques. Des indices climatiques représentant les températures de surface de la mer dans les océans Pacifique (Niño 3.4), Atlantique (AMO) et Indien (DMI) ont été sélectionnés. La cohérence des ondelettes révèle que la variabilité des précipitations et des débits est modulée par les téléconnexions climatiques ENSO, AMO et DMI. Pour les précipitations, les résultats révèlent une transition d'une cohérence dominante à basse fréquence (4-10 ans) au cours des premières décennies vers une cohérence à plus haute fréquence (1-3 ans) dans les dernières décennies. Cette évolution est moins marquée pour le débit des cours d'eau, probablement en raison d'influences climatiques indirectes. L'analyse du WTC entre l'indice Niño 3.4 et les précipitations des bassins versants montre une configuration similaire à celle observée entre le Niño 3.4 et le débit des cours d'eau. Dans les deux cas, les anomalies positives de la température de surface de la mer dans la région du Niño 3.4 sont corrélées à des anomalies négatives dans le nord du Bénin. Dans l'ensemble, nos résultats confirment ceux de plusieurs études antérieures.

Les indices DMI et AMO semblent être plus pertinents pour la variabilité des précipitations dans notre zone d'étude que l'ENSO. Ceci met en évidence le rôle déterminant des océans Indien et Atlantique sur les régimes climatiques régionaux. Des études antérieures ont souligné le rôle majeur de l'ENSO sur le climat de l'Afrique de l'Ouest. Cependant, nos résultats suggèrent que le DMI et l'AMO pourraient avoir un impact plus

important dans cette région, peut-être en raison des variations régionales des facteurs climatiques. Cependant, la cohérence à des fréquences plus basses (jusqu'à 15 ans) n'a pas été documentée dans cette région jusqu'à présent, offrant des aperçus de la variabilité à plus long terme du débit des cours d'eau. De manière générale, on observe une évolution dans la cohérence entre les indices climatiques et les précipitations du bassin versant, marquant un changement entre les premières et les dernières décennies. Dans une seconde phase de l'analyse, l'attention a été portée sur le potentiel prédictif des téléconnexions océaniques pour la prévision des anomalies pluviométriques saisonnières. Les résultats mettent évidence le rôle déterminant de ces téléconnexions dans l'amélioration de la prévisibilité. L'augmentation progressive des performances du modèle, avec un coefficient de détermination de R^2=0.58 en juin à R^2=0.70 en septembre, illustre l'efficacité croissante des prédicteurs tels que les indices Niño, TASI, SAT et SWIO pour capter la variabilité des précipitations. Afin d'évaluer l'ampleur des écarts entre les anomalies de précipitations observées et celles prédites par le modèle, l'erreur quadratique moyenne (MSE) a été calculée pour chaque mois : 0.150 en juin, 0.180 en juillet, 0.130 en août et 0,129 en septembre. Ces valeurs fournissent des indications précises sur la capacité du modèle à reproduire l'intensité des anomalies pluviométriques. Cela confirme le rôle central que jouent les téléconnexions dans la modulation des conditions climatiques régionales au fil de la saison.

- **Resultats et discussion pour l'étude des caractéristiques historiques des sécheresses hydrométéorologiques dans l'espace et dans le temps**

Les résultats révèlent que si 71 % des agriculteurs ont une bonne compréhension de la variabilité hydroclimatique locale, des lacunes importantes subsistent quant à ses causes sous-jacentes ; seuls 9 % attribuent les hausses de température au changement climatique global. L'analyse montre que l'âge et l'expérience sont positivement corrélés au score de connaissance, bien que faiblement. Les agriculteurs plus âgés et expérimentés tendent à mieux connaître la variabilité hydroclimatique et le changement climatique. Des différences significatives de score apparaissent selon la localisation et le niveau d'éducation, avec un score médian allant de 0.55 à 0.75. L'éducation formelle semble avoir un effet légèrement négatif sur la connaissance locale. D'autres facteurs

comme le genre, la prise en compte de la technoscience ou un emploi secondaire n'ont pas d'impact significatif.

Les facteurs clés qui influencent les niveaux de connaissance sont l'âge et l'expérience agricole, les agriculteurs plus âgés et plus expérimentés ont tendance à faire preuve d'une meilleure compréhension, tandis que l'éducation formelle n'a qu'un faible effet. Ces résultats mettent en évidence le rôle vital des connaissances endogènes dans le nord du Bénin, accumulées grâce à une interaction environnementale à long terme.

5. Conclusion

Les résultats de cette étude mettent en évidence des dynamiques climatiques complexes et des impacts socio-environnementaux significatifs dans les bassins versants étudiés, notamment dans le nord du Bénin. Une phase de récupération hydrologique après les graves sécheresses des années 1970 et 1980 a été observée, bien que des tendances inquiétantes, telles qu'une augmentation des périodes sèches (CDD) et une intensification des indices de sécheresse hydrologique (IDS), subsistent. L'analyse des téléconnexions climatiques a révélé l'influence marquée de facteurs océaniques comme ENSO, AMO et DMI sur la variabilité des précipitations et des débits, particulièrement en fin de saison de la mousson. Les modèles prédictifs basés sur des indices climatiques tels que Niño3.4, Niño1.2, SAT, TASI et SWIO se sont avérés efficaces pour expliquer la variabilité des précipitations saisonnières, avec des performances croissantes au fil des mois, culminant en septembre. Ces résultats soulignent le rôle critique des indices SST et des téléconnexions océaniques dans la prédiction des anomalies pluviométriques. Sur le plan socio-économique, les lacunes dans la compréhension des causes du changement climatique mondial par les agriculteurs, malgré une bonne connaissance locale de la variabilité hydroclimatique, mettent en lumière la nécessité de renforcer les capacités d'adaptation. L'intégration des connaissances indigènes accumulées par les agriculteurs plus expérimentés à des approches éducatives formelles apparaît comme une stratégie clé pour accroître la résilience climatique dans les régions vulnérables.

Table of contents

List of Acronyms

AIC	**:**	Association Interprofessionnelle du Coton
AMO	**:**	Atlantic Multi-decadal Oscillation
ATDA	**:**	Agence Territoriale de Développement Agricole
BPNRB	**:**	Beninese Part of the Niger River Basin
CHIRPS	**:**	Climate Hazards Group InfraRed Precipitation with Station data
DMI	**:**	Dipole Mode Index
ENSO	**:**	El Niño–Southern Oscillation
IPCC	**:**	Intergovernmental Panel on Climate Change
ModHyPMA	**:**	Hydrological Model based on the Least Action Principle
NAT	**:**	North Atlantic Tropical
PDO	**:**	Pacific Decadal Oscillation
SAT	**:**	South Atlantic Tropical
SDI	**:**	Standardized Drought Index
SETIO	**:**	South Eastern Tropical Indian Ocean
SPI	**:**	Standardized Precipitation Index
SPEI	**:**	Standardized Precipitation and Evapotranspiration Index
SST	**:**	Sea Surface Temperature
SWAT	**:**	Soil and Water Assessment Tool
SWIO	**:**	South Western Indian Ocean
TNI	**:**	Trans-Nino Index
TASI	**:**	Tropical Atlantic SST Index
WEF	**:**	World Economic Forum
WTIO	**:**	Western Tropical Indian Ocean

List of figures

List of tables

CHAPTER 1: GENERAL INTRODUCTION

This chapter first presents the study's context, problem statement, and literature review. In addition, it provides research questions as well as the thesis's main and specific objectives. It then outlines the main sub-sections of this thesis.

1.1. Context and problem statement

Rainfall is crucial to many aspects of human life in West Africa due to the region's heavy reliance on agriculture as a primary source of livelihood (Diatta et al., 2020; H. E. Thompson et al., 2010). West Africa is particularly vulnerable to climate change due to its high climate variability, its heavy dependence on rain-fed agriculture, and limited economic and institutional capacity. Its arid and semi-arid regions consistently rank among the most drought-prone regions in the world (Ndehedehe et al., 2020). Starting in the 1970s, West Africa experienced severe droughts linked to a northward shift of the monsoon. A substantial decrease of around 40% in total annual rainfall was recorded between 1968 and 1990, compared to the period 1931–1960 (Dai, 2011). Since the early 1990s, a partial recovery has been observed. This decadal-scale variability has prompted numerous studies, particularly on Sahelian droughts (Aich et al., 2015; Gal, 2016; Mahé & Paturel, 2009; Nicholson, 2013; Ouedraogo et al., 2014; Ozer et al., 2010; Tall et al., 2023; Zeng, 2003). Droughts are also a major concern for Benin, where our study area is located. According to the National Agency for Civil Protection, approximately 2.2 million people, or 18% of Benin's total population, are at risk of drought (MCVDD), 2019). The severe droughts in the 1970s and 1980s caused huge economic losses in Benin due to reduced agricultural production, loss of livestock, and reduced hydropower generation (Katz & Brown, 1992; Obada et al., 2021). An analysis of hydrometric station data across the national territory shows that streamflow and groundwater recharge decreased after the 1970s (MCVDD, 2019).

In contrast to changes in the mean behavior, changes in the variability of rainfall and streamflow are not well understood, and there is a lack of understanding of how rainfall varies concerning global warming (Akinsanola et al., 2020; Biasutti, 2019a; Pendergrass et al., 2017). Increased rainfall or streamflow variability can stress the environment and society, for instance, by reducing agricultural yields or increasing the intensity of heavy

rainfall and flooding (Akinsanola et al., 2020; Rowhani et al., 2011). Under global warming (Akinsanola et al., 2020) projected an increase in West African summer monsoon rainfall variability in the range of 10–28% over West Africa, which was consistent over a wide range of time scales, including seasonal, interannual, and decadal scales. However, it has also been suggested that rainfall variability does not change much under climate change (Hawkins & Sutton, 2011; D. W. J. Thompson et al., 2015). Furthermore, most results on changes in rainfall variability are based on model simulations, especially in regions such as West Africa, where there are few climate observations.

Although several studies have been conducted to explore past changes and future projections of rainfall variability in the region, there remains a need for more comprehensive research to fully understand the implications of a warmer climate on rainfall patterns, particularly due to the region's dependence on rainfall. Several studies have attempted to explain the causes of the rainfall variability and droughts in West Africa by relating rainfall variability and deficits to climate teleconnections (Bader & Latif, 2011; Fontaine & Bigot, 1993; Fontaine & Janicot, 1996; Giannini, 2010; Losada et al., 2012; Pomposi et al., 2016). Most of these studies have identified El Niño Southern Oscillation (ENSO) as the main driver of rainfall variability on interannual and decadal time scales. Gizaw & Gan (2017) reported that the occurrence of El Niño increases the probability of drought in the Sahel. Worou et al., (2020) identified ENSO, the South Atlantic Ocean Dipole (SAOD), and the Atlantic Niño (ATL3) as major modulators of the pre-monsoon and monsoon on the Guinean coast. In Central Equatorial Africa, the long-term drying observed in the period 1970–1990 has been linked to ENSO and atmospheric circulation changes associated with a weaker West African monsoon (Hua et al., 2016). In addition, the Atlantic Multidecadal Oscillation (AMO) and the Dipole Mode Index (DMI) have been found to influence rainfall variability in West Africa on a wide range of time scales, multidecadal time scales, and on interannual to decadal time scales, respectively (Fontaine & Bigot, 1993; Giannini et al., 2003; Nicholson & Selato, 2000; Pomposi et al., 2016).

The value of local knowledge is often underestimated in climate change studies. Farmers have valuable indigenous adaptation strategies, including early warning systems (Nyadzi

et al., 2021), and they recognize and respond to climatic changes (Thomas et al., 2007). For example, local communities in the Niger River Basin have responded to variations in water availability through the use of water harvesting, irrigation, and planting of drought-tolerant and early-maturing crop varieties (Jellason et al., 2021). Therefore, it has been argued that local knowledge of climate variability and adaptation measures is very valuable, particularly in the absence of reliable local observations and projections (Oyerinde et al., 2015) and some studies have demonstrated high agreement between local perceptions and observations (Oyerinde et al., 2015; Tambo & Abdoulaye, 2013; Thomas et al., 2007; West et al., 2008).

Given Benin's high vulnerability to rainfall variability and droughts, it is of utmost importance to understand the variability of rainfall and streamflow, and how this variability is linked to climate teleconnections. So far, studies in this region have been limited to the assessment of water resources (Badou et al., 2017, 2021; Gaba, 2015) and the impacts of climate variability and climate change on water (Alamou et al., 2017; Halissou et al., 2021; Vissin, 2007). This present work responds to this gap in understanding, characterizing, and predicting the state of drought in the basin. Therefore, improving the understanding of drought characteristics and their predictability over the region in climate change conditions is important for developing mitigation and adaptation plans.

The growing recurrence and severity of droughts in the Beninese part of the Niger River Basin (BPNRB) present not only environmental and socio-economic challenges but also critical policy implications. This issue aligns closely with Benin's National Drought Management Plan, which emphasises the development of effective early warning systems and the integration of climate information into decision-making for agriculture and water management. However, progress in understanding and predicting the occurrence of droughts has been constrained by limited observational coverage and data discontinuities. In particular, the scarcity of long-term, high-resolution hydro-meteorological records poses challenges to accurate drought monitoring and trend analysis. This study addresses these limitations by integrating multiple data sources, including satellite observations and sea surface temperature (SST) based large-scale climate teleconnection, to enhance drought predictability and support evidence-based decision-making in line with Benin's National Drought Management Plan. Through

improving the understanding of drought characteristics and their predictability over the region, this study contributes directly to the National Drought Management Plan's objectives of strengthening preparedness, reducing vulnerability, and enhancing resilience in climate-sensitive sectors.

1.2. Literature review

Due to the complex relationship between the different physical factors involved in the event and the duration of drought, it is difficult to precisely define drought. In this chapter, the different types of droughts, their underlying causes, and the indices commonly used to quantify their severity are reviewed. The literature is organized into thematic sub-sections: Climate Drivers, Hydrological Responses, Drought Prediction, Local Adaptation and Perception.

Types of droughts

There are several types of droughts: meteorological, hydrological, agricultural and socio-economic:

- **Meteorological drought** has been defined as a "period of more than some particular number of days with precipitation less than some specified small amount" (Great Britain Meteorological Office, 1951). Linsley R. K. (1958) referred to it as a "sustained period without significant rainfall. McGuire and Palmer (1957), for example, have referred to drought as a "period of monthly or annual precipitation less than some particular percentage of normal."
- **Hydrological drought** is generally related to the deficit of surface runoff, streamflow, reservoir, or groundwater level. Since it is directly linked to drought impacts, it is argued that more attention is needed to study hydrological drought (Fleig et al., 2011; Mishra & Singh, 2010). Overall, Hydrological drought is primarily influenced by climatic factors and catchment characteristics, with its prediction requiring meteorological inputs (particularly precipitation and temperature) alongside initial catchment conditions (Van et al., 2013)
- **Agricultural drought:** Agricultural drought definitions connect various aspects of meteorological drought to agricultural impacts, often emphasizing precipitation deficits, deviations from normal conditions, or a combination of meteorological

factors, including evapotranspiration (Almendra-Martín et al., 2021; Pan et al., 2024).

- **Socio-economic droughts**: Definitions of socioeconomic drought often integrate characteristics of meteorological, agricultural, and hydrological drought, emphasizing the imbalance between the supply and demand of economic goods and services. These definitions highlight the broader economic and societal impacts, such as reduced agricultural productivity, water scarcity, and disruptions to livelihoods (IPCC, 2023; Wilhite et al., 1985).

Figure 2 illustrates the progression and interconnection of various drought types, highlighting the sequence in which meteorological drought can cascade into agricultural, hydrological, and ultimately socioeconomic droughts.

This research focuses on meteorological and hydrological droughts, as they represent the most direct and measurable impacts of climate variability on water availability. These two types are particularly relevant for understanding seasonal water shortages and managing water resources in river basins such as the Niger, where both rainfall variability and river discharge are critical for agriculture, energy production, and ecosystem sustainability.

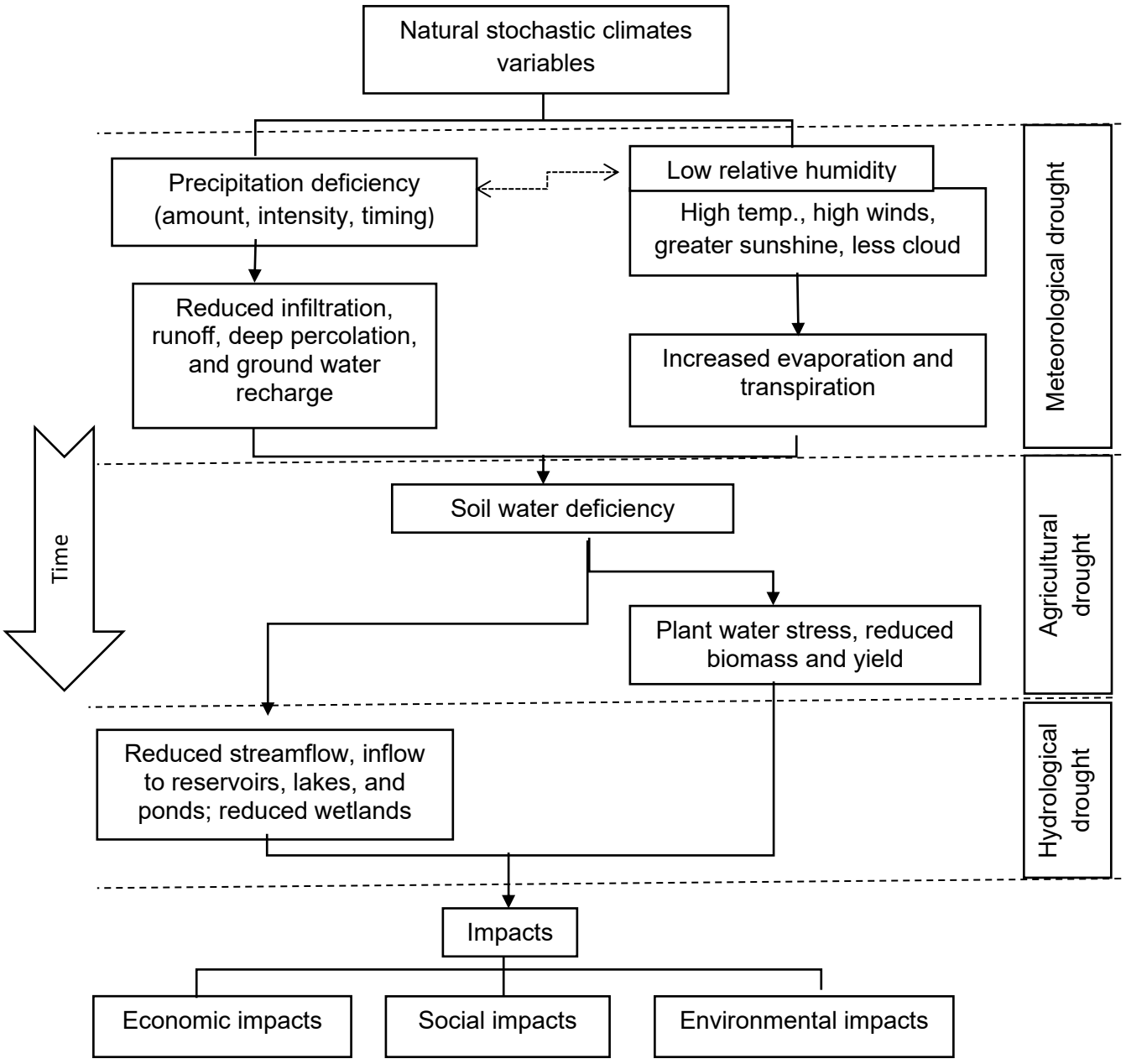

Figure 2 **:** The general sequence for the occurrence of different drought types. Modified from (National Drought Mitigation Center (NDMC), 2006).

Climate Drivers

Precipitation variability under global warming is closely tied to extreme events that threaten the environment and society (IPCC, 2012). These events can have devastating consequences for ecosystems, food supply, and economies (Handmer et al., 2012). Among the most significant extreme events associated with precipitation variability in

West Africa are droughts and floods, which result in severe detrimental impacts (Ebi & Bowen, 2016). The prolonged drought that affected West African countries starting in the 1970s is a particularly notable example, lasting several decades and described as one of "the most undisputed and largest recent climate changes recognized by the climate research community" (Dai & Trenberth, 2004).

West Africa's highly variable climatic conditions pose significant threats to water and ecological resources, making the region particularly vulnerable to the impacts of global climate change. For instance, Lake Chad, one of the world's most prominent freshwater bodies in a major interior drainage basin, has experienced a dramatic reduction in size from approximately 24,000 km² in the 1950s to just about 1,700 km² in recent years (Fougou & Lemoalle, 2022; Ndehedehe et al., 2016). This historic decline in Lake Chad's surface area is largely attributed to the persistent droughts of the 1960s and 1980s. These severe droughts, continental in scope, have been linked by diagnostic studies (Bader & Latif, 2011; Fontaine & Bigot, 1993; Giannini et al., 2003; Rodríguez-Fonseca et al., 2011) to large-scale climatological shifts and modifications in global sea surface temperatures (SSTs).

In the Volta Basin, rainfall variability has been a major driver of food production fluctuations (Kasei et al., 2010), while hydrological droughts have caused significant declines in the water levels of Lake Volta (Bekoe & Logah, 2013; Ndehedehe et al., 2016). Similarly, long-term drying observed in Central Equatorial Africa has been attributed to SST variations and circulation changes associated with a weaker West African monsoon (Hua et al., 2016).

The BPNRB is the largest zone for cotton and vegetable production in Benin, as well as cattle breeding. It is also home to the W-Park, which is one of the most important wildlife parks in West Africa. Climate change and population growth increasingly threaten these areas with deforestation for settlement, agriculture, and resource extraction (Vissin, 2007).

Studies in this region have primarily focused on the assessment of water resources (Badou et al., 2017; Gaba, 2015) and the impacts of climate variability and change on water availability and hydrological systems (Alamou et al., 2017; Halissou et al., 2021; Vissin, 2007). These studies have provided valuable insights into the challenges posed

by changing precipitation patterns and water resource management. However, there remains a critical gap in understanding the dynamics and predictability of droughts, which are among the most pressing climate-related challenges in Benin.

Given Benin's significant dependence on rain-fed agriculture and its high vulnerability to rainfall variability and droughts, understanding the frequency, intensity, and spatial distribution of droughts is essential. Additionally, the potential role of climate teleconnections, such as the El Niño-Southern Oscillation (ENSO), Atlantic Multidecadal Oscillation (AMO), and Indian Ocean Dipole (IOD), in influencing drought patterns in this region has not been adequately explored. Addressing these gaps is crucial for enhancing drought monitoring, improving water resource planning, and informing adaptive strategies to mitigate the adverse effects of climate variability on agricultural productivity and livelihoods.

Hydrological Responses

In Africa, hydrological variability and recurrent drought episodes have profoundly negative impacts on freshwater resources, biodiversity, food security, health, and other critical sectors. These adverse effects hinder economic development, such as reducing gross domestic product (GDP) (C. Brown & Lall, 2006), and exacerbate poverty in one of the world's poorest continents. Notably, the severe droughts of the 1970s and 1980s, coupled with the persistent impacts of climate variability on West Africa's socioeconomic systems, catalyzed a surge in climate research in the region.

A poor understanding of hydrological variability poses significant challenges to risk management and the prediction of extreme weather events (Vogel et al., 2015). For example, before the devastating droughts of the 1980s, Lake Chad played a vital role in regional economic stability. Similarly, surface water developments like Lake Volta and the Kainji Dam, which are essential for hydropower generation, have been negatively impacted by drought events (Ndehedehe et al., 2016).

Focusing on our study area in northern Benin, part of the Niger River Basin, similar challenges are evident. The region is highly vulnerable to rainfall variability and droughts, which significantly affect water availability for agriculture, drinking water supplies, and energy production. Despite this vulnerability, there is a limited understanding of the spatiotemporal variability of rainfall and streamflow in the area, as well as their

relationship with climate teleconnections. By addressing these gaps, our study provides critical insights into the hydrological dynamics of the region, offering a foundation for improved water resource management and drought preparedness tailored to the local context.

Drought prediction, Local Adaptation and Perception

Drought prediction and predictability in West Africa, particularly in Benin, have been the subject of limited but emerging research, reflecting the region's vulnerability to climate variability and heavy reliance on rain-fed agriculture. The complexities of drought prediction arise from the intricate interplay between local climatic factors and large-scale climate systems, including teleconnections such as the El Niño-Southern Oscillation (ENSO), Atlantic Multidecadal Oscillation (AMO), and Indian Ocean Dipole (IOD). Studies have demonstrated that these teleconnections significantly influence precipitation patterns across West Africa (S. E. Nicholson, 2013; Rodríguez-Fonseca et al., 2011).

Most drought predictability studies in the region have leveraged global climate models and seasonal forecasting systems, with varying degrees of success. For example, Giannini et al., (2003) analyzed the predictability of rainfall anomalies in West Africa, emphasizing the role of sea surface temperature patterns and their teleconnection impacts, while highlighting challenges associated with model limitations and uncertainty. In Benin specifically, research by Alamou et al., (2017); Halissou et al., (2021) have focused on assessing rainfall variability and its implications for drought events, but these studies often stop short of providing predictive frameworks.

Recent advancements in the use of sea surface temperature (SST) anomalies as predictors have shown promise in improving drought forecasts (Funk et al., 2015). SST indices such as Niño 3.4, the Tropical Atlantic SST Index (TASI), and the South West Indian Ocean SST Index (SWIO) have been linked to rainfall variability in West Africa and could provide a foundation for enhanced drought prediction systems in the region. However, the application of these predictors to localized scales, such as specific catchments in Benin, remains underexplored.

There is a growing consensus that incorporating observational data from dense station networks and improving the spatial resolution of forecasting models are critical for advancing drought prediction capabilities. In data-poor regions like Benin, integrating

satellite-derived datasets, such as CHIRPS, with in-situ observations offers a viable pathway to address data gaps and enhance predictability.

A major advance in drought (or climate) prediction has been the discovery of teleconnections between hydroclimatic anomalies and SST phenomena (Schubert et al., 2004), for which the combined ocean-atmosphere El Niño–Southern Oscillation (ENSO) phenomenon (with periods of 2–7 years) provides the most important source of seasonal predictability. ENSO affects seasonal climate over wide areas, including North and South America, Africa, India, Indonesia, southwest Asia and Australia (Schubert et al., 2014; Smith & Ubilava, 2017).

However, the value of local knowledge is often underestimated in climate change studies. Farmers have valuable indigenous adaptation strategies, including early warning systems (Nyadzi et al., 2021b), and they recognize and respond to climatic changes (Thomas et al., 2007). For example, local communities in the Niger River Basin have responded to variations in water availability through the use of water harvesting, irrigation, planting of drought-tolerant and early-maturing crop varieties (Jellason et al., 2021). Therefore, it has been argued that local knowledge of climate variability and adaptation measures is very valuable, particularly in the absence of reliable local observations and projections (Oyerinde et al., 2015), and some studies have demonstrated high agreement between local perceptions and observations (Oyerinde et al., 2015; Tambo & Abdoulaye, 2013; Thomas et al., 2007; West et al., 2008).

It has also been shown that integrating indigenous knowledge with scientific data can enhance climate adaptation strategies and improve resilience (Nyong et al., 2007). Meze-Hausken (2004) also reported that local perceptions are often based on the ability of the communities to recall key events, making them more accurate for recent climatic events (less than 30 years). Hence, there is limited understanding of how well the indigenous knowledge of rural households aligns with empirical data (Kalanda-Joshua et al., 2011). Despite growing concerns about hydroclimatic variability and climate change, little is known about how well the local perceptions of hydroclimatic variability and climate change align with empirical data, and what factors influence potential discrepancies. Understanding these differences is crucial for developing effective adaptation strategies.

1.3. Research questions

- **Q1:** Have droughts become more frequent and/or severe in recent decades in the study basin?
- **Q2**: How to improve the predictive skills and the predictability of droughts over the basin?
- **Q3:** How does farmers' indigenous knowledge contribute to drought management and climate change adaptation?

1.4. Thesis objectives

1.4.1. Main objective

The main purpose of this study is to improve hydro-meteorological drought prediction in the Benin Part of the Niger River Basin by enhancing the understanding of hydroclimatic variability and farmers' perception for better water management and adaptation strategies.

1.4.2. Specific objectives

Specifically, this study aims:

- ❖ Characterize spatially and temporally the historical meteorological and hydrological drought in the study basin;
- ❖ Evaluate the predictive skills and the predictability of droughts;
- ❖ Propose a design framework based on farmers' indigenous knowledge for drought risk management in the study area.

1.5. Novelty

The novelty of this study lies in its integrated approach, using wavelet analysis to link climate teleconnections with local rainfall and streamflow variability for enhanced drought predictability. Combining advanced analytics with local community knowledge provides a comprehensive framework for managing climate risks in highly sensitive regions.

1.6. Scope of the thesis

This study will help to better understand the historical drought characteristics and to predict hydro-meteorological drought events in the region. As a result, this will lead to designing a framework for drought management in the region that will include necessary preparatory actions to reduce the foreseeable impacts.

1.7. Expected results and benefits

The main expected result is a comprehensive understanding of drought dynamics in the sub-region, particularly in the study area, and an assessment of multiscale climate teleconnections for improved drought prediction. This will be an input for designing climate adaptation strategies to reduce climate change impacts. The knowledge of water availability and climate extremes trends in the study area will help in sharpening more realistic water resources management for sustainability. As Benin's economy is rainfed agriculture-based, the knowledge about the current and future water resources informs resource availability.

A drought management plan should be a gateway to achieving the Sustainable Development Goals (SDGs). Indeed, in Benin, the prioritized SDGs directly or indirectly related to drought are:

1. **SDG 6** – Clean Water and Sanitation
    - ✓ Ensuring sustainable water management, which is crucial for drought prediction and adaptation strategies.
2. **SDG 13** – Climate Action
    - ✓ Addressing hydroclimatic variability, improving drought prediction, and supporting climate adaptation.
3. **SDG 2** – Zero Hunger
    - ✓ Supporting farmers in adapting to climate variability, which helps improve food security.
4. **SDG 15** – Life on Land
    - ✓ Promoting sustainable land and water management to mitigate drought impacts on ecosystems.
5. **SDG 1** – No Poverty
    - ✓ Helping farmers adapt to droughts, reducing vulnerability, and improving livelihoods.

1.8. Outline of the thesis

The thesis is divided into the following seven chapters:

Chapter 1 presents the literature review, encompassing the problem statement, research questions, primary and specific objectives, research questions, thesis novelty, scope, as well as the expected outcomes and benefits of the study.

Chapter 2 provides an in-depth description of the study area, covering its location, topography, vegetation, climate, hydrology, soil characteristics, land use, and demographics.

Chapter 3 outlines the data, materials, and methods employed in the study.

Chapters 4, 5, and 6 detail the results corresponding to each specific objective.

Chapter 7 provides the general conclusion and future perspectives.

CHAPTER 2: DESCRIPTION OF THE STUDY AREA

This chapter presents the study area. Its geographic localization, relief, and vegetation cover are respectively described. In addition, climate, hydrography, soil and land use as well as demography of the study area are respectively presented in this chapter.

2.1. Localization

The Niger is the third longest river in Africa, with a stream length of 4,200 km, a drainage basin of 2,170,500 km^2, and an average discharge of about 6,000 m^3 /s (Mascaro et al., 2015). Nine countries share the Niger River Basin: Benin, Burkina Faso, Cameroon, Guinea, Ivory Coast, Mali, Nigeria, Chad, and Niger (Figure 3**:** Study area Beninese Part of the Niger River Basin (BPNRB).). At its northernmost point, the river enters the Sahara Desert in Mali before turning southwest and flowing about 1,500 km through Niger, Benin and Nigeria. The Beninese Part of the Niger River Basin is located in the north of Benin. Located between 1°32' and 3°50' East and 10° and 12°30' North, it covers an area of about 48,000 km², i.e., 42% of the total area of Benin (Halissou et al., 2021). It is shared by 17 municipalities and includes the three catchments Sota (B1; 13,449 km^2), Alibori (B2; 13,684 km^2), and Mekrou (B3; 10,552 km^2) (Figure 3**:** Study area Beninese Part of the Niger River Basin (BPNRB).). The study area is the largest zone for cotton and vegetable production in Benin, as well as cattle breeding. It is also home to the W-Park, which is one of the most important wildlife parks in West Africa.

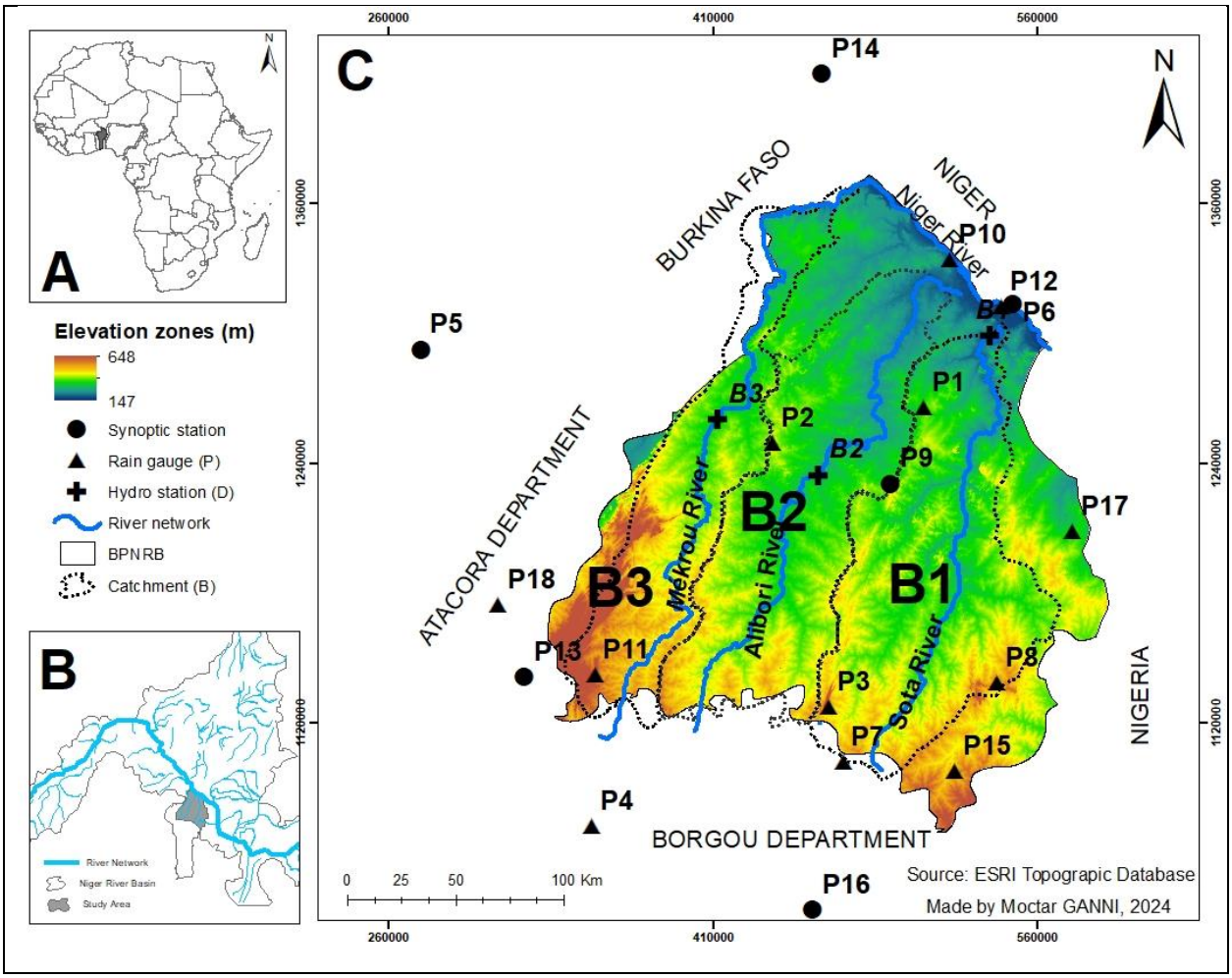

Figure 3: Study area Beninese Part of the Niger River Basin (BPNRB). (A) Location of Benin in West Africa. (B) Niger River Basin including the study area. (C) Study area BPNRB: topography, location of climate and discharge stations, and the three catchments (Sota River, B1; Alibori River, B2; Mekrou River, B3).

2.2. Relief

The Beninese part of the Niger River Basin, separated from the Ouémé and Mono basins by an east-west watershed at latitude 10° north, consists of two main topographic units: the crystalline peneplain and the Kandi sandstone plateau (Adam & Boko, 1993; Le Barbé L. et al., 1993). The southern granite-gneissic peneplain, with crystalline rocks and gently sloping hillsides, descends gradually from an altitude of 400 m near the watershed to meet the Kandi plateau. This area is interspersed with isolated hills (Bembéréké, Sinendé, Nikki, and Kalalé) and connects with the Atacora massif to the west and the Kandi plateau

to the north, creating a diverse topography across the B1, B2, and B3 sub-basins (Le Barbé et al., 1993).

The Kandi plateau, forming the basin's northern part, is notably flat, averaging 250 m in altitude, and dotted with small ferruginous buttes with low gradients. Slightly inclined toward the Niger River's alluvial plain, these formations, influence atmospheric flows, intensify diurnal heating, and encourage thunderstorms in the region (Adam & Boko, 1993). Both the peneplain and plateau are carved by valleys, through which the B1, B2, and B3 rivers flow northward along geological formations aligned NNE-SSW (Vissin, 2007). The Niger River, which forms a 135 km border between Benin and Niger, runs in a straight NW-SE course in this region and receives the B1, B2, and B3 tributaries on its right bank (Vissin, 2007).

2.3. Vegetation

Vegetation in the study basin thins progressively from south to north due to decreasing rainfall (Vissin, 2007). In the southern region, a wooded savannah—comprising trees up to 10 m, shrubs, and grasses (Le Barbé et al., 1993)—slows runoff. The plateau's lateritic soils support small dry forests of Isoberlinia doka, while wooded savannah with Hymenocardia acida, Entada abyssinica, and Cochlospermum spp. dominates slopes. Toward the north, forests contain Diospiros mespiliformis, Ficus spp., and Khaya senegalensis, with tree and shrub savannas of Adansonia digitata and Combretum spp. on lithosols (**Figure *4***).

The 2006 vegetation map shows savannah as the primary vegetation (54.3%), followed by farms and fallow lands (24.5%), with a 9% increase in agricultural land from 1995 due to rising demand for cotton fields (Badou, 2016). Protected areas include the W Park, covering lower Mékrou and Alibori basins, and classified forests (Goungoun, Sota, Trois Rivières), which span 30% of the Sota sub-basin. The Trois Rivières forest, covering 2,400 km², is the largest and most densely vegetated. However, these forests face human pressure and are vulnerable to climatic changes.

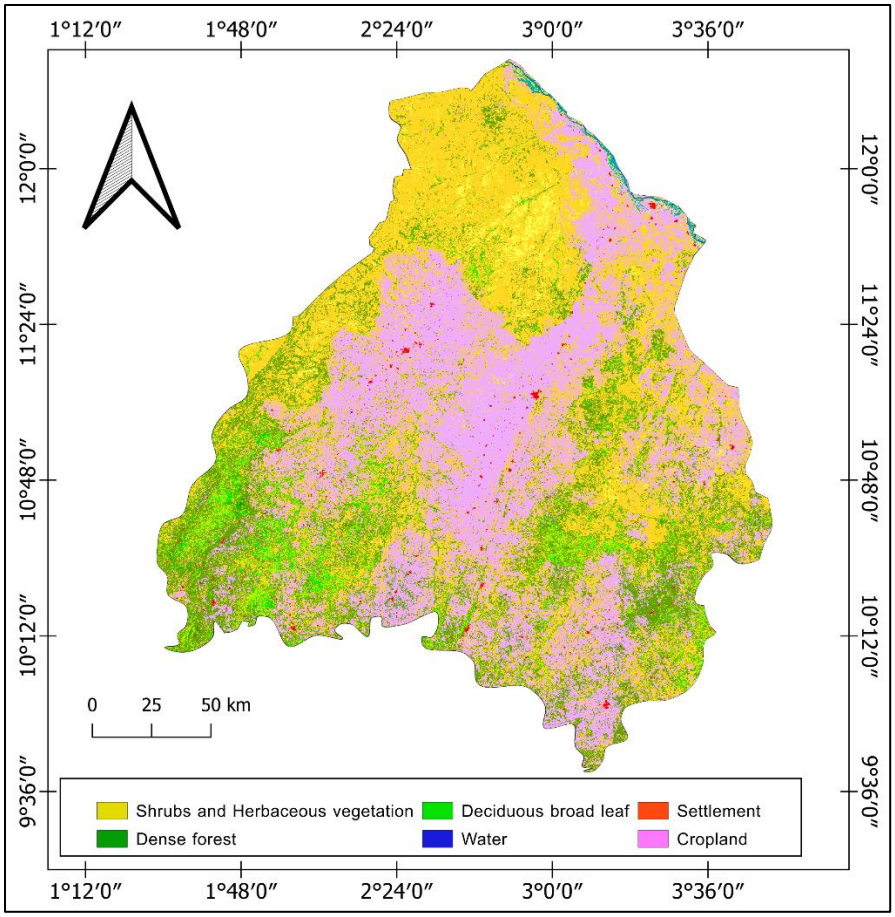

Figure 4: Land use map of the year 2024

2.4. Climate

The climate description is organized into six subsections: rainfall, temperature, Humidity, Potential Evapotranspiration, wind speedy and insolation.

2.4.1. Rainfall

The study area BPRNB has two contrasting seasons with a typical Sudano-Sahelian seasonal rainfall cycle (Fig. 5a–c). Approximately 97% of the annual rainfall occurs during the rainy season from April to October. August has the highest rainfall amounts with a median monthly rainfall of about 250 mm in the three catchments. The interannual variability of monthly rainfall is comparatively high. For example, the interquartile range of August rainfall over the period 1970–2020 is 200-260 mm, 215-275 mm, and 210-270 mm in catchments B1, B2, and B3, respectively. During the rainy season, the sky is typically characterized by intermittent cloud cover, often accompanied by brief

thunderstorms, partially influenced by the Inter-Tropical Convergence Zone (ITCZ) and the monsoon system (Vissin, 2007). Throughout the dry season from November to March, the study area experiences the prevailing dry north-easterly Harmattan wind, resulting in sparse rainfall.

Overall, the stations in the Benin basin of the River Niger have rainfall values that vary between 780 and 1200 mm over the sub-period 1970-2020. This rainfall value decreases with increasing latitude (Figure 5). The basin is characterized by three climatic zones: the first, located in the south between isohyets 1240 and 1050 mm, corresponds to the humid Sudanian type of climate (the stations in the extreme south of the basin are grouped in this zone); the second zone, located in the north of the basin, extends between isohyets 1050 and 950 mm and corresponds to the dry Sudanian type of climate; finally, the third class is located in the extreme north from isohyets 850 mm and above and corresponds to the Sudano-Sahelian type climate.

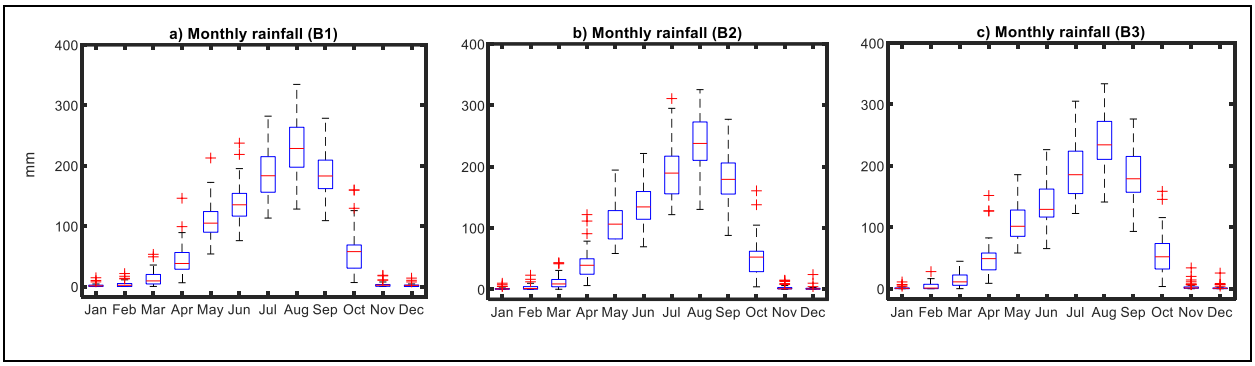

Figure 5: Catchment rainfall for B1–B3 for the period 1970–2020. **(a–c)** Monthly rainfall: Interannual variability represented by the median (red line), the interquartile range IQR (box), the range of the data (whiskers), and outliers (red cross).

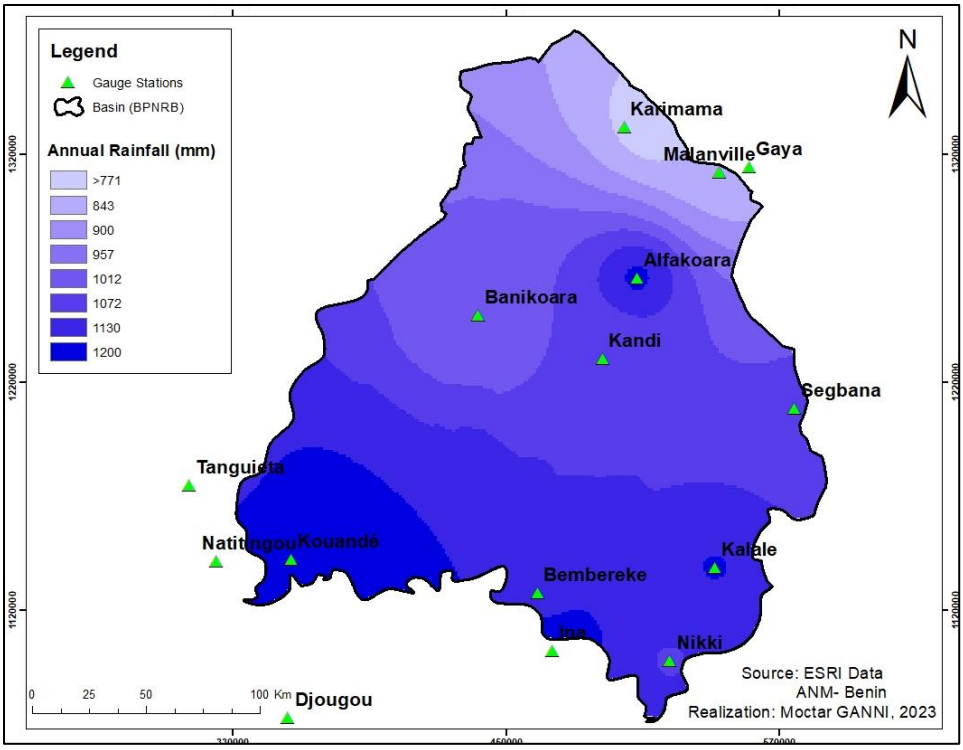

Figure 6 : Spatialization of rainfall over the BPNRB (1970- 2020)

2.4.2. Temperature

In the Benin Part of the Niger River Basin, the average monthly maximum temperature from 1970 to 2021 is 33.8°C, occasionally rising to around 40°C. The basin's average temperature is 27.63°C, with regional averages of 27.34°C in Natitingou and 28.25°C in Kandi. Across the basin, minimum temperatures vary from 16°C to 26°C (Figure 7).

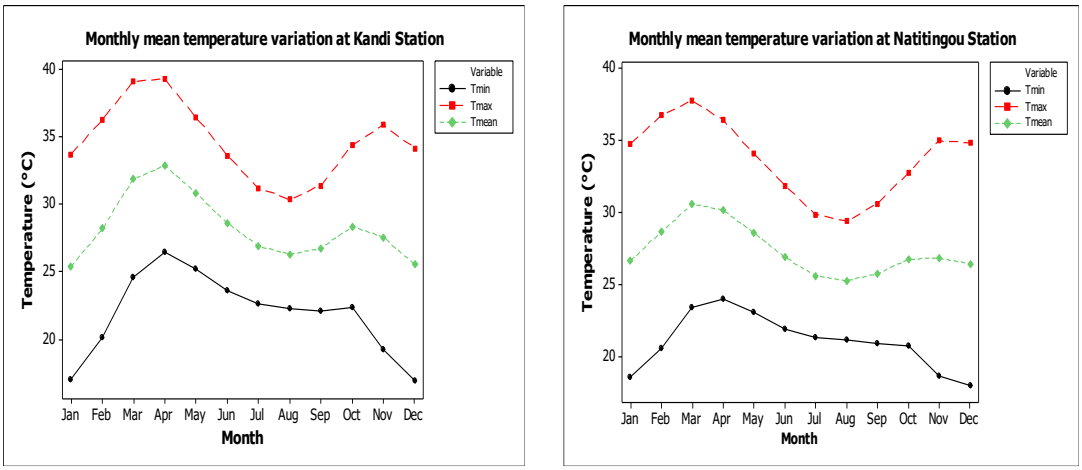

Figure 7: Monthly temperature variation (Average, Maximum and minimum) respectively at Kandi, and Natitingou synoptic stations from 1970 to 2020.

2.4.3. Relative humidity

On average, mean relative humidity in the basin ranges from 32.25% to 82%, with the lowest values occurring in January and February and the highest in August and September. At the station level, minimum mean relative humidity values are recorded as 26.8% at Kandi, 33.64% at Natitingou, and 33.5% at Parakou. Maximum values are 81.51%, 83.1%, and 81.6% at Kandi, Natitingou, and Parakou, respectively (Figure 8).

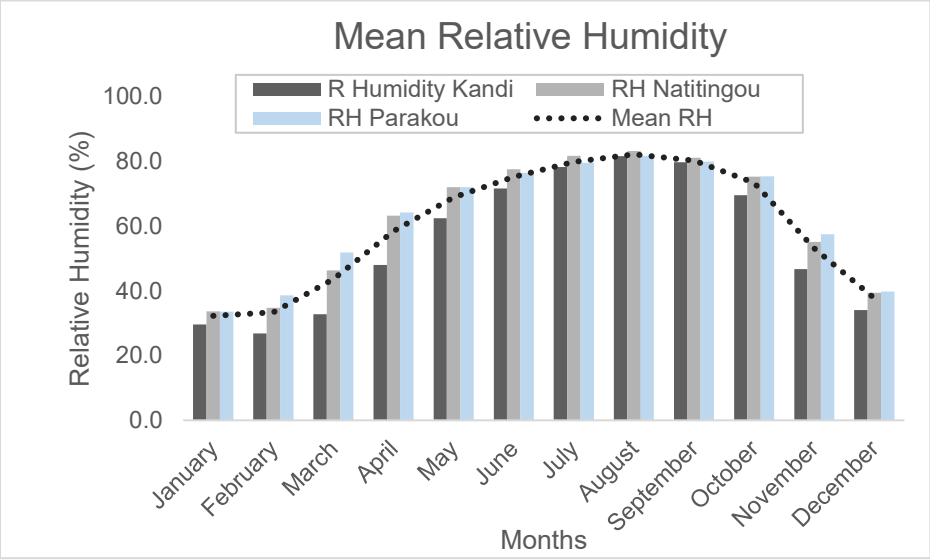

Figure 8 : Monthly average daily relative humidity variation from 1970-2021.

2.4.4. Potential Evapotranspiration (PET)

The Penman PET estimation used in this work incorporates various climatic parameters: radiation, temperature, humidity, and wind. Analysis of the daily PET series from 1985 to 2020 shows a range of 1.6 to 10 mm. Figure 9 illustrates that daily PET is lowest in July, August, and September (between 2 and 4 mm), coinciding with the rainy season when evaporative demand is reduced, leading to lower water loss by both surface evaporation and plant transpiration. The minimum PET occurs in early August, aligning with peak rainfall. Conversely, from October to May, decadal PET ranges from 4.13 to 6 mm across stations, reflecting heightened atmospheric evaporative demand during the dry season, which, along with a lack of rainfall, accelerates the drying of watercourses (Vissin, 2007).

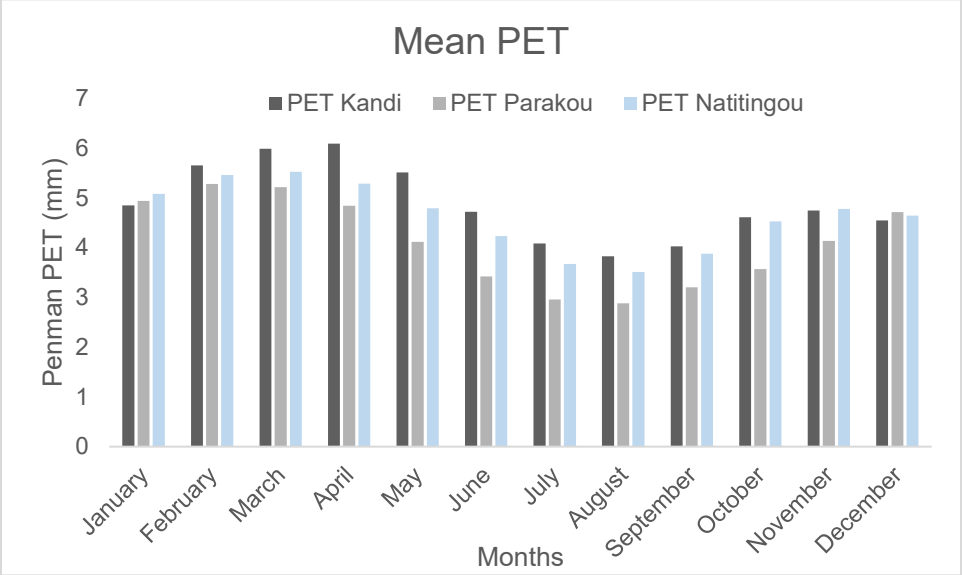

Figure 9: Monthly average of daily Penman Monteith PET from 1985-2020.

2.4.5. Wind Speed

The daily wind speed varies between 1.41 and 2.24 m/s from 1970 to 2021 (Figure 10). The maximum monthly average wind speed is observed in April while the minimum is reached in September in the basin. On the other hand, throughout the stations, the maximum monthly averages are 2.30, 2.29 and 2.42 m/s respectively at Kandi, Natitingou and Parakou stations. On the other hand, 1.25, 1.20 and 1.57 m/s, as respectively the minimum monthly values at Kandi, Natitingou and Parakou stations (Figure 10).

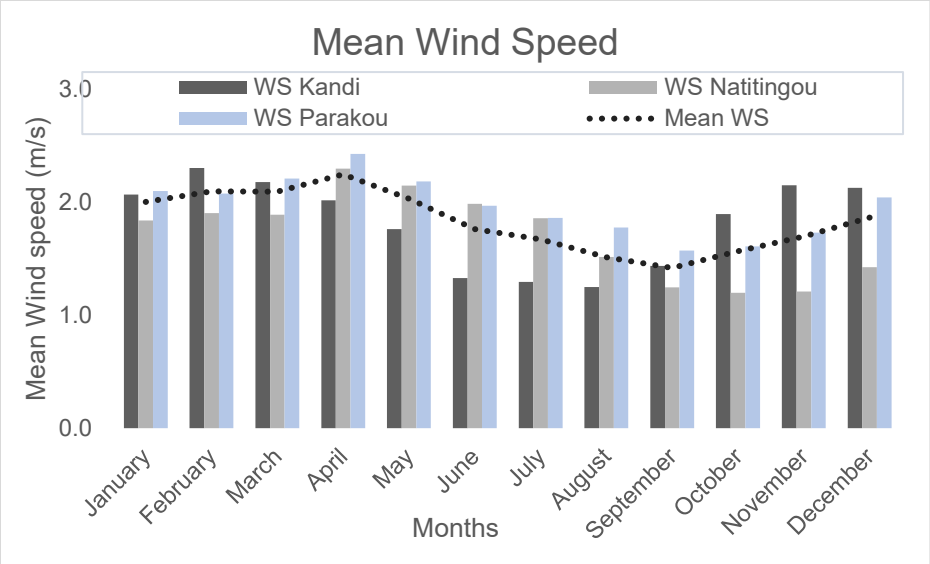

Figure 10 : Monthly average daily wind speed variation at 10m altitude from 1970-2020.

2.4.6. Average insolation

Figure 11 shows that at the basin scale, the insolation has an irregular rhythm over a year. The lowest values of insolation are recorded in August (4.95 h/day) and September (5.41 h/day) at the heart of the rainy season. The highest values are observed from October to February, with a maximum in November (8.80 h/day), which corresponds to the dry season. Those values vary from one synoptic station to another. The maximum values are 9.40, 9.35, and 8.38 h/day respectively at Kandi, Natitingou, and Parakou stations, while 5.61, 4.78, and 3.86 h/day as the lowest values at Kandi, Natitingou and Parakou stations (Figure 11).

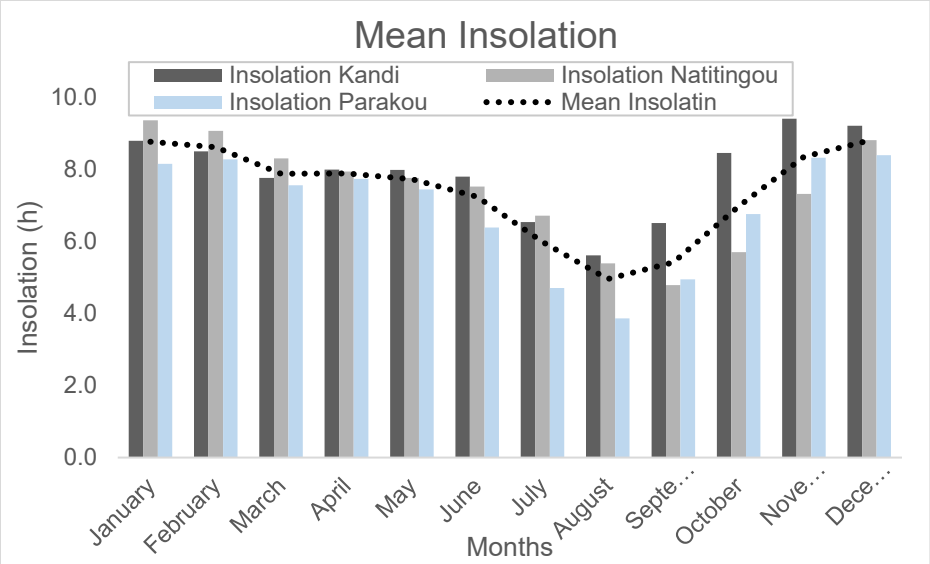

Figure 11: Monthly average daily insolation variation from 1970-2021.

2.5. Hydrology

In terms of hydrology, the two distinct seasons are evident in the monthly streamflow. All three rivers reach their maximum flow in September. The high flow lasts for three months (August–October), which together account for 80–90% of the annual runoff. This fraction increases to 97% for B2 and B3 if we add the flow in July and November. Catchment B1 has a slightly more regular regime, characterized by a perennial flow, while the rivers of B2 and B3 run dry in February–May. In the three catchments, streamflow recession starts abruptly in October and reaches critical levels in January. The interannual variability is high. For example, the interquartile range of September streamflow is 75–140, 65–138, and 60–115 m3/s in catchments B1, B2, and B3, respectively (Figure 12).

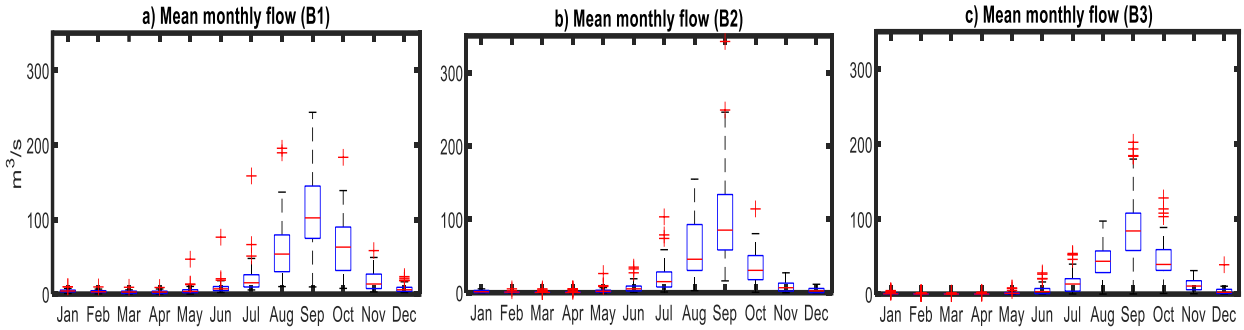

Figure 12: Monthly streamflow for B1–B3 for the period 1970–2020: Interannual variability represented by the median (red line), the interquartile range IQR (box), the range of the data (whiskers) and outliers (red cross).

2.6. Soil and Geology

The basin spans two main geological formations: basement formations in the west and south, and Kandi sandstone in the northeast (Adam & Boko, 1993; Le Barbé L. et al., 1993). The Mekrou basin mainly consists of primary terrains gneiss, orthogneiss, micaschist, and quartzite from the Atacora range with primary schists appearing in its lower basin (Vissin, 2007). The Alibori sub-basin comprises gneissic terrains, with granites and migmatites emerging near north-south fractures. Both sub-basins feature crystalline magmatic and metamorphic rocks, making them impermeable (Vissin, 2007). In the Sota sub-basin, the southern region around Gbassè is predominantly Precambrian granite-gneiss with gneiss, migmatites, micaschists, diorites, and quartzites, gradually descending toward the Kandi sandstone, which covers 20% of the area (Le Barbé L. et al., 1993; Vissin, 2007). The lower and middle Sota basins, north of Gbassè, include diorite, gneiss, and migmatite conglomerates overlain by sandstones, covering over 93% of the Sota to Couberi sub-basin (Figure 13). These consist of fine to coarse arkosic sandstones, siltstones, terminal continental conglomerates, and breccias (Vissin, 2007).

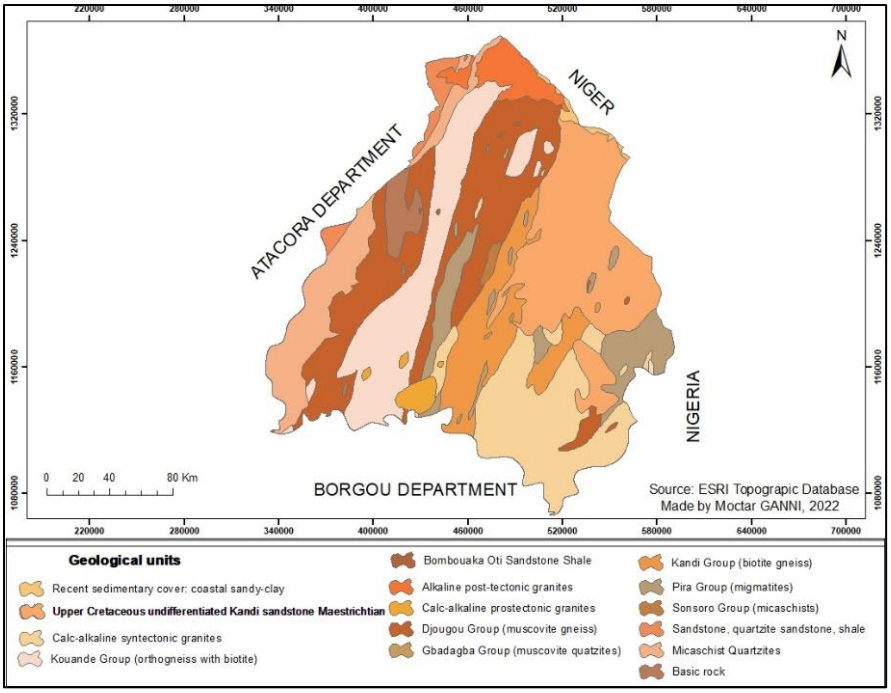

Figure 13: Geological units of the Benin basin of the Niger River

2.7. Demography

The basin supports a population of approximately 1,997,743 inhabitants, representing about 19.96% of Benin's total population, according to the 2013 General Population and Housing Census (RGPH 4) (INSAE, 2016). This marks an increase from 1,451,646 inhabitants in 2002 (INSAE, 2004), reflecting a growth of 546,097 people (about 37.62%) over 11 years. The communes within the Beninese Niger River basin have low population density but high growth rates, driven largely by significant immigration of agricultural households seeking arable land and rural-to-urban migration.

2.8. Socio-cultural groups

Attracted by the natural resources of the basin, the populations that occupy the territory of the Beninese basin of the Niger River are of several ethnic groups. They are the Baatombu (49%), the Fulbe and Gando (33%), the Boko, the Dendi (10%), the Gulmancé (2.5%), the Mokolé (2.2%), the Yowa (0.4%), and the Tchenga (0.9%). These various groups are thought to have come at different times from multiple African empires in the Middle Ages (Adam & Boko, 1993). All of these peoples, grouped in rural communities, are predominantly Muslim (72.6% Muslims compared to less than 9% Catholics) and have

developed different agrarian civilizations concerning the evolution of the agricultural history of the basin and the national economic context (Vissin, 2007).

2.9. Economic activities

Agriculture forms the economic backbone of the basin, though it remains largely traditional and rain-fed (Vissin, 2007). Local populations grow both food crops (yams, cassava, maize, millet) and cash crops (cotton, groundnuts). Livestock breeding, especially in northern Benin, is also significant but meets only around 6% of the population's annual protein needs. Key communes like Banikoara, Kandi, Kalalé, Nikki, and Bembéréké are major centers for cattle, goat, and sheep breeding; Banikoara, Kandi, and Kalalé alone represent 26% of Benin's cattle population, while Alibori and Borgou account for 69% of the nation's total (Adjinacou & Onibon, 2004). Other activities, though less prominent, include fishing in the Niger River and its tributaries, trade, and tourism.

2.10. Access to water for the populations

Water is crucial for sustaining life and is a primary natural resource supporting population settlement. In the Beninese Niger River basin, where most tributaries are temporary except for the Sota, groundwater serves as the main consistent drinking water source. To improve water access, the General Directorate of Water (DG-Eau) has initiated significant drilling and supply projects, establishing wells and standpipes across the basin. Additional sources include dams, overburden, modern large-diameter wells, and developed springs, which though now considered less safe still play an essential role in addressing local water needs.

Conclusion

This chapter outlines the study area's two primary topographic units: the crystalline peneplain and the Kandi sandstone plateau, composed of sandstone and bedrock. The Beninese basin of the Niger River experiences a unimodal rainfall pattern that diminishes from south to north, correlating with progressively sparser vegetation and rising temperatures in that direction. The basin's rapidly growing population, engaged in various economic activities, has diverse and substantial water needs.

CHAPTER 3: DATA, MATERIALS, AND METHODS

This chapter provides data, materials, and methods used for this research.
All data used are presented in section 3.2, from the first specific objective data in section 3.2.1 to the data for the third specific objective in section 3.2.3.
While all the materials used are presented in section 3.3, the last part of this chapter concerns the methods used to get the results that are contained in section 3.4.

3.1. Data

3.1.1. Data for the investigation of historical meteorological and hydrological drought characteristics spatially and temporally

Daily rainfall data from 21 climate stations for the period 1970–2020 were acquired from the Benin Meteorological Agency and neighbouring countries, i.e., the National Meteorological Service of Niger and the Burkina Faso Meteorological Agency. After quality control (see section 3.1 below), 18 stations were used for the analysis (Figure 3 and Table 12). Daily discharge data from four hydrometric stations (Gbassè, Couberi, Yankin, and Kompongou) for the four catchments were obtained over the same period from the Hydrological Service of Benin (DG-Eau) (see table 1).

Monthly values of three climate teleconnections were considered. Nino 3.4, DMI, and AMO were obtained from the NOAA Climate Prediction Center (CPC) website. For the preparation of the predictors, we calculated the sea surface temperature (SST) anomalies by subtracting the mean and then dividing by the standard deviation.

Data quality control and preprocessing

The 21 rainfall and three streamflow time series were quality-controlled prior to data analysis. Rainfall stations with more than 5% missing data in the rainy season were excluded. Gaps in the rainfall time series of the remaining 18 stations were filled using the ordinary kriging method following previous studies in the same area (Alamou et al., 2022; Badou et al., 2017). We applied the double-cumulation method to these 18-time series (Kohler, 1949). This method allows the detection of systematic errors in a time series; however, no systematic error was detected.

After these quality checks, we applied ordinary kriging to obtain a time series of catchment rainfall for the three catchments.

Regarding the daily discharge data obtained from the hydrological service, none of the four hydrometric stations has less than 20% of missing data. A good performance of the ModHyPMA model at each sub-basin allowed us to fill in the missing values in the discharges.

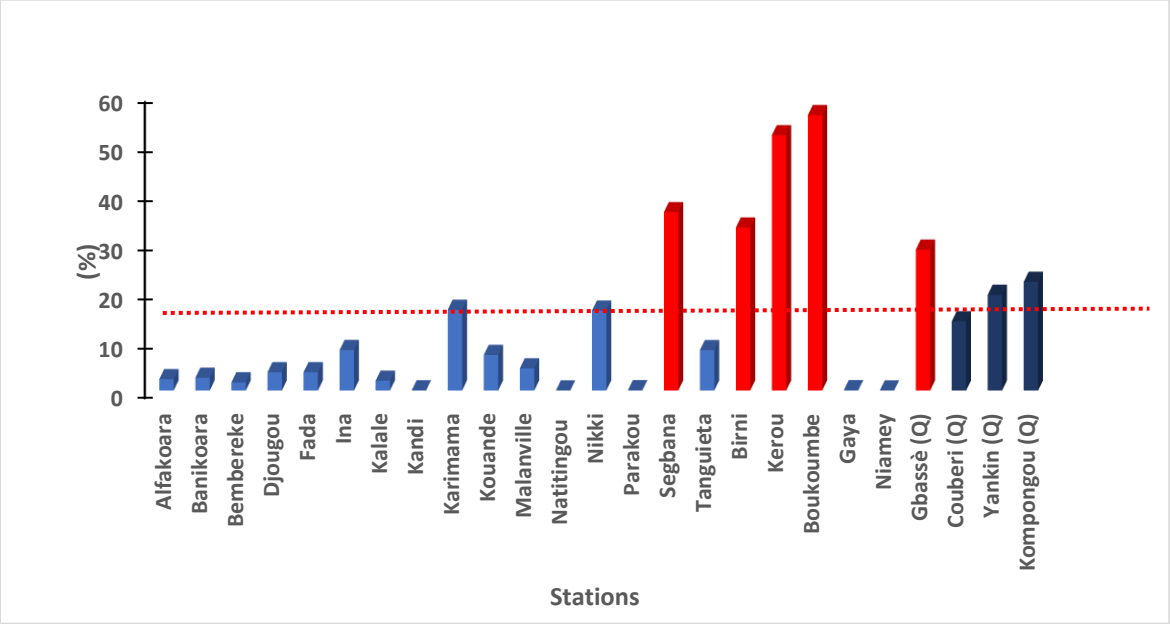

Figure 14: Percentage of missing data on the daily rainfall and streamflow throughout 1970-2020

For all three streamflow stations, substantial gaps occurred during the period 1993–2004 due to delays between the breakdown of the gauging instruments and their repair or replacement (Badou et al., 2017). The hydrological model ModHyPMA (Hydrological Model based on the Least Action Principle) was used to simulate river flows and to fill the missing data for the three catchments. ModHyPMA is widely used in West Africa (Afouda, et al 2004; Alamou, 2011; Gaba, 2015; Obada, 2016; Halissou, et al., 2021). It produced good results for the Mekrou River (catchment B3) (Gaba, 2015; Obada, 2016), the Beninese Part of the Niger River Basin (Halissou et al., 2021) and the Ouémé River in Benin (Houngue et al., 2020).

3.1.2. Data for the assessment of the predictive skills and the predictability of drought

CHIRPS satellite data

CHIRPS (Climate Hazards Group InfraRed Precipitation with Station data) satellite data provides high-resolution gridded precipitation estimates, which are crucial in data-scarce regions like West Africa. CHIRPS combines infrared satellite imagery with in-situ rainfall station data (Funk et al., 2015). It provides daily data with a spatial resolution of 0.05° (~5.3 km) from 1981 to the present. CHIRPS is widely used for drought monitoring, agricultural planning, and climate studies in data-scarce regions such as West Africa. Daily CHIRPS satellite rainfall from 1981 to 2020 was downloaded and used.

Comparison between Catchments and CHIRPS Rainfall Data

The quality of the catchment rainfall data from 1981 to 2020 was assessed by comparing it with CHIRPS satellite rainfall data for three catchments within the Niger River Basin. Figure 3 illustrates the daily variability between the satellite product and observed catchment rainfall. To evaluate the accuracy of the catchment rainfall data, statistical metrics such as the Nash-Sutcliffe Efficiency (NSE) (Nash & Sutcliffe, 1970) and the correlation coefficient (R) were applied (see Table 4).

$$NSE = 1 - \frac{\langle (Pr_1 - Pr_2)^2 \rangle}{\langle (Pr_1 - \langle Pr_2 \rangle)^2 \rangle} \quad (1)$$

$$R = \frac{\sum_{i=1}^{n} (P_{r1i} - \overline{P_{r1}})\,(P_{r2i} - \overline{P_{r2}})}{\sqrt{\sum_{i=1}^{n} (P_{r1i} - \overline{P_{r1}})^2} - \sqrt{\sum_{i=1}^{n} (P_{r2i} - \overline{P_{r2}})^2}} \quad (2)$$

Pr1 is the observed rainfall from the catchment, Pr2 represents satellite rainfall; $\overline{P_{r1}}$ and $\overline{P_{r2}}$ represent their average, respectively. An NSE value of 1 indicates perfect agreement between the satellite data and observations. In contrast, an NSE value of 0 suggests that the satellite product's mean square error is equivalent to using the mean observed value as the sole predictor.

Climate indices

The oceanic indices from three distinct ocean basins are based on previous studies since they have a significant association with the Western African monsoon. These include Pacific Decadal Oscillation (PDO), Nino 3.4, Nino 1.2, and Trans-Nino Index (TNI), representing the Pacific Ocean (Bader & Latif, 2011; Fontaine & Bigot, 1993; Fontaine & Janicot, 1996; Giannini et al., 2003; Losada et al., 2012; Pomposi et al., 2016); Atlantic Multi-decadal Oscillation (AMO), North Atlantic Tropical (NAT), South Atlantic Tropical (SAT), and Tropical Atlantic SST index (TASI) representing the Atlantic Ocean (Worou et al., 2020); and South Western Indian Ocean (SWIO), Western Tropical Indian Ocean (WTIO), South Eastern Tropical Indian Ocean (SETIO), and Dipole Mode Index (DMI) representing the Indian Ocean (Fontaine & Bigot, 1993; Giannini et al., 2003; Nicholson & Selato, 2000; Pomposi et al., 2016).

The monthly time series of these indices were obtained from the Extended Reconstructed Sea Surface Temperature version 5 dataset and the NOAA Climate Prediction Center (CPC) Website (https://www.ncei.noaa.gov/products/extended-reconstructed-sst)(Huang et al., 2017).

Table 1: Data sources, spatial resolution, and temporal coverage used

Dataset	**Source**	**Data Description/Properties**	**Study period**
Observed climate	National Meteorological Agency from Benin, Niger and Burkina Faso	Daily rainfall data from 18 climate stations and max and min temperature from the Synoptic stations	1970–2020
Hydrometric data	The Hydrology Department at General Directory of Water (DGEau, Benin)	Daily discharge data from three hydrometric stations (Couberi, Yankin, and Kompongou)	
Climate teleconnection indices	The Extended Reconstructed Sea Surface Temperature version 5 dataset and the NOAA Climate Prediction Center (CPC) Website (https://www.ncei.noaa.gov/products/extended-reconstructed-sst)(Huang et al., 2017).	Monthly values of 12 climate teleconnections: **PDO, Nino 3.4, Nino 1.2, TNI** representing the Pacific Ocean; **AMO, NAT, SAT, and TASI** representing the Atlantic Ocean; and **SWIO,**	

		WTIO, SETIO, and **DMI** representing the Indian Ocean	
CHIRPS	CHIRPS combines infrared satellite imagery with in-situ rainfall station data (Funk et al., 2015)	Daily data with a spatial resolution of 0.05° (~5.3 km) from 1981 to the present	1981–2020

3.1.3. Data for the Proposed design framework for drought risk management in the study area

Survey data

The data collection was limited to eight municipalities (L1 to L8 in Fig. 3) due to terrorism in the border areas of Burkina Faso and Niger. Isolated or sparsely populated areas were also excluded, as it was strongly discouraged due to the potential activities of armed groups and the associated risk of kidnapping.

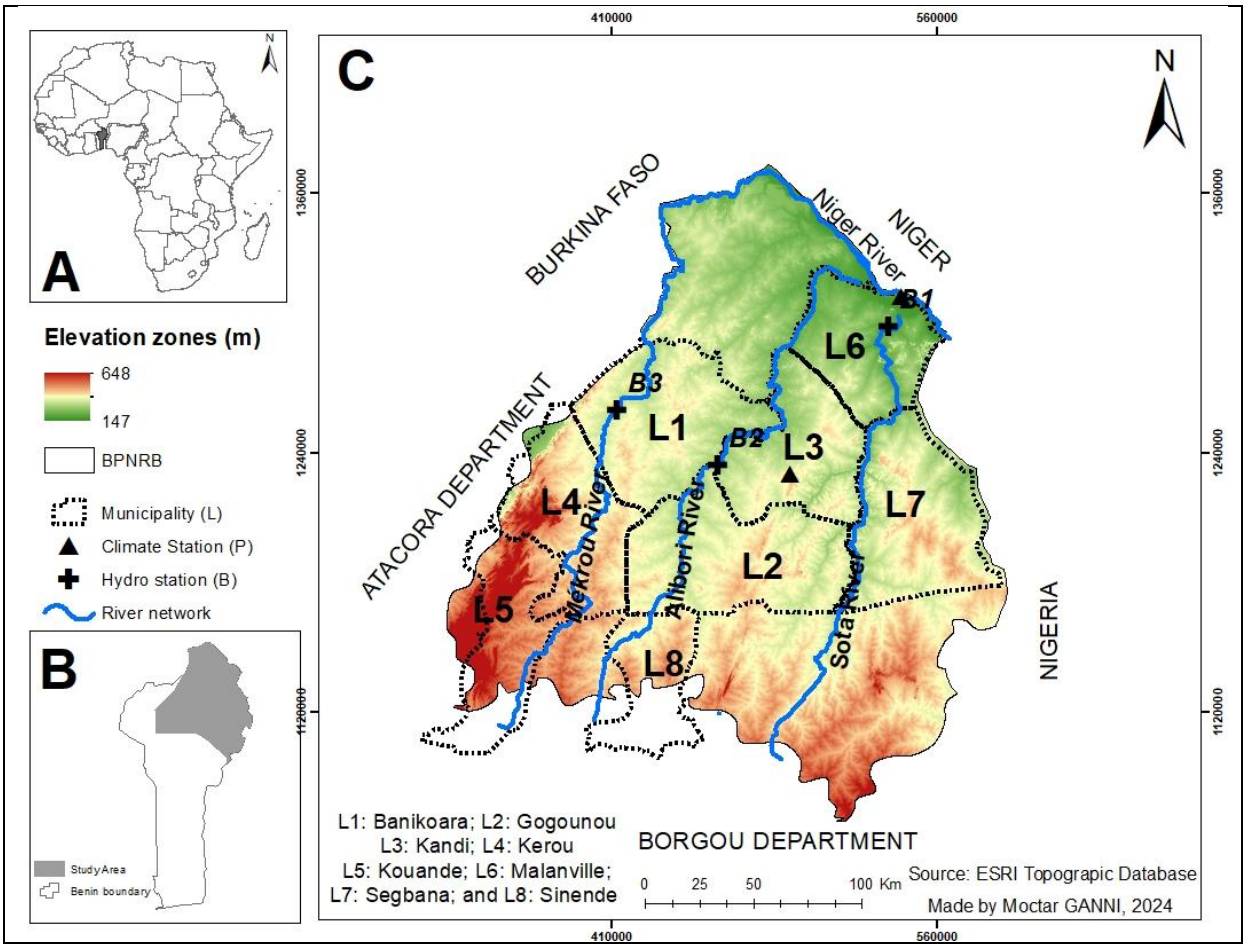

Figure 15: Case study area Beninese Part of the Niger River Basin (BPNRB). (A) Location of Benin in West Africa. (B) Benin including the study area. (C) Study area BPNRB: topography, location of climate and discharge stations, and the eight targeted municipalities

We collected historical records of rainfall, streamflow, and temperature to assess the correctness of farmers' perceptions of climate change and variability with actual climate data in the study area. For Kandi, daily rainfall and temperature data were available from 1970 to 2020. In Malanville, daily rainfall data for the same period were considered. Additionally, daily streamflow data from three hydrometric stations Couberi (B1), Yankin (B2), and Kompongou (B3), were obtained for the three catchments from the Hydrological Service in Benin.

3.2. Materials

3.2.1. Materials for the investigation of historical meteorological and hydrological drought characteristics

QGIS/Arc-GIS

ArcGIS 10.8 was used to clip the study area portion of DEM data, downloaded from USGS, with the study area shapefile (the Beninese Part of the Niger River Basin). and to design thematic maps.

Rstudio

RStudio was used to prepare and analyze datasets effectively for various data processing tasks, including data cleaning, transformation, statistical analysis, and visualization.

Microsoft Office

Microsoft Office applications, including Excel, Word, and PowerPoint, were used for data organization, report writing, and presentation preparation to support data analysis and communicate findings effectively.

3.2.2. Materials for the assessment of the predictive skills and the predictability of drought

Climate Data Operator (CDO)

Climate Data Operator version 2.5.0, used in the Ubuntu environment, was employed to extract gridded SST and CHIRPS data and prepare data before correlation analysis between the predictand and predictors. Various operations were applied, including fldmean for field averaging, splitmon for monthly data separation, and ymean for yearly averaging, among others.

MATLAB

MATLAB R2018a version 9.4.0 was used for advanced data analysis, mathematical modeling, and visualization, facilitating complex computations, algorithm development, and graphical representation of results.

3.2.3. Materials for the Proposed design framework for drought risk management in the study area

KoboToolbox version 2.023.21 is a powerful tool for designing, deploying, and managing data collection forms, particularly suited for use in challenging field conditions. In this study, the data were collected using surveys, coded, and deployed on kobotoolbox.

XLSForm

KoboToolbox relies on XLSForm, a standard form format in Excel, to structure survey forms with complex logic, question types, and data validation. It was used in this study to design the survey questionnaire.

Smartphone

A smartphone was used to run KoboToolbox in the field for data collection, enabling efficient entry of survey responses and capturing additional data points, such as images and GPS coordinates.

3.3. Methods

3.3.1. Methods for the investigation of historical meteorological and hydrological drought characteristics

3.3.1.1. Drought indices used

Four indicators were used to determine droughts: the Standardized Precipitation Index (SPI), the Standardized Precipitation Evapotranspiration Index (SPEI), the Streamflow Drought Index (SDI), and the Consecutive Dry Days Index (CDD). In addition, we calculated the drought duration and intensity to understand the space-time variation of droughts across the study area. These drought indices used in the present study are all recommended in the World Meteorological Organisation (WMO) guidelines for drought assessment. They are particularly relevant here because they have scarcely been applied in the study area, allowing this work to fill an important gap and to compare results with previous findings. The CDD index, used to characterise dry spells, was also calculated for the rainy season in this study, whereas earlier studies typically considered the entire year. This seasonal focus provides a more targeted understanding of dry-spell behaviour during the period most critical for agriculture

The **Standardized Precipitation Index (SPI)** is one of the most frequently used indicators of meteorological drought and was developed based on the normalization of precipitation probabilities (Mckee et al., 1993). This indicator defines a precipitation deficit and allows the monitoring of droughts in different time frames. The SPI is recommended by the World Meteorological Organization (WMO) for determining the phenomenon of drought (WMO & GWP, 2016). For more information on the formulation of SPI, its

advantages and limitations, readers can refer to (Fang et al., 2020; Guttman2, 1999; Lloyd-Hughes & Saunders, 2002).

The SPI was calculated based on daily precipitation for the meteorological stations in the BPNRB. The daily precipitation data were aggregated into 3-, 6-, and 12-month timescales, and a two-parameter gamma distribution function was fitted to these aggregated data. Depending on the drought impact in question, SPI values for 3 months or less might be useful for basic drought monitoring, values for 6 months or less for monitoring agricultural impacts, and values for 12 months or longer for hydrological impacts (WMO & GWP, 2016). In this study, we considered meteorological and hydrological droughts, thus aggregating precipitation data to timescales of 3-, 6- and 12-months. SPI values define the deviation from the mean expressed in units of standard deviation:

$$SPI = \frac{f(x)-u}{\sigma} \quad (3)$$

where f(x) is the transformed sum of precipitation,

u is the mean value of the normalized variable x,

and σ is the standard deviation of variable x

Based on the value of SPI, a period is classified as normal or dry, from moderately dry to extremely dry (Table 2).

The **Standardized Precipitation Evapotranspiration Index (SPEI),** which also includes the evapotranspiration besides precipitation, was calculated for the same timescales (3-, 6-, and 12-month). Different methods are used to calculate PET (potential evapotranspiration), like the Penman-Monteith, Hargreaves, or Thornthwaite's equations. The Penman-Monteith method requires observations of climate variables, which are not available at most meteorological stations in many countries (Krishnan et al., 2019). Hence, we calculated the SPEI by applying the Hargreaves method, which uses only radiation and minimum and maximum temperatures at a particular location. Daily PET was estimated based on Hargreaves' equation as:

$$PET = 0.0023\ Ra(\frac{T_{max}+T_{min}}{2} + 17.8)(T_{max} - T_{min})^{0.5} \quad (4)$$

where Ra is the extra-terrestrial radiation and Tmax and Tmin are the maximum and minimum temperature values, respectively. 0.0023 is the original empirical coefficient proposed by Hargreaves and Samani (Hargreaves & Samani A. Z., 1985). SPEI is based on the normalization of a simple water balance equation stated as follows:

$$D_i = P_i - PET_i \quad (5)$$

D_i indicates whether there is a water surplus or deficit. The Di values were aggregated to 3, 6, and 12 months as in the case of SPI. As recommended by Krishnan et al., (2019), a three-parameter log-logistic distribution was used to fit a distribution to the SPEI values. Drought classification based on SPEI values uses the same scheme as for SPI (Table 2). PET and SPEI were calculated using the R software package SPEI (Vicente-Serrano et al., 2010).

The **Streamflow Drought Index (SDI),** developed by (Nalbantis & Tsakiris, 2008), is calculated in the same way as SPI by using discharge instead of precipitation (Lorenzo-Lacruz et al., 2013). Classification of dry periods is the same as for SPI and SPEI (values smaller than -1.0), while wet periods are identified for values larger than 1.0.

Table 2: Drought classification using SPI, SPEI, and SDI values *(*Mckee et al., 1993; Nalbantis & Tsakiris, 2008*)*.

SPI and SDI Values	Category
-0.99 to 0.99	Near normal
-1.49 to -1.0	Moderately dry
-1.99 to -1.5	Severely dry
-2.0 or less	Extremely dry

The **Consecutive Dry Days index (CDD),** i.e., the maximum period of consecutive dry days (with rainfall ≤ 1mm), is another useful drought indicator (Frich et al., 2002). In contrast to the other indicators that represent water fluxes, CDD quantifies the variations of dry spells in a given region. To account for the distinct seasonality of rainfall, we calculated the CDD for the rainy season (April to September) and the entire year.

Drought **duration** is the time between the onset and the end of a drought. Onset and end are defined as the points in time when SPI falls below -1 (drought onset) and rises above -1 (drought end), respectively

Drought **intensity** is estimated as a ratio of drought magnitude and drought duration. It is presented in the equation (Haile et al., 2020; Wang et al., 2018).

Drought **magnitude** is the sum of all SPI values smaller than -1 during the drought period (Mckee et al., 1993).

3.3.1.2. Statistical analysis

Basic statistical indicators, e.g., the coefficient of variation (CV) and the Spearman correlation coefficient, were used to represent the variability and dependencies of rainfall and streamflow. To test for trends, the nonparametric Mann–Kendall test is widely applied. However, auto-correlation may bias the Mann–Kendall test results. To correct this bias, we used the Modified Mann-Kendall test (MMK) proposed by Hamed & Rao, (1998). As significance levels, we used α =0.05 and α =0.10. Trends were calculated by linear regression.

The MMK trend test is performed as follows:
Consider a sequence X_T and divide it by the mean of this series to obtain a new series Xt. Null hypothesis ($H0$): no trend in the series over time. The alternate hypothesis ($H1$): existence of an increasing or decreasing trend (Hamed & Rao, 1998).

$$\beta = median\left(\frac{x_i - x_j}{i-j}\right) \quad 1 \le i < j \le n \tag{6}$$

Where $\beta\beta > 0$ represents an upward trend and $\beta\beta < 0$ represents a downward trend.
If the trend part Tt of the new series Xt is linear then the trend part is removed to obtain the stationary series Yt.

$$Y_t = X_t - T_t = X_t - \beta \times t \tag{7}$$

The rank corresponding to series Y is calculated and its corresponding autocorrelation coefficient ri is obtained.

$$r_i = \frac{\sum_{k=1}^{n-i}(R_k - \bar{R})(R_{k+i} - \bar{R})}{\sum_{k=1}^{n}(R_k - \bar{R})^2} \tag{8}$$

where $\bar{R}$ is the average rank and Ri is the rank of yi.
The variance (S) of the trend statistic SS of autocorrelation series is obtained as follows:

$$V(S) = \eta \times \frac{n(n-1)(2n+5)}{18} \quad (9)$$

$$\eta = 1 + \frac{2}{n(n-1)(n-2)} \times \sum_{i=1}^{n-1}(n-i)(n-i-1)(n-i-2)r_i \quad (10)$$

The test statistic Z is calculated as

$$Z = \begin{cases} \frac{S-1}{\sqrt{V(S)}} & S > 0 \\ 0 & S = 0 \\ \frac{S-1}{\sqrt{V(S)}} & S < 0 \end{cases} \quad (11)$$

If $|Z_s| < Z_{0.05/2}$ for a given significance level α, then the hypothesis ($H0$) is accepted, otherwise rejected.

In this study, a default linear variogram model was applied. This choice was guided by the limited number of available stations in the basin.

3.3.2. Methods for the assessment of the predictive skills and the predictability of drought

3.3.2.1. Wavelet analysis

Wavelet analysis is a powerful tool for converting a continuous time series into the time-frequency domain, providing a multi-resolution approach that excels in analyzing non-stationary signals (Grinsted et al., 2004; Torrence & Compo, 1998). Compared to other signal processing techniques, it is superior in localizing both time and frequency features, making it particularly effective for identifying and analyzing non-stationary data (Torrence & Compo, 1998). This allows us to examine extreme and short-term events. This ability is crucial for studying hydroclimatic variability and teleconnections, where time series often exhibit significant variability over different time scales. We use wavelet analysis to understand whether catchment rainfall and streamflow variability in the three catchments are modulated by the selected climate teleconnections. All variables, i.e. climate indices,

catchment rainfall, and streamflow, were first normalized to obtain anomalies of annual values:

$$Z = \frac{X-\mu}{\sigma} \quad (12)$$

where X is the variable averaged over the rainy season, μ and σ are the mean and standard deviation of all years of the investigation period.

The continuous wavelet transform (CWT) is employed to decompose a time series into the time-frequency space, revealing how the frequency content of the data changes in time. The CWT of a time series X(t) is expressed as:

$$W_X(a,b) = \int_{-\infty}^{\infty} X(t)\psi^*_{(a,b)}(t)dt \quad (13)$$

Where $W_X(a,b)$ is the wavelet coefficients for the input time series $X(t)$, representing the transformed signal at scale a (frequency) and position b (time). $\psi^*_{(a,b)}(t)$ is the Conjugate of the scaled and shifted version of the mother wavelet $\psi(t)$ defined as:

$$\psi_{(a,b)}(t) = \frac{1}{\sqrt{|a|}}\psi\left(\frac{t-b}{a}\right) \quad (14)$$

The variability of the dominant mode with time was analyzed using the CWT, with the Morlet wavelet (wavenumber $w_o = 6$) as the mother wavelet. The choice of the Morlet wavelet is based on its very good ability to extract features that are highly localized in time and frequency (Grinsted et al., 2004). We used the CWT to analyse the variability of catchment rainfall and streamflow of the three catchments. In addition, we also derived the power spectrum for these time series. The power spectrum shows how the variance (or power) of a time series is distributed across different frequencies.

Based on the CWT of two time series $X(t)$ and $Y(t)$, the cross-wavelet transform (XWT) allows the evaluation of the relationships between these time series in the time-frequency domain. In our study, $X(t)$ stands for the time series representing the catchment rainfall or streamflow anomaly of the three catchments, respectively. $Y(t)$ stands for climate the

index anomaly, i.e. Niño 3.4, AMO and DMI, respectively. The XWT identifies common power areas between two time series, allowing for the exploration of shared temporal variability. Mathematically, the XWT of two time series $X(t)$ and $Y(t)$ is defined as (Grinsted et al., 2004):

$$W_{XY}(a,b) = W_X(a,b) \times W_Y^*(a,b) \tag{15}$$

Where $W_{XY}(a,b)$ is the cross wavelet transform coefficients, $W_X(a,b)$ is the CWT of $X(t)$ and $W_Y(a,b)$ is the CWT of $Y(t)$, $W_Y^*(a,b)$ is the complex conjugate of $W_Y(a,b)$.

The XWT is adequate to evaluate the time evolution of mutual intensity between two time series (Grinsted et al., 2004). However, the cross-wavelet power obtained through XWT can sometimes be misleading due to coincidental high-power areas (Maraun & Kurths, 2004). To address this problem, the wavelet transform coherence (WTC) is used to provide a more nuanced understanding of the correlation between two time series in the time-frequency domain. WTC is similar to a localized correlation coefficient, but in the time-frequency space, offering a robust measure of the co-movement between time series across scales (Lin & Weng, 2024; Longobardi et al., 2020). According to Torrence & Compo (1998), the WTC of two time series is defined as:

$$R^2(a,b) = \frac{|S(W_{XY}(a,b))|^2}{S(|W_X(a,b)|^2) \times S(|W_Y(a,b)|^2)} \tag{16}$$

where $R^2(a,b)$ is the Wavelet coherence ranging from 0 (no coherence) to 1 (perfect coherence). S is the smoothing operator in both time and scale, which ensures that coherence is localized and robust to noise. This definition is very close to the traditional correlation coefficient, but localized in the time-frequency space (Lin & Weng, 2024; Longobardi et al., 2020). The statistical significance of the wavelet coherence is estimated using Monte Carlo methods with red noise (Fang et al., 2021; Okonkwo, 2014). We generate a distribution of coherence values under the null hypothesis (assuming no relationship between the climate index and the hydroclimatic target variable) using red noise, where the power spectrum decreases with increasing frequency. This distribution is used as the baseline against which the significance of the wavelet coherence is

evaluated. Detailed information about the methodology of WTC can be found in Grinsted et al., (2004); and Torrence & Compo, (1998).

3.3.2.2. Most promising predictors's selection

This study focuses on enhancing the seasonal predictability of rainfall, aiming for forecasts two months in advance. To achieve this, three-month average Sea Surface Temperature (SST) data from overlapping periods were used: OND (October–November–December), NDJ (November–December–January), DJF (December–January–February), JFM (January–February–March), FMA (February–March–April), MAM (March–April–May), and AMJ (April–May–June). These SST averages were used to predict rainfall anomalies for June, July, August, and September, respectively. Incorporating all relevant variables and indicators, 12 potential predictors were identified. Before employing multivariate models, refining this comprehensive set to a more parsimonious subset of predictors is essential. This step ensures optimal model performance and interpretability. Various statistical methods were applied to systematically select the most robust predictors, capable of explaining rainfall variability across the three catchments.

3.3.2.3. Multiple Regression Approach

The climate indices that influenced rainfall must first be known to apply multiple linear regression models. Multiple regression model was chosen over other machine learning (ML) approaches primarily for its interpretability, robustness with limited datasets, and suitability for establishing explicit statistical relationships between predictors and drought indicators. Multiple regression provides a clear analytical framework to quantify the contribution of individual predictors such as sea surface temperature (SST) indices to drought variability

All possible combinations of the 12 predictors for constructing multiple linear regression models were considered. The range of combinations to reduce the computational time has been limited, and because assuming the best model to lie within this range and that fewer or more predictors would result in a too simplified or too complex model, respectively to avoid overfitting during the predictor selection (Lever et al., 2016).

To ascertain the dependence of the dependent variable on the selected independent variables, multiple linear regressions were applied to generate a regression equation of the form:

$$y = \beta_0 + \beta_1 x_1 + \beta_2 x_2 + - - - - - - - - \beta_n x_n + \varepsilon \quad (17)$$

Where; x_1, x_2 ---------- x_n are the selected independent variables (SST predictors), y = the dependent variable (Rainfall anomalies), β_0 is the intercept; $\beta_{1,\ldots,}\beta_n$ are the regression coefficient (weights); ε is the deviation (error term).

The data is split randomly into five subsets and each subset once serves as test data to evaluate the performance of an MLR model trained on all remaining data (Hastie et al., 2009). The best model within each cross-validation fold is selected based on the lowest Bayesian Information Criteria (BIC). To analyze the degree of predictor multicollinearity, the variance inflation factor (VIF) for each of the best predictor combinations per subset was computed (Hirsch et al., 1992).

3.3.3. Methods for the Proposed design framework for drought risk management in the study area

To investigate farmers' understanding of hydroclimatic variability, 14 questions (Table 8) that allow a clear comparison between the farmers' perceptions and observed climate data were selected. Each respondent was assigned a knowledge score based on the degree to which their responses to these 14 questions matched observations. These questions were either binary (wrong, right) or more nuanced (wrong, mostly wrong, mostly right, right). Each answer was assigned to one of these classes and then the knowledge of the respondent for each question was determined (questions with 2 options: wrong = 0; correct = 1; questions with 4 options: wrong = 0; mostly wrong = 0.33; mostly correct = 0.67; correct = 1). The assignment of the answers to these classes is given in Table 8. In a second step the results for all 14 questions were averaged. Thus, a respondent who answers all questions correctly will obtain a knowledge score of 1, whereas a respondent who gives only incorrect answers will receive a knowledge score of 0.

The aim is to identify those factors that enhance people's understanding of hydroclimatic variability, climate change and appropriate adaptation measures. Potential factors that

were included in our survey are gender (male, female), age, experience (number of years of farming practices), education level (none, primary, high), secondary work engagement (yes, no), location (municipalities L1 to L8), and technology/science-oriented view (yes, mixed, no). The latter factor was not asked directly to the respondents, but was inferred from their answers to questions that were related to their farming practices and their approaches to increasing their agricultural yields. Households that used pesticides and agricultural equipment were classified as favourable to a technology/science-oriented view. Households that relied on community-based practices and the use of religious rites in their farming activities were classified as not technology/science-oriented. The mixed class was assigned to those farmers who used both types of approaches, such as using pesticides and religious rites.

To understand the relationships between the variables surveyed, the Spearman correlation coefficient (r_s) was calculated for the continuous variables (age, experience, and knowledge):

$$r_s = 1 - \frac{6 \sum d_i^2}{n(n^2 - 1)} \tag{18}$$

Where:

- $d_i^2 = R(X_i) - R(Y_i)$ is the difference between the ranks of each pair of values in the two datasets.
- n is the number of observations.
- $R(X_i)$ and $R(Y_i)$ are the ranks of X_i and Y_i, respectively.

For the categorical variables, we used the Mann-Whitney U test for the binary variables (gender, secondary work) to determine whether there is a significant difference between the two groups. For two independent groups A and B, the U statistic is calculated as:

$$U = n_1 n_2 + \frac{n_1(n_1 + 1)}{2} - R_1 \tag{19}$$

or

$$U = n_1 n_2 + \frac{n_2(n_2 + 1)}{2} - R_2 \tag{20}$$

Where:

- n_1 and n_2 are the sample sizes of groups A and B, respectively.

- R_1 and R_2 are the sums of ranks for groups A and B, respectively.
- The smaller U value is used for statistical significance testing.

Z-score for significance testing:

$$Z = \frac{U - \mu_U}{\rho_U} \tag{21}$$

Where:

- $\mu_U = \frac{n_1 n_2}{2}$ is the mean of U
- $\rho_U = \sqrt{\frac{n_1 n_2 (n_1 + n_2 + 1)}{12}}$ is the standard deviation of U

The Kruskal-Wallis H test was applied for the variables with more than two categories (level of education, location, technology/science-oriented view). The Kruskal-Wallis H test checks if at least one of the groups has a different median compared to the others. The H statistic is calculated as:

$$H = \left(\frac{12}{N(N+1)}\right) \sum_{i=1}^{k} \frac{R_i^2}{n_i} - 3(N+1) \tag{22}$$

Where:

- K is the number of groups
- N is the total number of observations across all groups
- n_i is the number of observations in group i
- Ri is the sum of ranks for group i

For large sample sizes ($n_i > 5$) , the H statistic follows a chi-square distribution with k-1 degrees of freedom.

Both tests analyze whether the populations from which the samples are drawn are different.

To understand whether and how a certain factor contributes to farmers' understanding of hydroclimatic variability and climate change, represented by the knowledge score over all 14 questions, we applied the Random Forest and Accumulative Local Effects methods. Random Forest is a robust machine-learning algorithm known for its ability to handle large datasets and complex interactions among variables (Breiman, 2001). A Random Forest is an ensemble of many regression trees. Each regression tree is trained on a random

subset of the data, which helps to ensure that the trees are uncorrelated and reduces the risk of overfitting. The Random Forest method is particularly suitable for our analysis due to its flexibility and high accuracy in classification and regression tasks. Random Forests perform well compared to many other methods, including discriminant analysis, support vector machines, and neural networks (Liaw & Wiener, 2002). The data set of 509 records was split into a training set, which consisted of a random subset representing 80% of the data, and a holdout set, comprising the remaining 20%. A random forest was generated using 500 conditional inference trees as base learners (Hothorn et al., 2015), which are unbiased towards variables with numerous potential split points unlike regular regression trees (Hothorn et al., 2006). Model performance was assessed using out-of-bag (OOB) predictions, providing conservative accuracy measures akin to cross-validation for multiple linear regression models (Liaw & Wiener, 2002). The random Forest package in R was used to fit random forest models to the training data (Liaw & Wiener, 2002).
Random Forests are black-box models that do not allow us to understand how a certain predictor influences the target variable. To shed light on these influences, the accumulated local effects (ALE) plots were calculated (Apley & Zhu, 2020; Robette, 2020). ALE plots estimate the change in model predictions across small intervals of each predictor, unaffected by collinear input variables (Molnar, 2021). They thus show how each predictor influences, possibly in a non-linear way, the target variable.

Figure 16 illustrates the steps of our analysis.

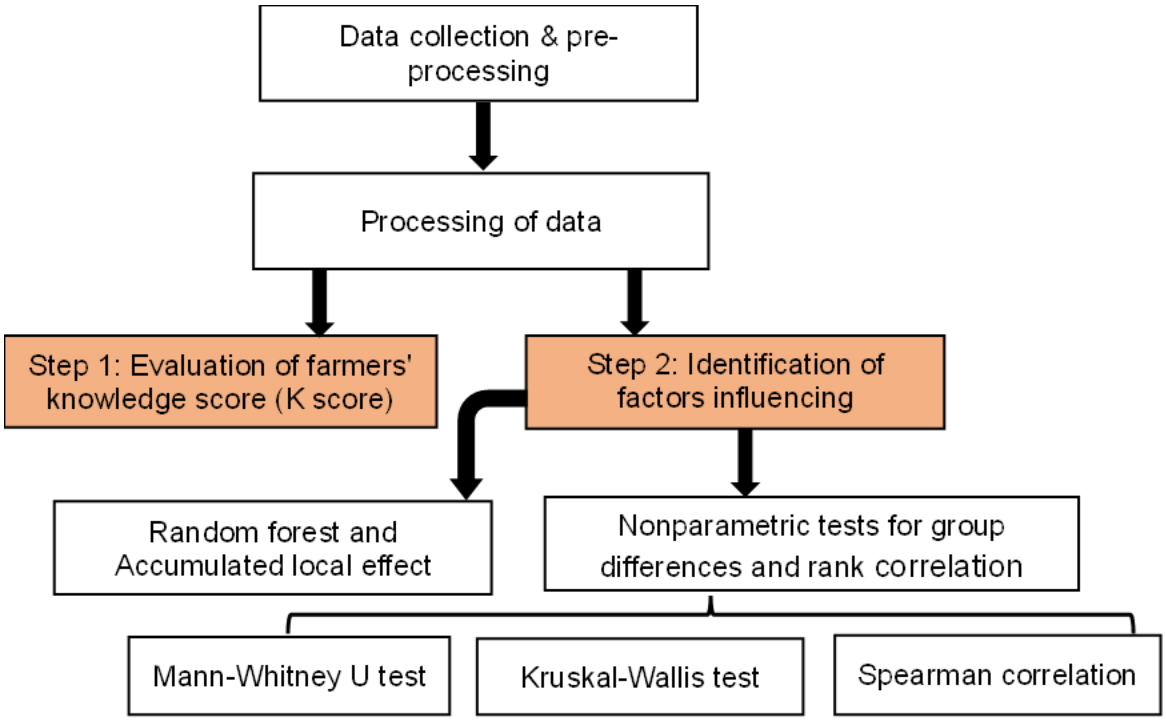

Figure 16: Flowchart outlining the steps of the analysis

Conclusion

The data used in this study consist of hydrological, meteorological, and climatic datasets. CHIRPS satellite data and climate indices from various oceans were incorporated to analyze climate teleconnections and enhance predictive capabilities. Developing a framework for drought risk management requires a thorough understanding of historical hydroclimatic variability, as well as insights from local community knowledge. To gather this local knowledge, field surveys were conducted using tools such as KoboToolbox and XLSForm, with RStudio employed for data processing. Ultimately, this study examined past hydro-meteorological drought characteristics, hydroclimatic variability, multiscale climate teleconnections, improved drought predictability, and established a comprehensive framework for drought risk management in the study area.

CHAPTER 4: INVESTIGATION OF HISTORICAL METEOROLOGICAL AND HYDROLOGICAL DROUGHT CHARACTERISTICS SPATIALLY AND TEMPORALLY

This chapter provides results of the historical meteorological and hydrological drought characteristics over the Benin Portion of the Niger River Basin. The major significant results presented in sections 4.4, in particular 4.4.1, 4.4.2, and 4.4.3, have been published in published in Journal of Hydrology: Regional Studies (Elsevier, 2025, Vol. 59, 102319) and are available at the following link: https://doi.org/10.1016/j.ejrh.2025.102319.

4.1. Analysis of meteorological drought (Standardized Precipitation Index (SPI))

4.1.1. Trends of SPI and SPEI

Figure 17 shows the temporal evolution of the spatial mean of SPI and SPEI across various timescales over the basin, capturing the alternation between wet and dry cycles from 1970 to 2020. An upward trend is observed in SPI, while SPEI displays a downward trend. Both indices frequently fluctuate around zero, exhibiting a broad range. Notably, longer timescales reveal a more pronounced drought trend. Although the variations in SPI and SPEI appear similar across different timescales, slight differences in fluctuation values are evident. The Modified Mann-Kendall test indicates a significant trend in both SPI and SPEI across all timescales, except for SPI-3 and SPEI-12. The significant trend is upward for SPI and downward for SPEI (Table 14 & 16 in the annex).

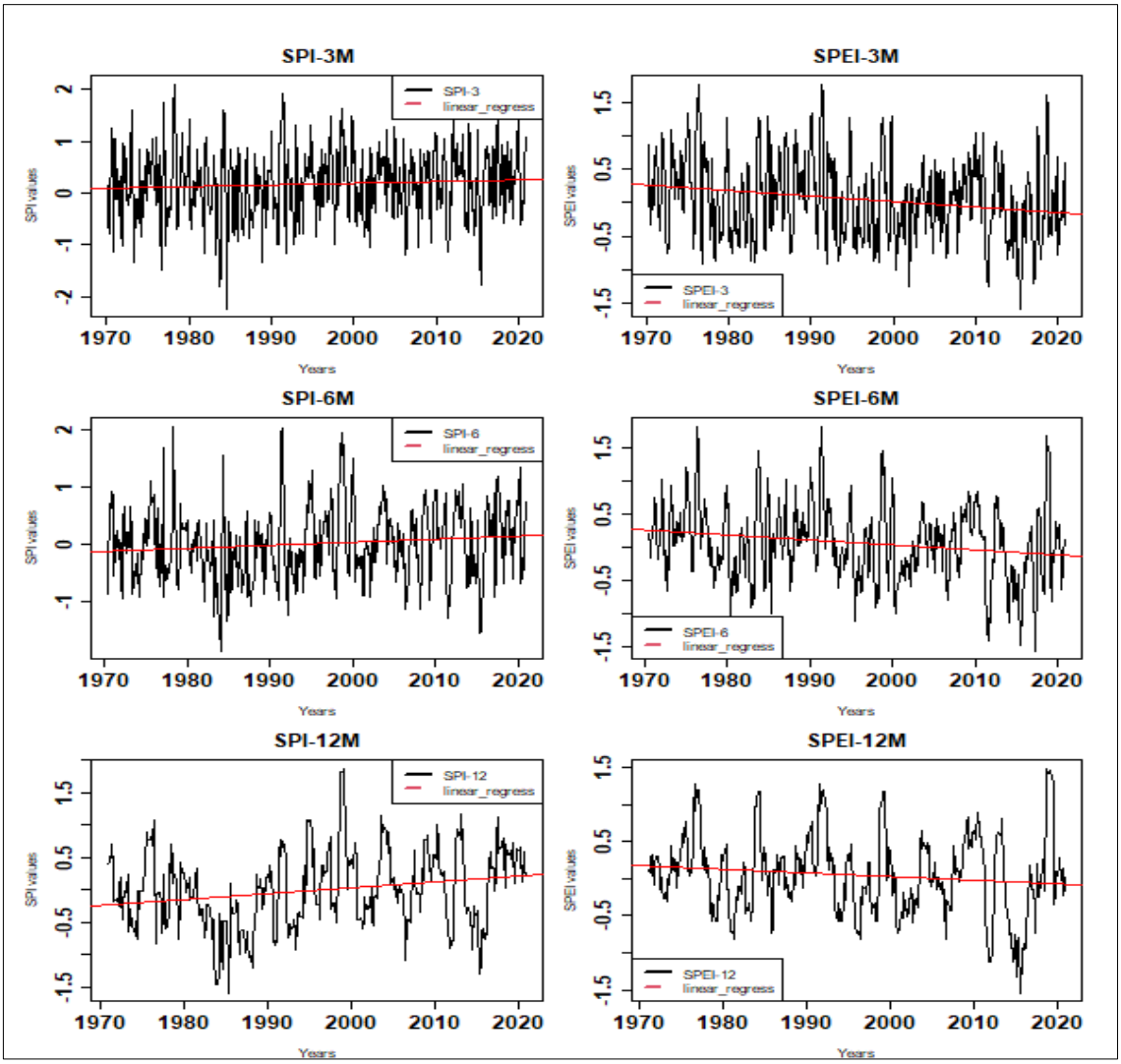

Figure 17: The temporal evolution of the standardized precipitation index (SPI) and standardized precipitation evapotranspiration index (SPEI) at 3-, 6-, and 12-month timescales over the BPNRB during 1970–2020.

4.1.2. Occurrence of meteorological drought

Figure 18 shows the average occurrence of different types of droughts in the BPRNB over the period 1970-2020. The acquired occurrences are based on the classification of drought as defined (Mckee et al., 1993; Nalbantis and Tsakiris, 2008) (Table 2). It appears from this figure that on the BPRNB globally, SPI values show a high occurrence percentage of near normal drought (alternate of wet and dry: SPI varies from -0.99 to 0.99) of almost 80%, and a very low percentage for the other classes of drought, 12%, 7% and 1% relatively for moderate, severe and extreme drought respectively. During the

3-month SPI, near-normal drought is higher than at the 6- and 12-month timescales. Moderate and extreme droughts are felt more at the 12-month scale, whereas severe drought is felt more at the 6-month scale. Since droughts are better characterized by the moderate, severe, and extreme classes, at the 12-month interval, the sum of these three drought classes is higher than at the other time intervals. We can therefore conclude from this analysis that on a 12-month scale, drought is felt more acutely in the study basin (Figure 18).

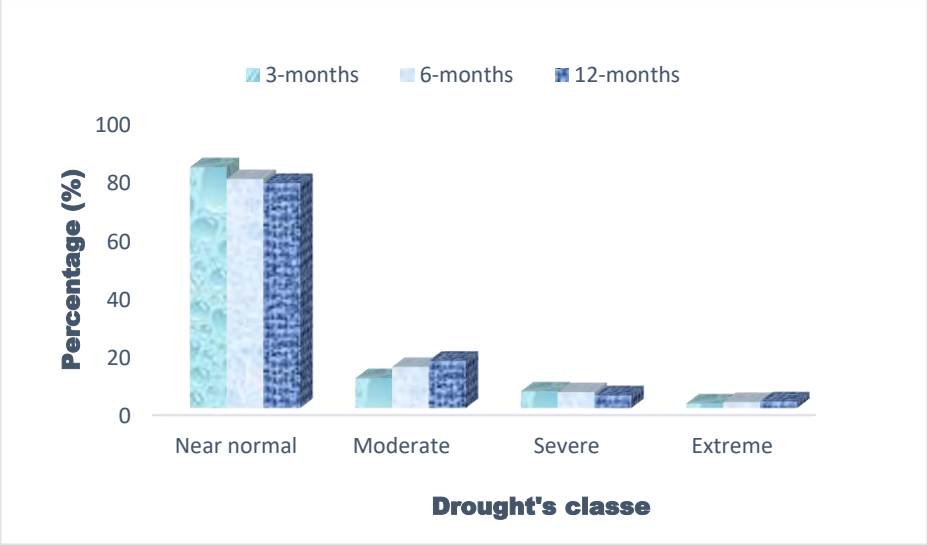

Figure 18: Average occurrence percentage of drought classes using the spatial mean of SPI

4.1.3. Spatial variations of drought occurrence over the basin

Figure 19 shows the Spatialization of the drought-type percentage of occurrence using the SPI values. The SPI values obtained at each station were classified based on Table 2 and then spatialized.

Spatially, during the near-normal drought, the percentages of occurrence vary between 76-88%. Its spatial distribution shows a latitudinal gradient that increases from the south to the north of the basin (Figure 19). During moderate drought, the extreme southeast and southwest of the basin show the highest values of drought occurrence (Figure 19). These values vary between 6-14%. On the other hand, severe drought has its highest values in the middle of the basin on a diagonal and varies between 2-7% (Figure 19). Finally, extreme drought is only felt in the northernmost of the basin, with values varying between 2-5% (Figure 19).

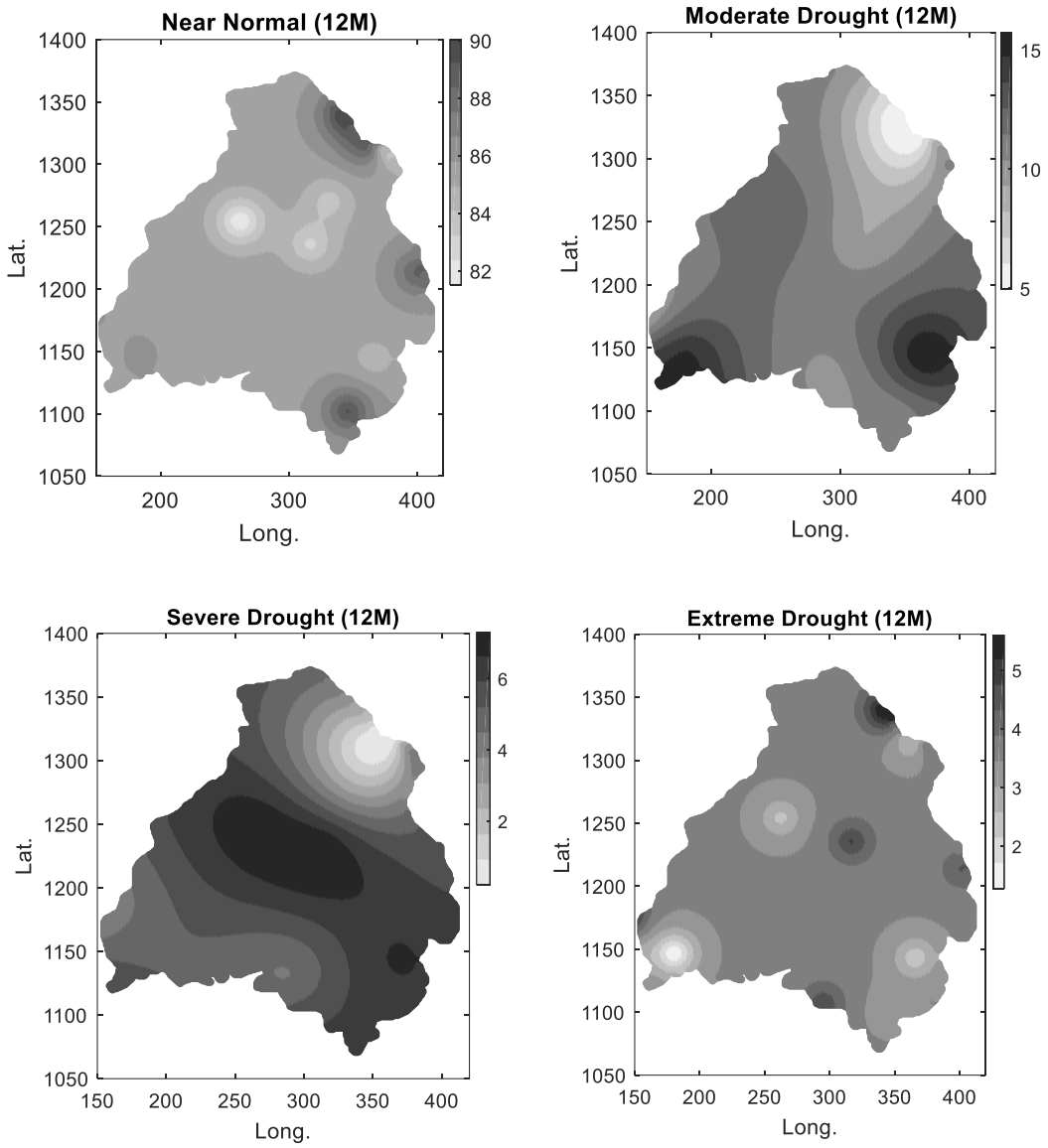

Figure 19: Spatialization of drought-type percentage of occurrence using the SPI values

4.1.4. Drought's duration and intensity

Figure 20 illustrates the spatialization of droughts duration and intensity at 3- and 12-month timescales. For each timescale, the duration and peak of drought were calculated using the SPI values for each station. These values were then interpolated using the Kriging method. It appears from Figure 20 that the duration of the drought is on average 3.2 and 16.41 months for the SPI-3 and SPI-12 months respectively in the study basin. We note a decrease in the durations of the 12-month SPI with increasing latitude. The durations are more pronounced in the south than in the north of the basin with long durations (maximum) (Figure 20).

The average intensity of SPI-3 and 12 months are -1.77 and -1.73 respectively. All these average values plunge the basin into a severe drought situation. This situation is noticeably recorded in the extreme areas of the north and southeast of the basin (Figure 20).

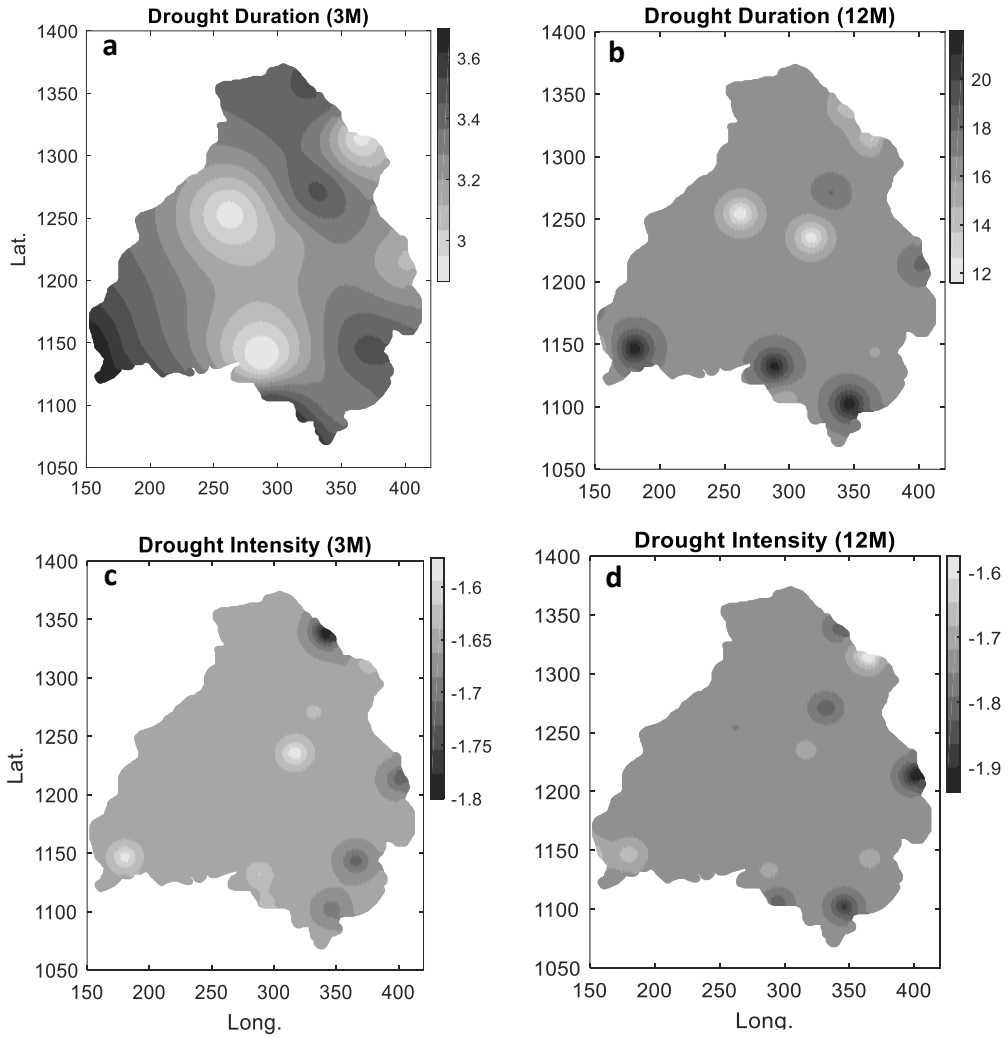

Figure 20: Spatiotemporal variations of drought duration (a-3month and b-12month) and intensity (c-3month and d-12month) using SPI values

4.2. Analysis of the Consecutive Dry Days (CDD) index

The CDD values obtained for each station during the study period were kriged and then spatialized over the entire study area. Figure 21 shows the spatialized mean CDD values (plots 21-a and b) and the trend results (plots 21-c and d).

The spatial characteristics of CDD during 1970–2020 show great differences between the rainy season (AMJJAS) and the entire seasons (both rainy and dry seasons). For the entire season over the BPNRB from 1970 to 2020, the CDD ranged from 80 to 180 days (plots 21-a and c). This index increases with the latitude of the stations. It showed a chronological upward trend of 0.1 days/year, which was statistically significant in the central-west (plot 21-d). In the rainy season, the CDD, which corresponds to dry spells, varies from 9 to 18 days. Its maximum was recorded in the northern part of the basin (plots 21-b and d). The MMK test showed a statistically significant increasing trend in the northern and northeastern parts of the basin (Table 17 & 18).

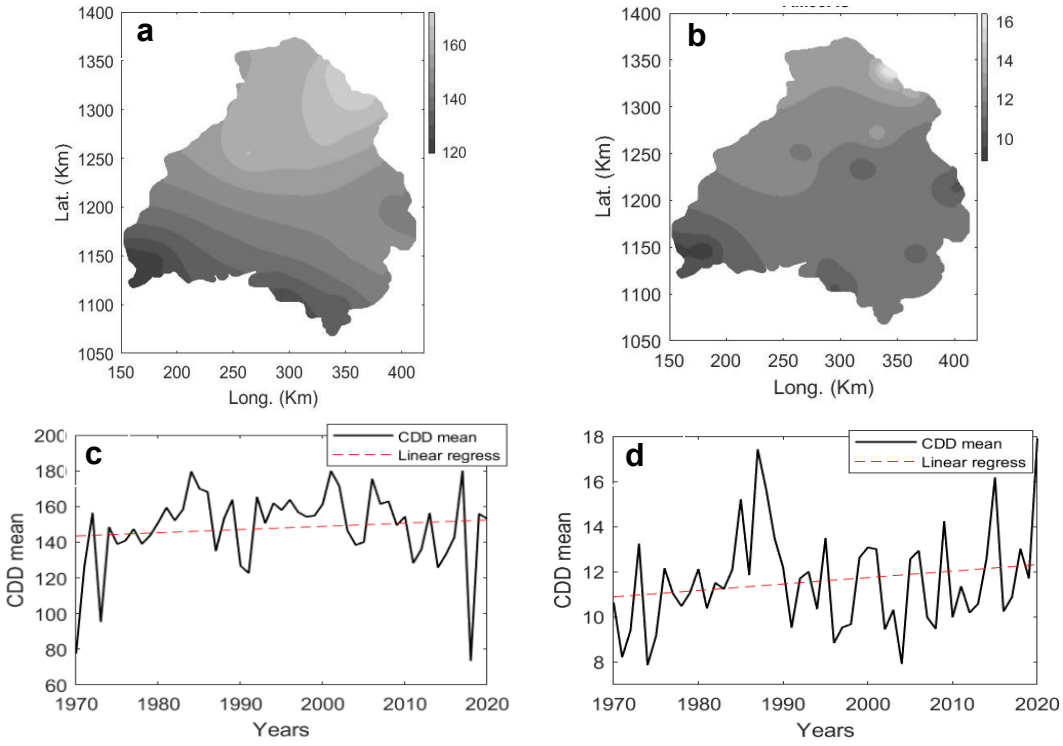

Figure 21: Spatialisation and trends of averaged CDD annually and in the rainy season

4.3. Analysis of the hydrological drought in the Benin Portion of the Niger River Basin

The SDI values obtained for each time scale at each hydrometric station and were analyzed and subjected to the MMK test. These SDI values, classified according to Table 2, were also used to calculate the duration and peak of drought at each hydrometric station. The temporal distribution of the SDI indices, the duration, and the intensity of hydrological droughts for different reference timescales are depicted in Figure 22.

Figure 22 shows the fluctuations in the wet and dry periods for the whole hydrometric stations of BPNRB during 1970–2020. A significantly (level=5%) upward trend was noted for the SDI at the various timescales except for 3-month at Couberi and Kompongou stations and 12-month at Yankin station. Duration and intensity of drought were comparatively higher at longer time scales of 6- and 12-month and they seemed to increase as the time scale increased.

For instance, the longest drought duration was recorded at Gbassè station, where the drought intensity is the lowest compared to other stations. Additionally, the highest drought intensity occurred in a longer timescale (SDI-12), noted as −2.4, and was recorded at Kompongou station. Regarding the severe drought conditions, the Couberi station is leading followed by the Gbassè station (Figure 22).

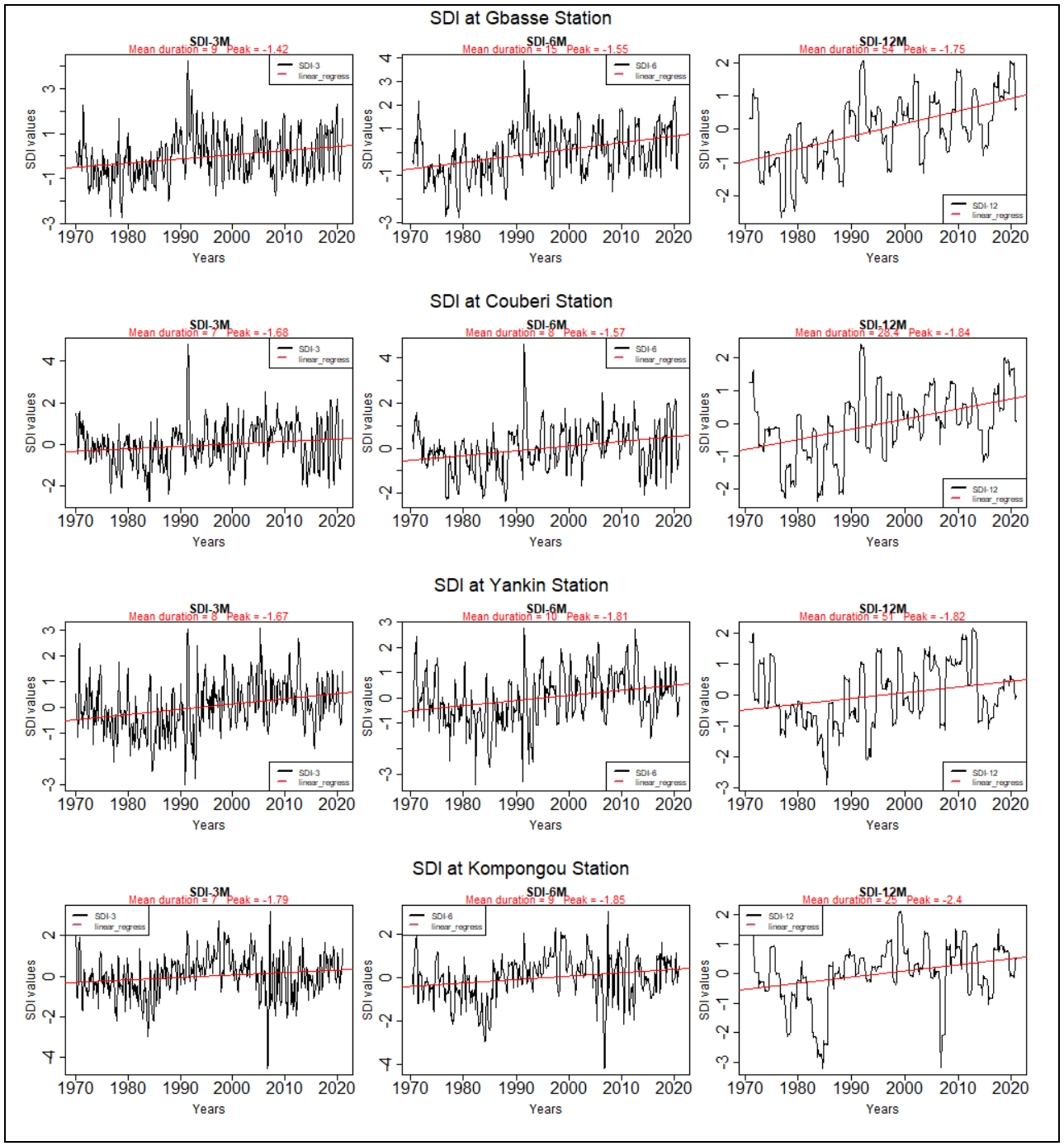

Figure 22: The temporal evolution of the SDI, Duration, and Peak values at each hydrological station at 3-, 6-, and 12-month timescales in BPNRB during 1970–2020.

4.4. Rainfall and streamflow variability across the study area

4.4.1. Rainfall variability patterns

Figure 23 provides a more detailed picture of the temporal variability for the three catchments. Total rainfall within the rainy season (Figure 23a–c) shows a high variability at the interannual scale, often a zigzag pattern at the bi-annual scale, i.e. rainfall tends to fluctuate between high and low values. In dry tropical regions like our study area, rainfall exhibits high interannual variability, unlike wetter parts of the tropics where rainfall tends to be more consistent (Obarein & Lee, 2022). There is also a clear variability at the decadal scale. For example, the 1980s were particularly dry, followed by a decade with much higher rainfall. Over the period 1970–2020, we find significant upward trends for B1 and B3 (5% significance level) and B2 (10% significance level). The early decades before the 1990s were characterized by a severe and persistent drought, while the more recent decades are marked as a recovery from the drought period. This pattern applies not only to our study area and to the entire Republic of Benin (Badou et al., 2017, Adechina et al., 2022, Ahokpossi (2018), but also to West Africa as a whole (New et al., 2006;Giannini & Kaplan, 2019; S. Nicholson, 2005; OZER et al., 2010).

The number of wet days (days with rain > 1 mm) within the rainy season shows a strong increase from about 120 to more than 140 days. This means that rainfall occurs (somewhere) in each catchment in two out of every three days. This increase is significant at the 5% level and consistent across the catchments (Figure 23d–f). In contrast, the mean daily rainfall (Figure 23g–i) decreases for B1 (significant at 5%), B2 (significant at 10%) and B3 (non-significant). The increase in total seasonal catchment rainfall is therefore a consequence of the higher number of wet days. An increase in the number of wet days was also reported by Ahokpossi (2018) for July–September at some stations in the Republic of Benin.

The variability of daily rainfall (wet days in the rainy season) is represented by the standard deviation (Figure 23j–l) and the coefficient of variation (Figure 23j–l). The variability of daily rainfall is rather high with CV values between 70% and 110%. High variability has also been reported by Oguntunde et al. (2006) and Orke & Li (2021) in the Volta River Basin and the Bilate watershed in Ethiopia, respectively. In line with the decreasing mean daily rainfall, the variability of daily rainfall also decreases over the

period 1970–2020. Both variability indicators show significant decreasing trends at the 5% significance level for B1 and B2. For catchment B3, the decrease is less pronounced. Extreme daily rainfall, represented by the 99th percentile, shows downward trends across the three catchments (Figure 23p–r). However, these trends are only significant in catchment B2.

To understand whether the spatial distribution of daily rainfall has changed over the period 1970–2020, we quantify the mean number of climate stations receiving rainfall on the same days for each catchment (Figure 23s–u). For instance, 3.2 stations out of 7 stations in catchment B2 received rain on the same day in the 1970s, while this number decreased to 2.6 in the 2020s. This trend shows a significant increase in the spatial variability of daily rainfall (at 5% significance level). A significant increase in spatial variability is also observed in catchment B2.

The analysis of daily rainfall at the catchment scale shows a number of significant changes that are broadly consistent across the three catchments. The total rainfall in the rainy season has increased over the last five decades. This increase is driven by a higher number of wet days. In contrast, the mean daily rainfall, its variability, and extreme daily rainfall have decreased over the study period. These results indicate more rainfall and less variable rainfall in recent years. However, this development should not be interpreted as a sign that the risk of drought has faded, as we find high interannual variability of rainfall and streamflow in northern Benin.

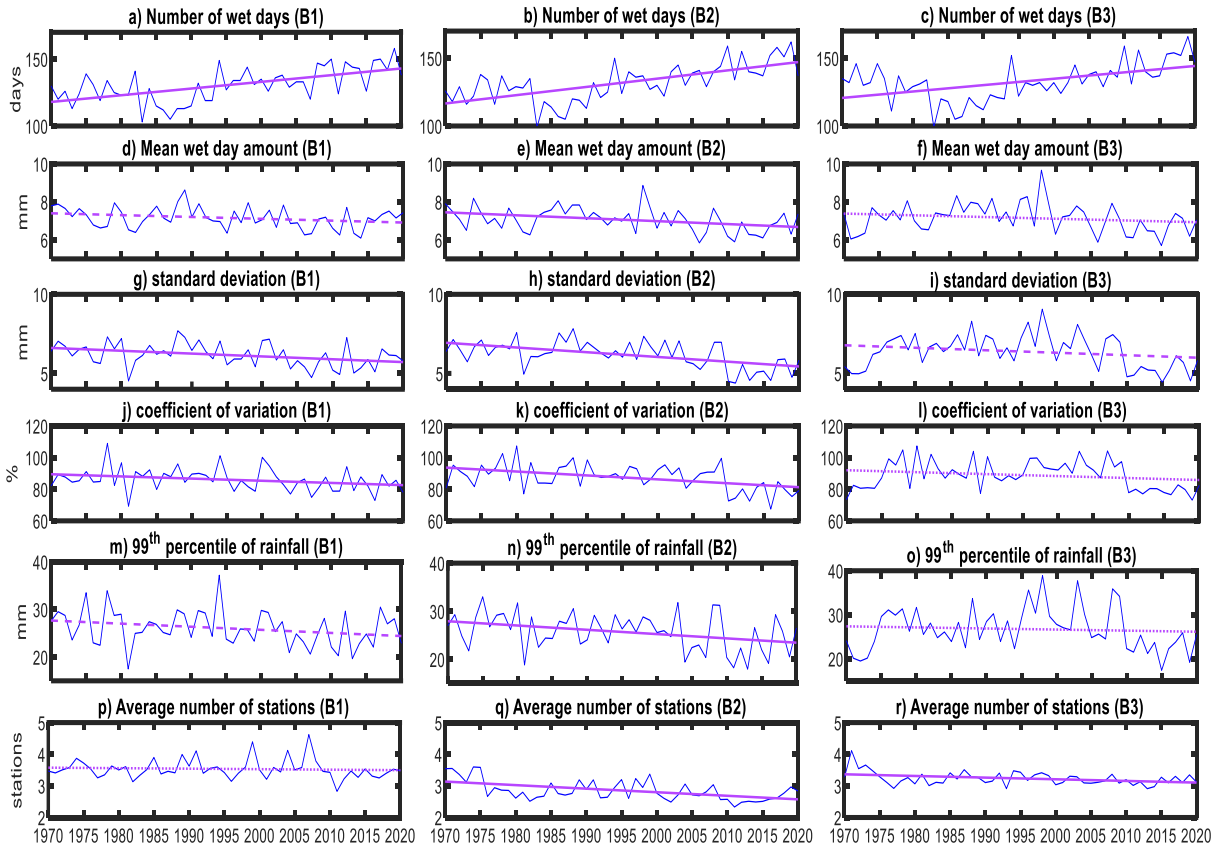

Figure 23: Time series and linear trends (solid: significant at 5%; dashed: significant at 10%) of catchment daily rainfall in the rainy season for the catchments B1–B3 for 1970–2020. (a–c) Number of wet days. (d–f) Mean wet day amount. (g–i) Standard deviation of wet day amounts. (j–l) Coefficient of variation. (m–o) 99th percentile of wet day amounts. (p–r) Average number of climate stations receiving rainfall on the same day.

4.4.2. Streamflow variability patterns

To understand whether the observed changes in catchment rainfall translate into similar changes in streamflow, we analyze the monthly interannual variability and trends in the mean and variability of streamflow. The two distinct seasons are also evident in the monthly streamflow (Figure 24a–c). All three rivers reach their maximum flow in September. The high flow lasts for three months (August–October), which together account for 80–90% of the annual runoff. This fraction increases to 97% for B2 and B3, if we add the flow in July and November. Catchment B1 has a slightly more regular regime, characterized by a perennial flow, while the rivers of B2 and B3 run dry in February–May. In the three catchments, streamflow recession starts abruptly in October and reaches

critical levels in January. The interannual variability is high. For example, the interquartile range of September streamflow is 75–140, 65–138, and 60–115 m^3/s in catchments B1, B2, and B3, respectively.

The mean streamflow during the rainy season shows considerable interannual variability, characterized by zigzag fluctuations and upward trends in all catchments (Figure 24d–f). However, only the trends in B1 and B3 are statistically significant (5% level). Similar to the total catchment rainfall, we observe decadal variability in the mean streamflow. The severe drought in the decades prior to the 1990s is also evident in the streamflow observations.

The variability of daily streamflow, represented by the standard deviation and coefficient of variation, shows a mixed behavior across the three catchments. While the standard deviation increases significantly (5% level) for B1 and B3 (Figure 24g–i), it decreases slightly (non-significant) for B2. The coefficient of variation of daily streamflow decreases over time with significant trends (5%) for B2 and B3 (Figure 24j–l).

The analysis of streamflow shows that some patterns in rainfall variability are translated into similar patterns in streamflow. We find similar short-term (zigzag) and decadal fluctuations in rainfall and streamflow. Furthermore, the increase in total rainfall is reflected in an increase in mean streamflow in all three catchments. However, the trends of decreasing variability in daily rainfall across the three catchments do not lead to similarly consistent trends in streamflow variability. The less consistent behavior of streamflow across the three catchments can be explained by the additional effects that catchment processes and human activities, such as evapotranspiration, land use change and water abstraction, have on streamflow.

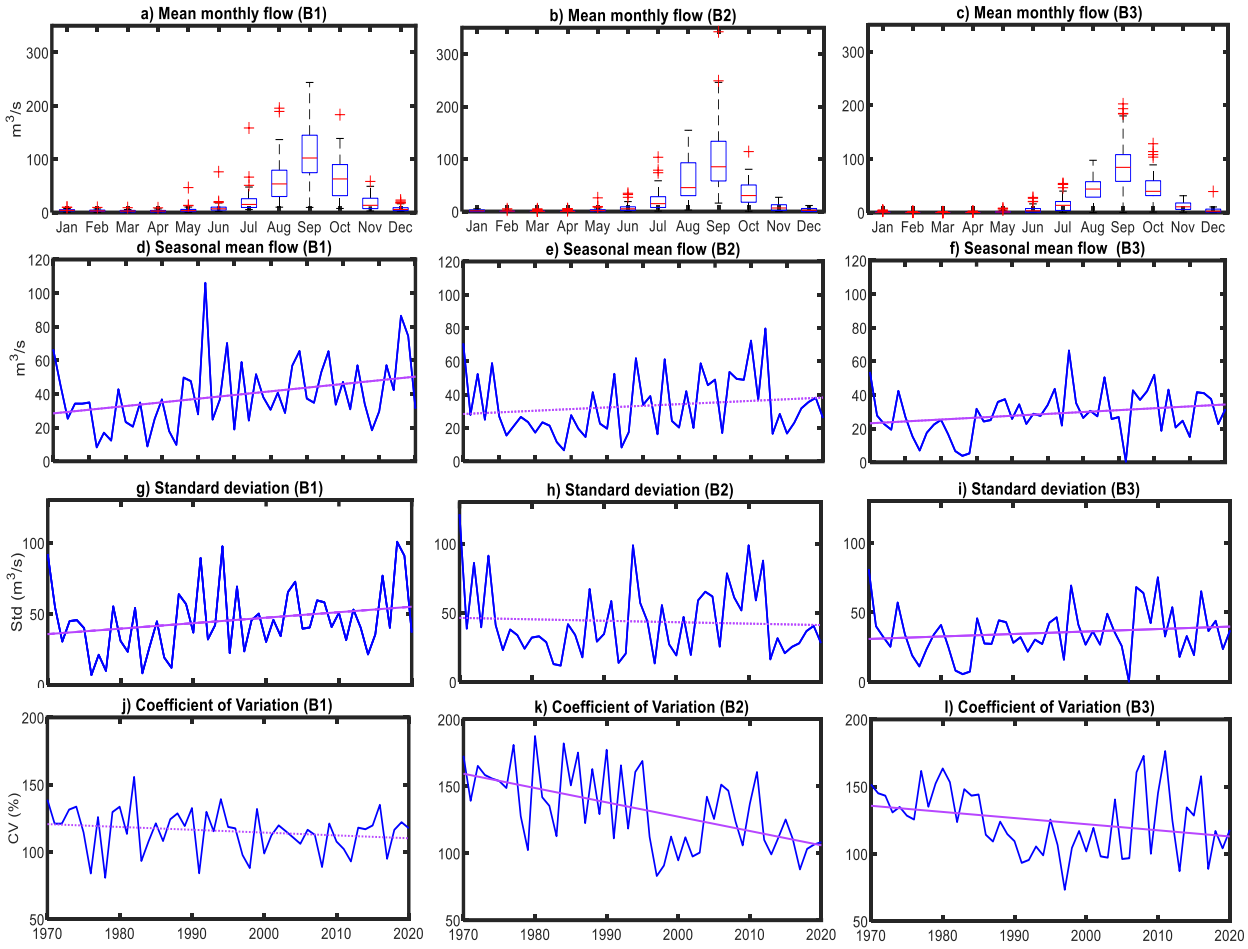

Figure 24: Streamflow of the rainy season for B1–B3 for 1970–2020. (a–c) Monthly streamflow: Interannual variability represented by the median (red line), the interquartile range IQR (box), the range of the data (whiskers), and outliers (red cross). (d–f) Mean daily streamflow. (g–i) Standard deviation and (j–l) Coefficient of variation of daily streamflow.

4.4.3. Dependence between rainfall, streamflow and temperature

To understand whether the observed changes in catchment rainfall and streamflow are correlated with changes in surface temperature, we correlate several rainfall and streamflow indicators with the mean seasonal temperature (Table 3). The latter is obtained from climate station P9, which is centrally located in the study area (Figure 3). The mean temperature of the rainy season shows a substantial variability at the interannual scale with frequent fluctuations between high and low values (Figure 25). Over the period 1970-2020, the mean temperature shows an increasing trend significant at the 5% level.

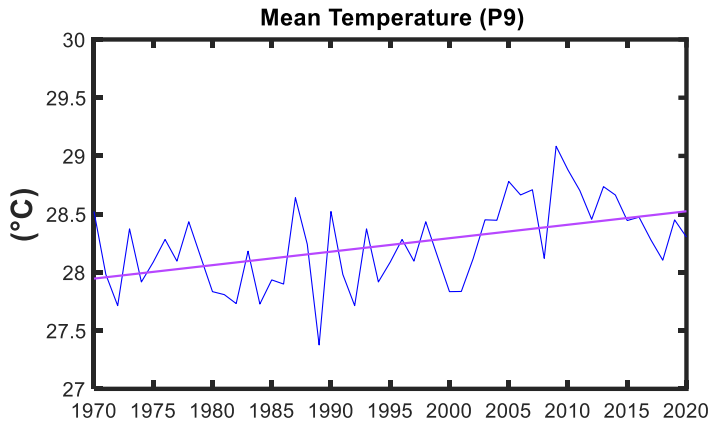

Figure 25: Mean temperature of the rainy season at Kandi station (P9, see Fig. 3) for the period 1970–2020. The linear trend is significant at 5%.

Table 3: Spearman correlation coefficient between catchment rainfall, streamflow, and temperature in the rainy season for the catchments B1–B3. P-values are given in brackets and bold numbers indicate significant correlation at the 5% level.

	B1	**B2**	**B3**
Rainfall variables			
Number of wet days	**0.29** (0.04)	**0.41** (<0.01)	**0.36** (0.02)
Total rainfall	0.02 (0.89)	0.03 (0.84)	0.10 (0.48)
Mean wet day amount	**-0.32** (0.02)	**-0.40** (<0.01)	-0.18 (0.20)
Standard deviation	**-0.45** (<0.01)	**-0.39** (<0.01)	-0.14 (0.32)
Coefficient of variation	-**0.38** (<0.01)	**-0.23** (<0.1)	-0.10 (0.48)
99th percentile	**-0.44** (<0.01)	**-0.29** (0.04)	-0.10 (0.46)
Streamflow variables			
Mean	0.13 (0.38)	0.22 (0.11)	0.18 (0.20)
Standard deviation	0.06 (0.68)	0.17 (0.23)	0.16 (0.25)
Coefficient of variation	-0.17 (0.24)	-0.26 (0.07)	-0.06 (0.69)

A significant correlation is found for the number of wet days for all three catchments (Table 3). This positive correlation between a number of wet days and mean temperature in the rainy season could be a consequence of more convective events in a warmer atmosphere, which could also explain the higher spatial variability of daily rainfall in more recent decades.

We find a significant correlation for all indicators related to daily rainfall for catchments B1 and B2. The correlation coefficients for daily rainfall for B3 follow the same pattern as those for B1 and B2, but are not significant. This could be a consequence of the location of climate station P9, which is on the border between B1 and B2 and quite far from B3. In

addition, B3 contains areas at higher altitudes whose climate may not be well represented by station P9. Mean wet day amount, the variability of daily rainfall and extreme daily rainfall decrease with higher temperature in B1 and B2. We find a decrease of 8.4 % and 9.5% in the mean daily rainfall and of 15.0% and 14.2% in the standard deviation with 1K increase in temperature for B1 and B2, respectively. (e.g. Pendergrass et al., 2017; Zhang et al., 2021). We find similar changes in the mean and the standard deviation of daily rainfall.

The correlation coefficients between streamflow and temperature are only partially consistent with the correlation coefficients between rainfall and temperature. For all three catchments and all three indicators, the correlation between streamflow and temperature is not significant (Table 3). The increase in mean streamflow with higher temperature is consistent with the increase in total rainfall.

4.5. Discussion

The spatiotemporal distribution of SPI and SPEI from 1970 to 2020 reveals alternating wet and dry phases across the basin, with considerable spatiotemporal variability in drought distribution. SPI shows an upward trend, while SPEI trends downward, indicating an increase in drought intensity. These findings align partially with (Katchele et al., 2017), who reported a downward SPEI trend from 1901 to 2010 in Sub-Saharan Africa. Severe to extreme drought events occurred in about 1-5% of the basin, most acutely in the north and southeast, with prolonged droughts more common in the south. SPI and SPEI peak values were recorded in the northern and southeastern extremes, underscoring the basin's severe drought conditions. This trend aligns with African-wide declines in rainy days and wet sequences since the 1970s (Balliet et al., 2016; New et al., 2006).

Using daily precipitation data from 18 stations across the BPNRB, this study documents spatial and temporal characteristics of consecutive dry days (CDD) during the rainy season (May-September) and annually. CDD exhibited notable latitudinal variation, reaching up to 180 days annually, while dry spells during the rainy season lasted up to 18 days. Both annual and rainy-season CDD showed a statistically significant increase ($p < 0.05$), consistent with Alamou et al., (2022) and Quenum et al., (2019), who reported

rising CDD trends in the BPNRB and Sahel. These trends pose challenges for rain-fed agriculture, especially in rural areas.

An analysis of SDI fluctuations also highlights dry-wet cycles with a significant upward trend at most hydrometric stations ($p < 0.05$) over 1970-2020. A prolonged dry period from 1970-1990 affected all stations, with drought duration and intensity varying across the basin. The Sota sub-basin (Gbassè and Couberi stations) had the longest droughts, while the Mekrou sub-basin (Kompongou station) showed the highest intensities, likely influenced by distinct geographic and human pressures. These findings align with Badou et al., (2017), who documented precipitation and runoff declines consistent with a major drought ending in 1992.

A cross-analysis of the time series for SPI, SPEI, and SDI reveals upward trends for SPI and SDI, with a downward trend for SPEI. The divergence between SPI and SPEI is largely due to the effects of evaporation and temperature in the SPEI calculation, reflecting increased evaporative demand from rising temperatures. These findings align with other studies, including (Hulme et al., 2001) on the Niger River Basin, (Sun et al., 2023) in China, and (Mohammed et al., 2022) and (Alsafadi et al., 2022) in other regions.

Additionally, a notable mismatch between SPI (rainfall) and SDI (discharge) peaks may relate to the "Sahelian paradox." While decreased rainfall might logically reduce water resources, the Sahel has paradoxically seen a net increase in runoff and surface water. First documented by (Albergel et al., 1989) in Burkina Faso, this paradox remains widely debated, intersecting with broader discussions on desertification versus regreening in the Sahel.

In general, the trends in rainfall and streamflow variability observed in the Niger River catchments of northern Benin from 1970 to 2020 align with patterns reported across West Africa, but they raise interesting questions about regional differences. For total rainfall, our results show an increase largely driven by a higher number of rainy days. We also find an increasing spatial variability, which aligns with earlier findings by Salack et al. (2016) and Sanogo et al. (2015). They pointed to increasing rainfall variability across the region, particularly in sub-seasonal rainfall patterns. This change could reflect the

weakening of the monsoonal system so that rain is delivered more evenly across the region (Biasutti, 2019).

Our analysis reveals negative trends in mean wet day amount and rainfall variability at the catchment scale (as indicated by the standard deviation and coefficient of variation) across the study area. This result is in contrast to the general expectation and to other studies on the relation between rainfall variability and climate change, which suggest higher variability in a warmer world (Pendergrass et al., 2017; Zhang et al., 2021). There are several possible reasons for this mismatch. Firstly, the spatial scale plays a role. Our analysis is based on catchment rainfall time series. At the point scale of the 18 stations, we find a different behavior in terms of trends (not shown). At the station level, we find little changes in the mean wet day amount; the few stations that show statistically significant trends show upward trends. The mismatch between the station level and catchment level can be explained by the increasing spatial rainfall variability over the study period. The catchment mean wet day amount is higher in the earlier periods, because a higher number of stations receive rainfall at the same day. In the later periods, with more localized rainfall, the catchments tend to include also dry areas which decreases the average catchment rainfall on wet days. Secondly, other studies are often based on climate model simulations. For instance, Pendergrass et al. (2017) find for West Africa that the CMIP5 multi-model mean of the standard deviation of daily rainfall increases in 2071–2100 relative to 1976–2005. Scaled by the change in global mean surface air temperature, this increase is around 5-10% per 1K and is considered a robust result, with at least 67% of models in agreement on the sign of the change. Observation-based studies are rare, particularly in West Africa. The global analysis by Pendergrass et al. (2017) also presents changes in the standard deviation of daily rainfall based on observations. However, their analysis does not include a single station across West Africa. In addition, their station-based analysis demonstrates that, although the global median change in rainfall variability is positive (~10% per 1K), there is a huge spread in observation-based results from -100% to + 200% per 1K. This spread can be explained by the manifold mechanisms at play in rainfall generation, comprising thermodynamic and dynamic changes in a warmer world (Zhang et al., 2021). The increasing variability has been explained by increasing atmospheric moisture availability in a warmer atmosphere

(Akinsanola et al., 2020; J. R. Brown et al., 2017). On the other hand, the weakening of tropical atmospheric circulation in a warmer world has been hypothesized to counteract increasing variability (He & Li, 2019). Moreover, we find similar changes in the mean and the standard deviation of daily rainfall. This similarity suggests that the decrease in variability that we observe in the catchment rainfall follows from the decrease in mean rainfall. For example, scaling the values of a positive variable by a constant results in a change in the standard deviation equal to the change in its mean (Pendergrass et al., 2017; Rind et al., 1989). The observed decline in extreme daily rainfall (99th percentile) across the three catchments may be attributed to catchment-wide rainfall, which, being spatially averaged, may not fully capture extreme events (Luini & Capsoni, 2012). In monsoon-dominated regions such as West Africa, changes in circulation patterns can lead to an extended rainy season with more frequent but less intense rain events. Some studies suggest that the West African Monsoon (WAM) onset is occurring earlier, contributing to more rainy days overall (Akinsanola et al., 2020; Salack et al., 2016). Shifts in monsoon dynamics and reduced monsoon intensity can weaken individual rain events, leading to less intense wet days (Dunning et al., 2018).

Conclusion

This study examined the spatiotemporal patterns of meteorological and hydrological droughts in the Beninese part of the Niger River Basin from 1970 to 2020. Meteorological droughts were assessed using SPI and SPEI based on daily precipitation data from 18 climate stations, while hydrological droughts were determined through SDI from daily discharge data at four hydrological stations (Yankin on the Alibori, Gbassè and Couberi on the Sota, and Kompongou on the Mekrou). Key findings include the following: -Significant spatiotemporal variability in drought distribution was observed, with meteorological and hydrological droughts prevalent from 1970 to 1990. Short-duration droughts were widespread, while prolonged droughts were concentrated along the basin's borders with Niger and Burkina Faso; -CDD values showed a statistically significant increase ($p < 0.05$) both annually and during the rainy season, with up to 180 rainless days and 18-day dry spells; -SDI values fluctuated from 1970 to 2020, indicating an overall rise in drought duration and intensity across sub-basins since the 1970s.

Northern Benin is a drought-prone region and is highly vulnerable to climate variability as its main economic activity is rain-fed agriculture. Understanding the variability of rainfall and streamflow, and how this variability relates to global warming and climate teleconnections is highly relevant for drought management and climate adaptation. With access to a comparatively dense network of stations, we analyze the catchment rainfall and streamflow for three tributaries of the Niger River for the period 1970–2020.

We find that total rainfall and mean streamflow during the rainy season show a high interannual variability, often a zigzag pattern at the biannual scale. There is also substantial decadal-scale variability. While the first two decades are characterized by persistently dry conditions, the last three decades show a recovery with increasing total rainfall and mean streamflow. The long-term changes in seasonal rainfall show an intricate pattern, consistent across the three catchments. Total catchment rainfall has increased despite a significant decrease in the mean wet day amount of rainfall. This counterintuitive result is explained by a strong increase in the number of wet days. The spatial variability of daily rainfall also increased during our study period. These results can be summarized as ‘increased total rainfall, but less intense and with higher spatial variation’. Contrary to the general expectation, our results show a decrease of daily rainfall variability at the catchment scale with higher temperature in northern Benin. This decrease may be a consequence of the decrease in the mean wet day amount, which in turn is a consequence of the increase in spatial rainfall variability.

CHAPTER 5: ASSESSMENT OF THE PREDICTIVE SKILLS AND THE PREDICTABILITY OF DROUGHT

Weather and climate significantly impact agricultural production in many regions worldwide. In tropical and subtropical areas, monsoon rainfall is especially crucial for the income of many smallholders (Shikwambana et al., 2021). Typically, normal rainfall conditions are associated with better crop yields. Conversely, prolonged dry periods or delayed onset of the rainy season can result in crop failures, threatening food security (Dobor et al., 2016; Waongo et al., 2015). Thus, providing reliable rainfall forecasts for the upcoming rainy season is essential for many national weather services in these regions. The climate in this area is primarily influenced by the West African Monsoon and its large-scale patterns. The main results presented in Sections 5.1 and 5.2 have been published in Journal of Hydrology: Regional Studies (Elsevier, 2025, Vol. 59, 102319) and are available at the following link: https://doi.org/10.1016/j.ejrh.2025.102319.

5.1. Teleconnections between ENSO, AMO, DMI, and rainfall and streamflow

Here, we investigate to what extent rainfall and streamflow variability in the three catchments are modulated by climate teleconnections. We select climate modes representing sea surface temperatures of the Pacific (Niño 3.4), Atlantic (AMO), and Indian (DMI) oceans. The WTC (wavelet transform coherence) is used to understand the multiscale association between these climate indicators and rainfall (Figure 26) and streamflow (Figure). In this study, correctly interpreting the Cone of Influence (COI) is essential for accurate analysis of periodicities and climate variability. The COI defines the region in a wavelet power spectrum where edge effects become significant due to the finite length of the time series. As wavelet analysis involves convolution with a localized function, the accuracy of computed power is reduced near the boundaries, leading to uncertainty in these regions. The COI is typically represented as a cone-shaped area at both ends of the time axis, often shaded or marked by a lighter color to indicate where results should be interpreted with caution (Grinsted et al., 2004; Torrence & Compo, 1998). The light area in the figure typically represents the Cone of Influence (COI). This region is often shaded lighter or marked differently to indicate where edge effects make

the wavelet power estimates less reliable. In contrast, the dark area represents the region where wavelet power values are more trustworthy.

Before analysing the coherence between variables, we performed a wavelet analysis for the individual variables. Catchment rainfall and streamflow of the three catchments show statistically significant (at the 5% level) variations at the time scale of 2–7 years and 2–4 years, respectively (Fig. 37 in the annex). However, these are episodic in nature, from a few years to up to 15 years. Nino 3.4 shows significant variability at the time scale of 3–6 years during the period 1980–2000. DMI and AMO show significant periodicities of 2–4 years, but for shorter episodes. Possible decadal periodicities of these two indices cannot be well identified with the given time series length of 50 years.

A significant coherence between Nino3.4 and catchment rainfall is found at the timescale of 4–7 years from 1971 to the early 1980s for all three catchments (Figure 26a–c). In addition, short periods of coherence are found at the 1–2 year and 3–4 year timescales for catchment B3 from around 1997 to 2005. At all scales, positive SST values in the Niño 3.4 region were associated with a rainfall deficiency in North Benin. A positive association between ENSO and a rainfall drought index at the timescale of 4–8 years was also reported by Ogunrinde et al. (2024) for the Sahel Region of Nigeria during 1981-1999.

Regarding the relationship between AMO and rainfall, a significant coherence is evident at the decadal scale for the early decades for all three catchments (Figure 26d–f). The direction of the arrows reveals that a positive anomaly in the Atlantic Ocean led to a positive rainfall anomaly in North Benin. However, this coherence at the decadal timescale ended in the early 1990s. Similar to the CWT of ENSO and rainfall, there are episodic periods of coherence at the scale of 1–4 years for B2 and B3. Previous studies reported that a decline in Sahel rainfall during the 1980s is linked to a positive phase of the tropical Atlantic Ocean at the decadal timescale (Camberlin et al., 2001; Dieppois et al., 2015).

The WTC between the DMI (representing the Indian Ocean) and rainfall shows significant coherence at 4–8 years from the 1970s to the late 1980s across the three catchments (Figure g–i). Both signals are out of phase, indicating that a positive phase of the Indian

Ocean was associated with a rainfall deficit in North Benin. Significant coherence is also found at the decadal scale for the period 2005–2020. Here, the two signals are positively correlated. However, this region of coherence is outside the COI.

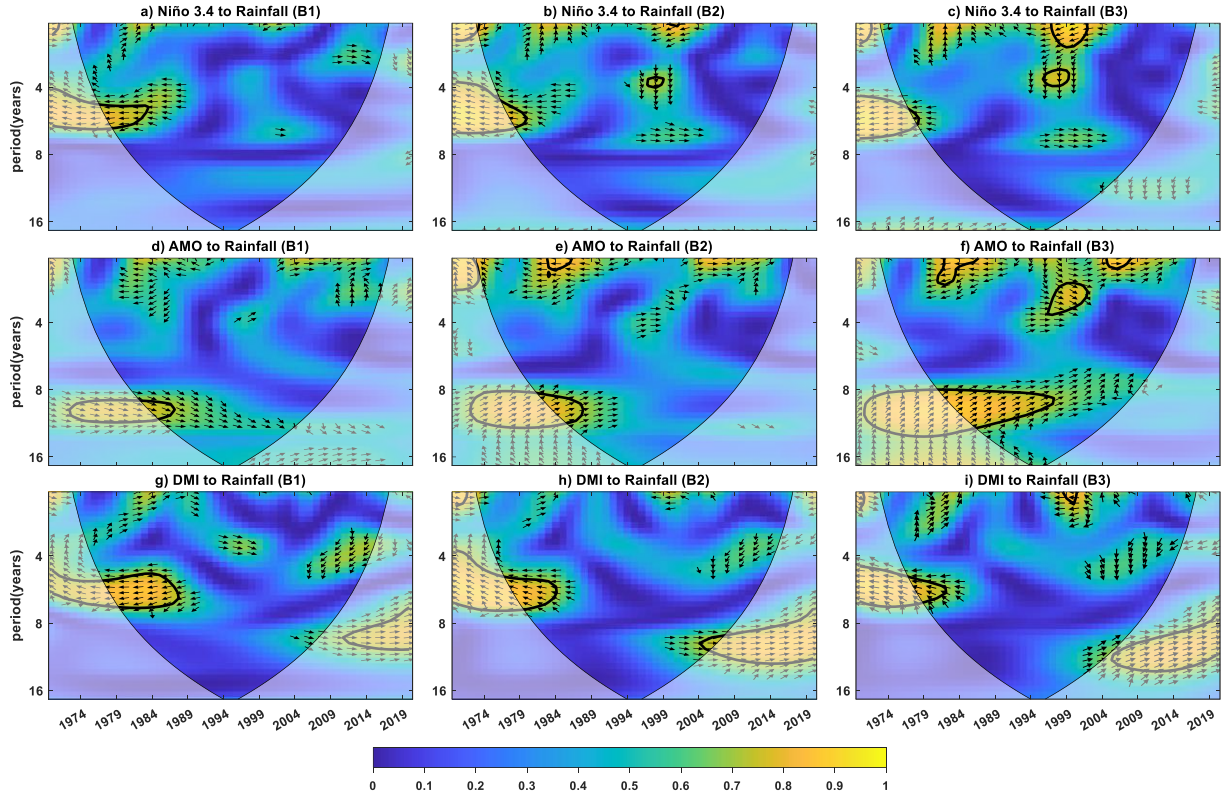

Figure 26: Wavelet transform coherence between climate teleconnections ENSO (a–c), AMO (d–f), DMI (g–i) and annual catchment rainfall for B1–B3. Colors code the coherence between the two signals and black contours represent statistical significance at the 5% significance level.

Figure 27 shows the relation between the three climate teleconnections and streamflow for the catchments B1–B3. The arrows indicate the lead-lag relationship: pointing to the right: both signals are in phase and positively correlated; pointing to the left: signals are anti-correlated; pointing down/up: the ocean index leads the rainfall by 90°/270°. The cone of influence (COI) is indicated by a thin solid line and shows the region where the results are affected by edge effects. A significant coherence between Nino3.4 and streamflow is found at the 3–7 year timescale for the 1970s for all three catchments (Figure a–c). However, this coherence is influenced by edge effects and not reliable. Catchment B3 shows coherence at the scale of 1–4 years for 1996–2004 and at the scale of 10–14 years for 1976–2020. Most of the areas of coherence indicate a negative

correlation between ENSO and streamflow. Overall, the coherence between ENSO and streamflow in the three catchments is mostly consistent with the coherence between ENSO and rainfall. Similar to rainfall, our results indicate that ENSO modulated streamflow variability in our study area. However, the association at the decadal scale is not significant in the WTC of ENSO and rainfall.

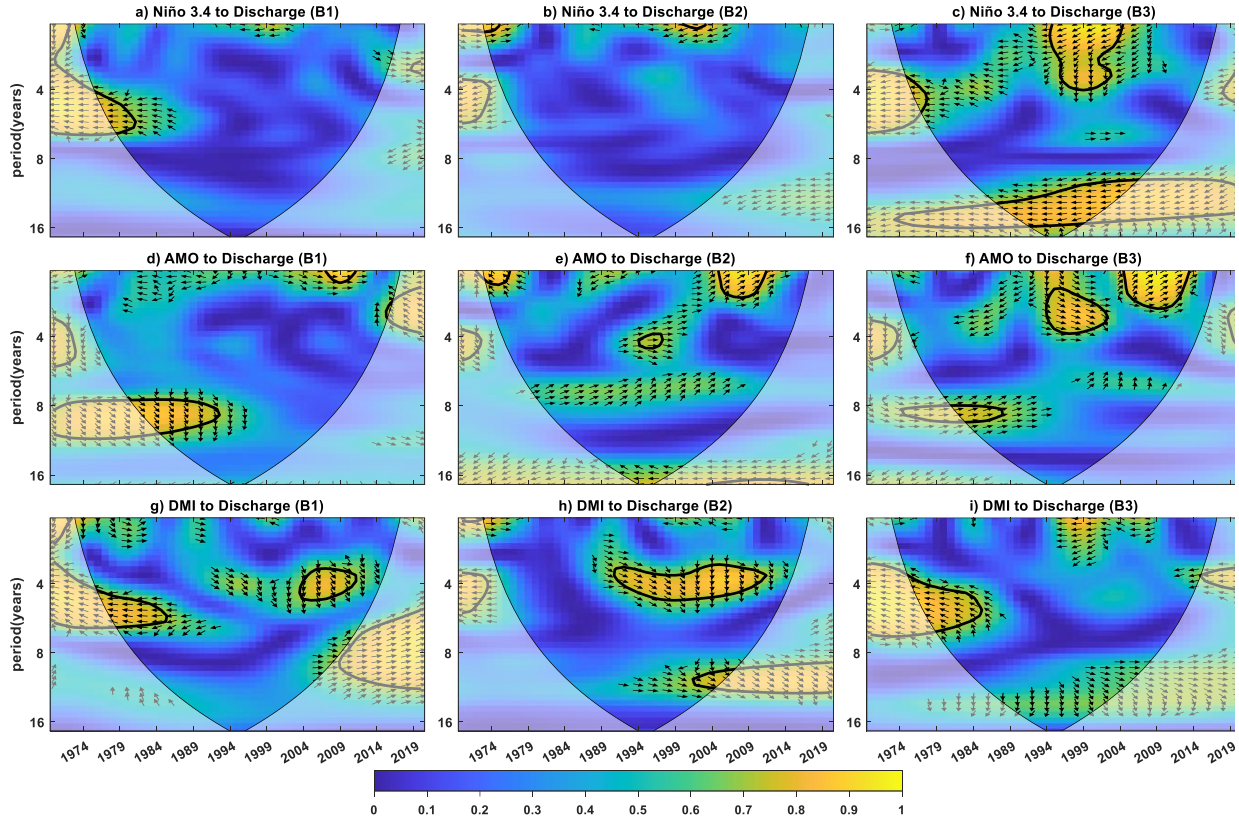

Figure 27: Wavelet transform coherence between climate teleconnections ENSO (a–c), AMO (d–f), DMI (g–i) and annual streamflow for B1–B3. (Colors etc. as in Figure 26.)

The WTC between AMO and streamflow shows significant coherence at the 8–10 year scale for the early decades in B1 and B3 (Figure 27d-f). For all three catchments, short periods of significant coherence are found at the interannual scale (1–4 years). All coherence periods are characterized by a positive association between AMO and streamflow. Overall, the coherence characteristics between AMO and streamflow agree broadly with those of AMO and rainfall. However, care must be taken while interpreting due to the imputation of a few missing data.

Regarding the association with DMI, a significant anti-phase relationship at the 3–7 year timescale is found for B1 and B3 for the early decades (Figure g-i). In the second half of our study period, significant coherence occurs at the 3–5 year timescale, with DMI leading streamflow variability by approximately three years. In all three catchments and in the recent decades, coherence is found at lower frequencies (up to 15 years), however, this coherence is mostly outside the COI.

Our findings reveal that Niño 3.4 and AMO are important to understand the changes in the rainfall at the 1-4 year timescale for the catchments B2 and B3. There is a tendency for a change in the coherence between the climate indices and rainfall between the first and the last decades. In the first decades, we find mostly coherence at lower frequencies (around 4–10 years), while in the last decades, we find episodic periods of coherence at the timescales of 1–3 years. This pattern in the last decades was not reported in earlier studies. In relation to streamflow, there are some periods of significant coherence, however, the similarity between the catchments is much lower compared to rainfall. This is explained by the additional processes that impact catchment streamflow.

5.2. Evaluation of the CHIRPS rainfall data

After applying a spatial mask corresponding to the catchment boundaries, daily catchment rainfall was obtained by spatially averaging the rainfall data across all grid points within a catchment. We find a very good agreement with Spearman correlation coefficients of about 0.95 between the catchment rainfall obtained from these two data sources (Figure 28 and Table 4).

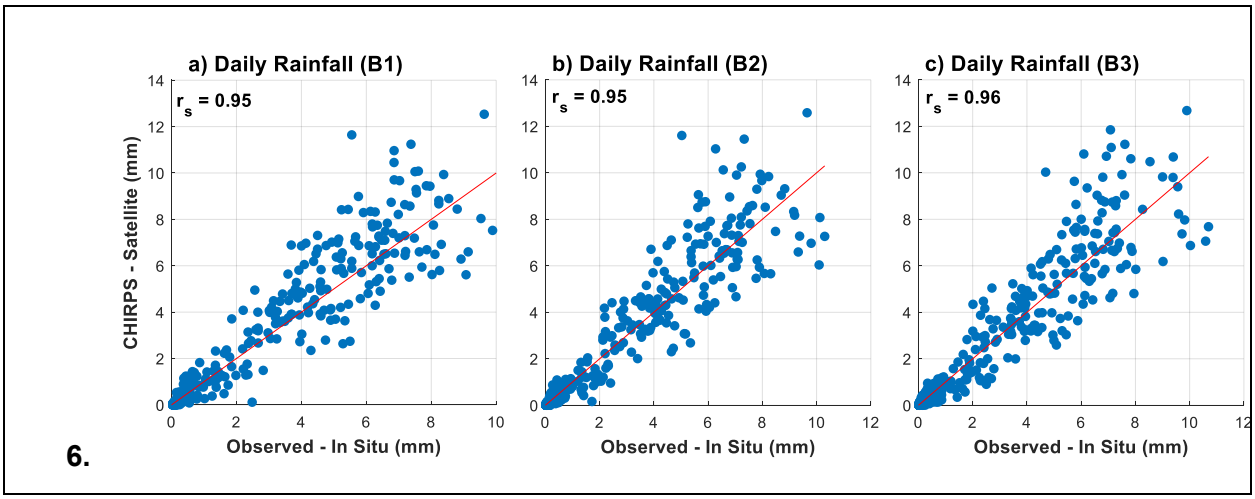

Figure 28: Comparison of daily catchment rainfall derived from the 18 stations and from CHIRPS satellite data for the three catchments B1 – Sota River (a), B2 – Alibori River (b), and B3 – Mekrou River (c).

Table 4: Comparative statistical analysis between CHRIPS and catchment-based rainfall data at a daily scale for the three catchments B1-B3.

Sub-basins	Statistical Indicators		
	NSE	R Spearman's rs	Spearman (p-Value)
Sota (B1)	0.84	0.95	$<2.2\times10^{-16}$
Alibori (B2)	0.85	0.95	$<2.2\times10^{-16}$
Mekrou (B3)	0.84	0.96	$<2.2\times10^{-16}$

5.3. Selection of the most promising predictors

A total of 12 climate teleconnection indices were considered as potential predictors. Before applying multivariate models, it is crucial to select the most relevant ones. To do this, we use the Spearman correlation coefficient to identify the strongest predictors of rainfall anomalies. This process involves analyzing the correlation between CHIRPS rainfall during the rainy season and SST indices, with statistical significance assessed at the 5% level. Grid points where the correlation is significant are highlighted in sky blue (Figure 29), and the total number of significant points is reported in Table 5. A higher number of significant grid points indicates a stronger predictor.

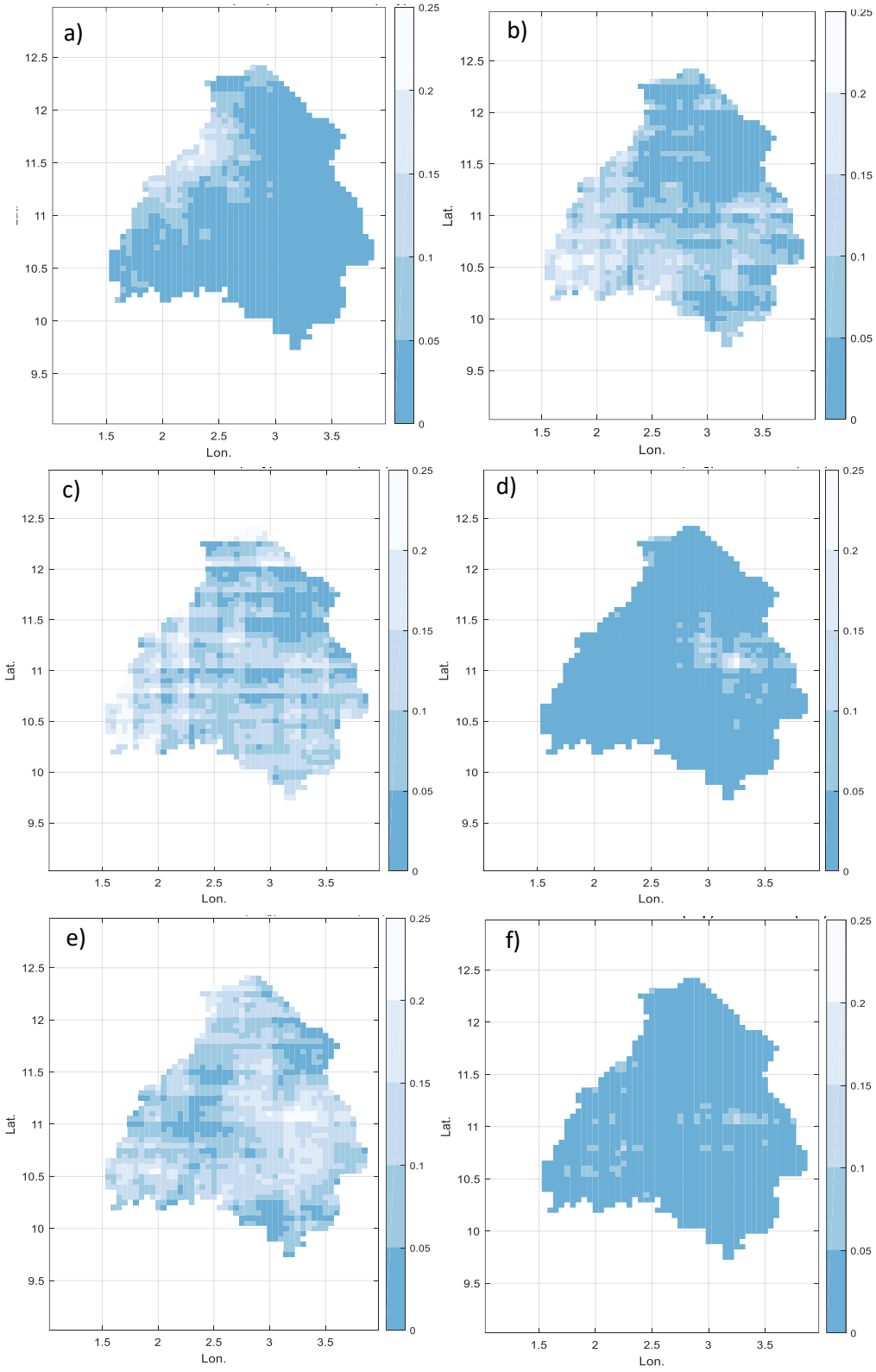

Figure 29: Correlation between seasonal rainfall anomalies and predictors: a) Nino 3.4 SST (May) vs. Anomalies (June), b) PDO SST (Oct) vs. Anomalies (July), c) PDO SST (Nov) vs. Anomalies (July), d) DMI SST (Oct) vs. Anomalies (Aug), e) DMI SST (Nov) vs. Anomalies

(Aug), f) DMI SST (Nov) vs. Anomalies (Sep). Sky-Blue represents statistical significance at the 5% level, while light color indicates no significance in the grid cell.

Table 5: The most promising predictors were identified based on the Spearman correlation coefficient was used between CHIRPS rainfall during the rainy season and various SST indices. The number of grid points where the correlation is significant at the 5% level is reported in brackets. The month associated with each SST index represents the time period for which the SST value was considered.

SSTpredictors	**Predictand (June)**	**Predictand (July)**	**Predictand (Aug)**	**Predictand (Sep)**
AMO	Oct (68.4%) Nov (69.2%) Dec (39.7%)	Oct (22.7%) May (31.0%)	Jan (<1%) Feb (2.3%)	Mar (<1%)
DMI	oct (61.0%) Nov, Dec (100%)	Oct (41.2%) Nov (95.8%) Dec (99.9%)	Dec (82.3%) Nov (92.3%) Oct (15.2%)	Oct (38.2%) Nov (76.8%) Dec (42.0%)
PDO	oct (71.2%) Nov (95.8%) Dec (69.8%)	Oct (23.5%) Nov (18.3%) Dec (23.5%)	Jan (4.2%) Fev (3.8%)	-
Nino34	oct (98.9%) Nov (96.9%) Dec (96.29%) May (80.4%)	Oct (92.6%) Nov (92.8%) Dec (95.0%)	Apr (83.9%) May (92.3%) Oct (99.9%) Nov (99.9%)	Oct (100%) Nov(100%) Dec(100%)
Nino12	Oct (97.5%) Nov (93.1%) Dec (95.0%) Apr (97.5%)*	Oct (99.9%) Nov (100%) Dec (100%)	Oct (100%) Nov (100%) Dec (100%)	Oct (100%) Nov (100%) Dec (100%)
NAT	Oct (68.4%) Nov (69.2%) Dec (39.7%)	Oct (22.7%) Nov (5.1%)	Feb (2.3%)	-
SAT	Jan (99.8%) Feb (100%) Mar (99.8%)	Oct (98.3%) Nov (93.5%) Jan (92.4%) Feb (87.9%)	Jan (13.6%) Oct (84.5%) Nov (63.9%) Dec (11.9%)	Oct (71.6%) Nov (47.6%)
SETIO	Oct (93.5%) Nov (100%) Dec (100%)	Oct (46.3%) Nov (93.9%) Dec (99.6%)	Nov (44.6%) Dec (42.7%)	Nov (28.9%) Dec (11.0%)
SWIO	Oct (64.6%) Nov (100%) Dec (100%)	Oct (60.1%) Nov (99.6%) Dec (100%)	Oct (17.5) Nov (98.9%) Dec (99.5%)	Oct (43.1%) Nov (89.6%) Dec (79.6%)
TNI	Oct (99.1%) Nov (100%) Dec (99.6%)	Oct (61.1%) Nov (72.5%) Dec (68.3%)	Jun (2.5%) Dec (6.9%)	May (19.4%) Jun (28.3%) Dec (6.9%)
TASI	Oct (99.9%) Nov(100%) Dec (99.9%)	Oct (89.6%) Nov (13.2%) Dec (9.6%)	Oct (<1%)	Jun (4.7%)
WTIO	Oct (61.0%) Nov (100%) Dec (100%)	Oct (41.2%) Nov (95.8%) Dec (99.9%)	Oct (15.2%) Nov (92.3%) Dec (82.3%)	Oct (38.2%) Nov (76.8%) Dec (42.3%)
Proposed Best predictors	Nino34, Nino12, SAT, TASI, SWIO	Nino34, Nino12, SAT, SWIO	Nino34, Nino12, SWIO, DMI	Nino34, Nino12, SWIO

5.4. Building and improvement of a multilinear regression model for each predictand

The multilinear regression model plays a crucial role in understanding and predicting rainfall anomalies, which are essential for drought forecasting. The model summary provides an overview of the relationship between climate predictors, such as SST indices, and rainfall, highlighting how well these variables explain the observed anomalies. The coefficients reveal the strength and direction of each predictor's impact, with statistically significant predictors providing insight into which oceanic or atmospheric factors most influence rainfall variability. The residuals allow for a check on model fit, ensuring that the model appropriately captures the variance in rainfall patterns without systematic errors. Meanwhile, the fitted values provide the predicted rainfall anomalies, offering a forecast that can inform early warning systems and agricultural decision-making.

The most promising predictors were used to build a multilinear regression model for each predictand, representing rainfall anomalies for June, July, August, and September. The metrics values progressively improve like R-squared from 0.58 in June to 0.7 in September, indicating that the chosen predictors capture a significant portion of the variability in the rainfall anomalies, with better performance in the later months.

The increasing metrics suggest that the selected predictors, such as SST indices, have a stronger relationship with rainfall anomalies as the season progresses. This may be linked to seasonal patterns where oceanic teleconnections (like Niño indices, Indian Ocean SSTs, or Atlantic Ocean SSTs) influence rainfall more distinctly during mid to late monsoon months.

Table 6: *Parameters of the multilinear regression model for each predictand.*

Model	Beta				Standard Error				t-Statistic				P-value			
	Jun	Jul	Aug	Sep	Jun	Jul	Aug	Sep	Jun	Jul	Aug	Sep	Jun	Jul	Aug	Sep
Intercept	-0.00	-0.000	-0.00	-0.000	0.094	0.082	0.079	0.069	-2.04e-06	-2.93e-06	-1.99e-06	-3.36e-06	1	1	1	1
X_1	-0.526	-0.365	-0.055	-0.347	0.763	0.452	0.642	0.381	-0.689	-0.809	-0.085	-0.911	0.499	0.429	0.933	0.375
X_2	-0.817	-0.433	0.264	-0.307	0.517	0.293	0.225	0.247	-1.582	-1.475	1.174	-1.249	0.132	0.158	0.257	0.232
X_3	-0.952	0.382	-1.763	0.546	0.643	0.303	0.678	0.255	-1.480	1.262	-2.600	2.136	0.157	0.223	0.019	0.047
X_4	1.018	-1.864	-0.320	-1.603	0.846	0.705	0.467	0.594	1.203	-2.644	-0.685	-2.696	0.245	0.017	0.503	0.015
X_5	-1.390	2.223	0.802	-0.478	0.805	1.043	0.611	0.409	-1.726	2.132	1.313	-1.167	0.102	0.047	0.207	0.259
X_6	1.640	0.833	0.439	-1.622	1.192	0.635	0.480	0.882	1.376	1.312	0.914	-1.839	0.186	0.206	0.373	0.083
X_7	0.961	0.657	2.20	2.0229	0.725	0.499	1.00	0.879	1.325	1.316	2.19	2.299	0.202	0.205	0.043	0.034
X_8	-0.955	-0.949	-0.618	1.086	0.556	0.487	0.468	0.535	-1.716	-1.949	-1.319	2.027	0.104	0.067	0.205	0.058

Table 7: Multilinear regression model performance for each predictand

Predictand	R^2	MSE	RMSE	P-value	Predictors' months	Associate equation ($\beta_0 = 0$)
June	0.58	0.150	0.38	0.09	$Nino3.4_{oct}$, SAT_{oct}, $SWIO_{oct}$, $TASI_{oct}$, $Nino3.4_{nov}$, SAT_{nov}, $SWIO_{nov}$, $TASI_{nov}$	$y = -0.526(Nino3.4_{oct}) - 0.817(SAT_{oct}) - 0.952(SWIO_{oct}) + 1.018(TASI_{oct}) - 1.390(Nino3.4_{nov}) + 1.640(SAT_{nov}) + 0.961(SWIO_{nov}) - 0.955(TASI_{nov})$
July	0.60	0.18	0.42	0.07	$Nino3.4_{nov}$, $Nino1.2_{nov}$, $SWIO_{nov}$, SAT_{nov}, $Nino3.4_{dec}$, $Nino1.2_{dec}$, SAT_{dec}, $SWIO_{dec}$,	$y = -0.365(Nino3.4_{nov}) - 0433(Nino1.2_{nov}) + 0.382(SWIO_{nov}) - 1.864(SAT_{nov}) + 2.223(Nino3.4_{dec}) + 0.833(Nino1.2_{dec}) + 0.657(SAT_{dec}) - 0.949(SWIO_{dec})$
August	0.62	0.13	0.36	0.05	$Nino3.4_{nov}$, $Nino1.2_{nov}$, DMI_{nov}, $SWIO_{nov}$, $Nino3.4_{may}$, $Nino1.2_{dec}$, DMI_{dec}, $SWIO_{dec}$	$y = -0.05(Nino3.4_{nov}) + 0.264(Nino1.2_{nov}) - 1.763(DMI_{nov}) - 0.320(SWIO_{nov}) + 0.802(Nino3.4_{may}) + 0.439(Nino1.2_{dec}) + 2.20(DMI_{dec}) - 0.618(SWIO_{dec})$
September	0.70	0.129	0.35	0.04	$Nino3.4_{nov}$, $Nino1.2_{nov}$, DMI_{nov}, $SWIO_{nov}$, $Nino3.4_{oct}$, $Nino1.2_{dec}$, $Nino3.4_{dec}$, $SWIO_{dec}$	$y = -0.347(Nino3.4_{nov}) - 307(Nino1.2_{nov}) + 0.546(DMI_{nov}) - 1.603(SWIO_{nov}) - 0.478(Nino3.4_{oct}) - 1.622(Nino1.2_{dec}) + 2.023(Nino3.4_{dec}) + 1.086(SWIO_{dec})$

Interpretation

- In June (R^2 = 0.58): The model performs moderately. This may manifest as noticeable deviations from the straight line on the Q-Q plot, particularly at the tails (Figure 30-a). This indicates challenges in capturing the variability of rainfall anomalies early in the monsoon season. This may be due to the transitional nature of early monsoon patterns, where a wider range of factors influences variability, and atmospheric patterns may not yet be fully established.
- For July (R^2 = 0.6): The predictands show improved alignment with standard normal quantiles, though some deviations may still be visible, reflecting better but not perfect model performance (Figure 30-b). The slight improvement suggests better predictive capacity, possibly due to more stable monsoon conditions, where ocean-atmosphere interactions become more pronounced.
- In August (R^2 = 0.62): Predictands likely align closely with standard normal quantiles, particularly in the central portion of the distribution, indicating that the model effectively captures the mid-season rainfall patterns (Figure 30-c). The model continues to improve, reflecting stronger relationships between rainfall and SST indices. This is typically the peak of the rainy season, and the predictors capture significant rainfall variability.
- As for September (R^2 = 0.7): The highest R^2 value implies the strongest alignment between predictands and standard normal quantiles (Figure 30-d). This reflects the model's robust performance in capturing late-season rainfall variability. The best performance is observed, likely due to the well-established teleconnection impacts by the late season. Oceanic conditions during this period may be more predictive of rainfall anomalies.
- In addition, the RMSE values obtained for the four predictands were 0.38 (June), 0.42 (July), 0.36 (August), and 0.35 (September), indicating relatively low prediction errors and acceptable model performance across months.

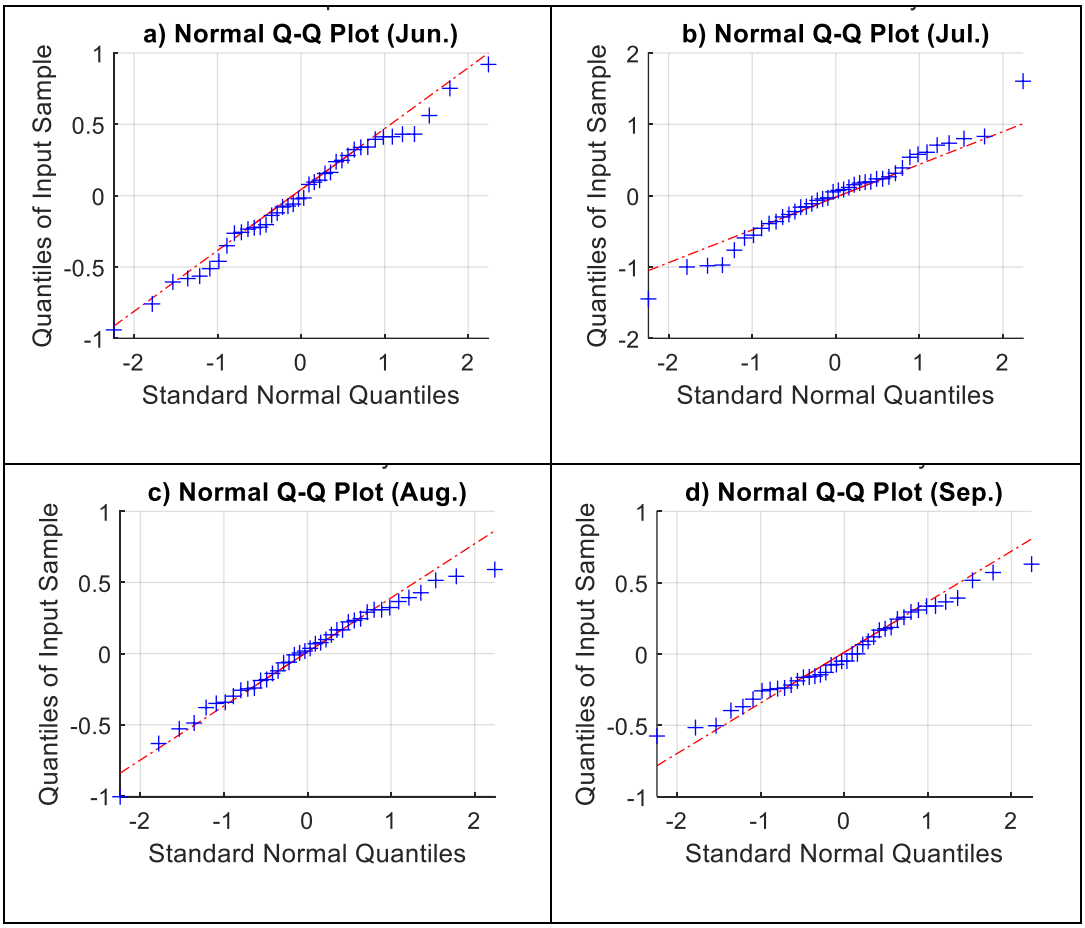

Figure 30: Quantiles of predictands (a) June, (b) July, (c) August, (d) September Vs. standard normal quantiles.

5.5. Discussion

The climate teleconnections ENSO, AMO and DMI, representing sea surface temperature anomalies in the Pacific, Atlantic, and Indian Oceans, respectively, have some association with catchment rainfall and streamflow in Northern Benin. The WTC between Nino 3.4 and catchment rainfall is similar to the one between Nino 3.4 and streamflow. In both cases, positive sea surface temperature values in the Niño 3.4 region are associated with negative anomalies in North Benin. Overall, our results agree with earlier studies that have emphasized the role of ENSO for climate variability in West Africa and that have linked El Niño to droughts in West Africa (Nicholson, 2000; Roudier et al., 2014, Ogunrinde et al., 2024). ENSO is known to significantly affect the Walker Circulation, which in turn influences weather patterns in the tropical regions of West Africa (Yeh et al.,

2018). During a positive ENSO phase (El Niño), the Walker Circulation weakens or shifts eastward, resulting in changes in atmospheric circulation patterns that typically lead to drier conditions in many regions of West Africa. This weakening can disrupt the westward flow of moist air from the Atlantic, reducing the convergence of moisture over West Africa, which can lead to a decrease in rainfall and thus to potential drought conditions. Based on these dynamics, one would generally expect a positive ENSO (El Niño) event to be associated with rainfall deficiencies in West Africa. Our results indicate some coherence between ENSO and Northern Benin rainfall variability, which is consistent with this expectation. However, significant coherence is only found for rather short episodes. Regional factors, such as the position and strength of the Intertropical Convergence Zone (ITCZ) and the West African Monsoon, can modulate these general patterns.

The relationship between AMO and catchment rainfall or streamflow, respectively, shows a statistically significant coherence at the decadal time scale for the early decades for all three catchments (with the exception of B2 streamflow). A positive anomaly in the Atlantic Ocean led to a positive anomaly in North Benin. This coherence at the decadal time scale ended in the early 1990s, after which short episodes of coherence are found at the time scales of 1–4 years. However, most of the episodic periods of high coherence are largely outside the Cone of Influence (COI) region.

In terms of DMI, we find significant anti-phase coherence at 4–8 years (1970s–1980s), emphasizing early decadal impacts and a notable positive correlation at decadal scales (2005–2020), which suggests an evolving influence of IOD in recent decades. However, some regions of coherence fall outside the Cone of Influence (COI), requiring cautious interpretation. Earlier studies (Nicholson & Selato, 2000) emphasized DMI's role in rainfall variability, with limited attention to hydrological responses. Our work shows DMI leading streamflow variability by approximately 3 years at the 3–5 year scale, providing new evidence of delayed hydrological responses to DMI.

The DMI and the AMO patterns appear to be more relevant for rainfall variability in our study area compared to ENSO. This highlights the significant influence of the Indian and Atlantic Oceans on regional climate patterns. While previous studies have emphasized the high influence of ENSO on West African climate, our findings suggest that DMI and

AMO may have a stronger impact in this particular region, possibly due to regional variations in climate drivers. However, the coherence at lower frequencies (up to 15 years) has not been documented in this region so far, offering insights into longer-term streamflow variability. Our analysis shows that ENSO, AMO and DMI are associated with rainfall variability in North Benin. Overall, we find a tendency for a change in the coherence between these climate indices and catchment rainfall between the first and the last decades. In the first decades, we find mostly coherence at lower frequencies (around 4–10 years), while in the last decades, we find episodic periods of coherence at the time scales of 1–3 years. These patterns in the last decades were not reported in earlier studies. In this study, we described these patterns at different frequencies over time. This has improved the understanding of how these teleconnections are associated with rainfall and streamflow at the catchment scale.

In relation to streamflow, there are some periods of significant coherence, however, the similarity between the catchments is lower compared to rainfall. This is explained by the additional processes that impact streamflow. The three catchments exhibit distinct land use changes, agricultural expansion, and resource pressures (Agblonon Houelome et al., 2022; Global Water Partnership & & PNE-Bénin, 2015; Sambieni et al., 2023, 2024). B1 is heavily impacted by intensive cotton farming and livestock production, leading to deforestation and high-water demand. B2, which includes conservation areas like Parc W, faces threats from cotton monoculture and unsustainable farming. B3 is experiencing rapid agricultural expansion, driving extensive land clearing and environmental degradation. While all catchments face deforestation and agricultural pressure, B1 has the highest land conversion rate, B2 balances conservation with agricultural threats, and B3 sees increasing mechanized expansion, especially for cotton. Water extraction is most severe in B1, while B2's protected areas provide some buffer. These differences in land use agricultural expansion, and resource pressures have altered runoff processes in different ways.

It is essential to acknowledge the limitations related to the relatively short length of our investigation period (1970–2020) when examining the influence of longer-term climate oscillations like AMO. The relatively short period of our observational data means that the

long-term phase shifts of the AMO may not be fully captured. Further research with extended time series data or climate model projections is needed to better isolate the influence of long-term climate oscillations and improve the robustness of the conclusions.

The analysis underscores the critical role of oceanic teleconnections in improving the predictability of seasonal rainfall anomalies. The progressively improving performance metrics, from R^2=0.58 in June to R^2=0.70 in September, highlight the effectiveness of predictors such as Niño indices, TASI, SAT, and SWIO in capturing rainfall variability. These findings emphasize the increasing relevance of ocean-atmosphere interactions as the monsoon season advances, where teleconnections play a pivotal role in modulating regional climatic conditions.

The teleconnections identified between sea surface temperature anomalies and drought patterns in the Niger River basin, particularly in northern Benin, provide valuable information for improving early warning and drought preparedness. Integrating these predictors into forecasting systems can improve the accuracy of seasonal forecasts, provide longer lead times, and facilitate adaptive planning. Such integration would strengthen water resource management and agricultural decisions through improved planting schedules, irrigation planning, and the promotion of drought-resistant crops, thereby promoting a shift from reactive to proactive and climate-resilient management.

Although CHIRPS and SST-based approaches provide valuable information in regions with limited observations, they also present notable limitations in data-sparse areas such as West Africa. The reliability of CHIRPS rainfall estimates is constrained by the scarcity of ground gauges used for bias correction, which can lead to spatial and temporal inconsistencies and underestimation of extreme rainfall events. Similarly, SST-based predictions face challenges due to the weak and non-stationary nature of teleconnections between oceanic anomalies and regional rainfall, as well as the limited representation of local climate and socio-environmental drivers such as land–atmosphere interactions and vegetation feedback. These limitations highlight the need for caution when interpreting drought or rainfall predictions and underscore the importance of integrating multiple data sources and hybrid modelling approaches to enhance prediction skill and robustness in

West Africa. Moreover, the integration of uncertainties would indeed enhance the robustness of the wavelet-based teleconnection analysis.

Conclusion

The wavelet transform coherence finds periods of significant coherence between the three climate indices and rainfall in the three catchments. Overall, there is a tendency of a shift from lower-frequency coherence (around 4–10 years) in earlier decades to higher-frequency coherence (1–3 years) in recent decades. These patterns are less pronounced for streamflow, which is more indirectly influenced by climate teleconnections. However, some regions of coherence fall outside the Cone of Influence (COI), requiring cautious interpretation. The steady improvement in performance metrics underscores the effectiveness of predictors such as Niño indices, TASI, SAT, and SWIO in capturing rainfall variability. These results highlight the growing influence of ocean-atmosphere interactions as the monsoon season progresses, with teleconnections playing a crucial role in shaping regional climate patterns. This influence is particularly important for seasonal prediction, as understanding the relationship between sea surface temperature anomalies and rainfall variability enhances forecast reliability. Such insights are invaluable for water resource management, agricultural planning, and disaster preparedness, especially in regions like West Africa, where rainfall variability significantly affects livelihoods and ecosystems.

CHAPTER 6: PROPOSED DESIGN FRAMEWORK FOR DROUGHT RISK MANAGEMENT IN THE STUDY AREA

Developing an effective Framework for Drought Risk Management begins with a thorough spatial and temporal assessment of historical hydro-meteorological droughts. By analyzing past drought events in both time and space, the framework can identify patterns of drought occurrence, intensity, and duration. This historical analysis provides crucial insights into the region's vulnerability to droughts over time and the areas most frequently affected. Survey-based insights are vital for understanding farmers' perceptions of climate change and hydroclimatic variability. By quantifying their knowledge, the framework reveals gaps in understanding drought drivers, highlighting the influence of factors such as age, education, and agricultural experience. In the northern part of Benin, no study has looked at the interrelationships between the perceptions, knowledge, and adaptation strategies of the populations in the face of climate change. The relevance of this study lies in quantifying farmers' understanding of hydroclimatic variability and identifying the factors that contribute to their understanding. The main results presented in Section 6.1, in particular 6.1.1, 6.1.2, 6.1.3, and 6.1.4, have been published in Frontiers Water Journal (Section Water and Climate, Volume 7-2025, 1530395) and are available at the following link: https://doi.org/10.3389/frwa.2025.1530395.

6.1. Case Study

6.1.1. Farmers' understanding of hydroclimatic variability

The understanding of the surveyed farmers of different aspects of hydroclimatic variability and climate change is summarized in

Figure 31. Averaged over all 14 questions, we found a 20.2% error rate and a 71% accuracy rate. This result reflects a substantial alignment between local perceptions and observed data. However, there are specific areas where knowledge is lacking, such as the link between global climate change and temperature increase (question 10). Here, more than 70% of the respondents were classified as wrong or mostly wrong. Our results also suggest that farmers have difficulties in understanding past changes in streamflow (questions 11, 12).

The 14 selected questions were used to quantify the knowledge of the farmers and the assignment of knowledge scores to the answers given. Questions with 2 options: wrong = 0; correct = 1; questions with 4 options: wrong = 0; mostly wrong = 0.33; mostly correct = 0.67; correct = 1.

Table 8: Assignment of knowledge score applied to answers given to the selected questions

No	Content of questions	Answers given	Assignment of knowledge score
Q1	How many rainy seasons do you have in your area?	1 rainy season 2 rainy seasons	1 0
Q2	In which month does the rainy season start in your locality?	April May June	1 1 0
Q3	How many months (n) does the rainy season last?	0< n < 3 3 ≤ n < 4 4 ≤ n ≤ 5 6 ≤ n ≤ 7	0 0.33 0.67 1
Q4	Has the start date of the rainy seasons changed?	Yes No	1 0
Q5	During the rainy season, are there days when it doesn't rain?	Yes No	1 0
Q6	If so, what is the average number of days (n) without rain?	0 < n < 3 3 ≤ n < 7 7 ≤ n < 10 10 ≤ n	0 0.33 0.67 1
Q7	How many months (n) does the dry season last?	5 ≤ n ≤ 6 others	1 0
Q8	In which month does the dry season begin in your locality?	October others	1 0
Q9	Do you think it is warmer than it used to be?	Yes No	1 0
Q10	If yes, what is the cause of the increase in temperature?	God's will; any religious or cultural beliefs that people assume as cause Bush fire, agriculture Deforestation, desertification, decline in rainfall Climate change, global warming	0 0.33 0.67 1
Q11	Has the average level of the rivers (B1, B2 and B3) fallen or risen compared with 30 years ago?	Fallen Risen	0 1
Q12	Do rivers dry up during the dry season?	Yes No	1 0
Q13	If yes, give the frequency with which the rivers dry up.	Every year Others	1 0
Q14	Did these rivers dry up with the same frequency 30 years ago?	Yes No	0 1

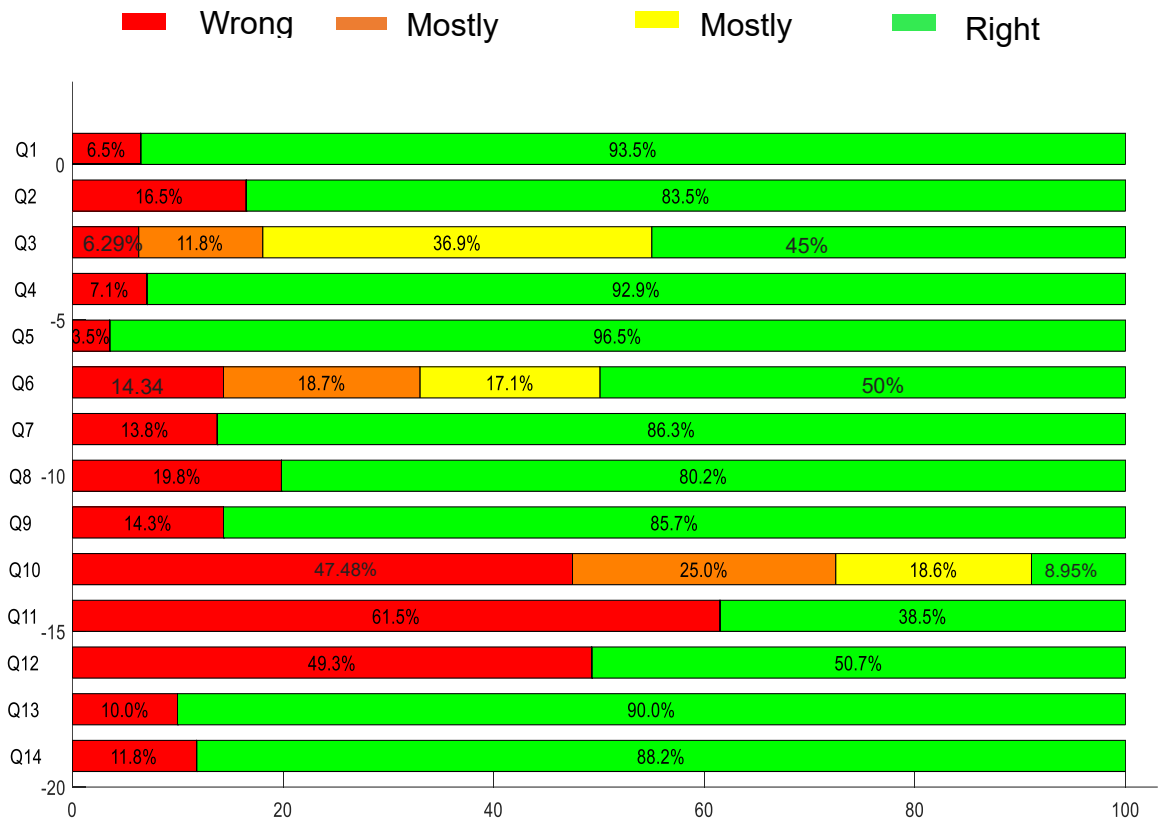

Figure 31: Correctness of the answers, averaged across all 509 farmers, to the 14 selected questions that allow comparison with observed hydroclimatic data.

6.1.2. Factors that contribute to the farmers' understanding

6.1.2.1. Distributions of the factors and the target variable

Before analyzing which factors influence how well the farmers understand hydroclimatic variability and climate change, we present how these factors and the target variable, i.e., the knowledge score, are distributed among the 509 respondents (Figure 32). More than 90% of the farmers are men, highlighting a significant gender imbalance in the agricultural sector (Figure 32-a). The majority of respondents are between 35 and 60 years old (Figure 32-b), with their experience in farming generally spanning from 10 to 40 years (Figure 32-c). The age distribution indicates that a significant proportion of the farmers are in their mid-to-late careers. However, this distribution is influenced by the age restrictions applied in the selection of the respondents (older than 35 years). Education within the agricultural

sector remains a challenge, as 63% of the farmers are either uneducated or have only completed primary school, while those with higher education (high school or university) are less involved in agricultural activities, leaving farming largely to the uneducated (Figure 32-e). 38% of the surveyed households engage in secondary activities to supplement their livelihoods, which is encouraged by the nature of rain-fed agriculture (Figure 32-f). The seasonal nature of farming allows for other income-generating activities during the off-season. This diversification helps mitigate risks from crop failure due to climate variability, improving financial stability and household resilience (Ozor, 2010). The large majority (77%) of the farmers show a technology/science-oriented view towards farming (Figure 32-g). Due to the poor quality of harvests, often attributed to climate variability, land degradation, and soil infertility, farmers seem to recognize the need for modern agricultural tools, fertilizers, and pesticides to improve yields. The distribution of the knowledge score indicates that many farmers in northern Benin are well aware of hydroclimatic variability, with an average knowledge score of 0.67 (Figure 32-h).

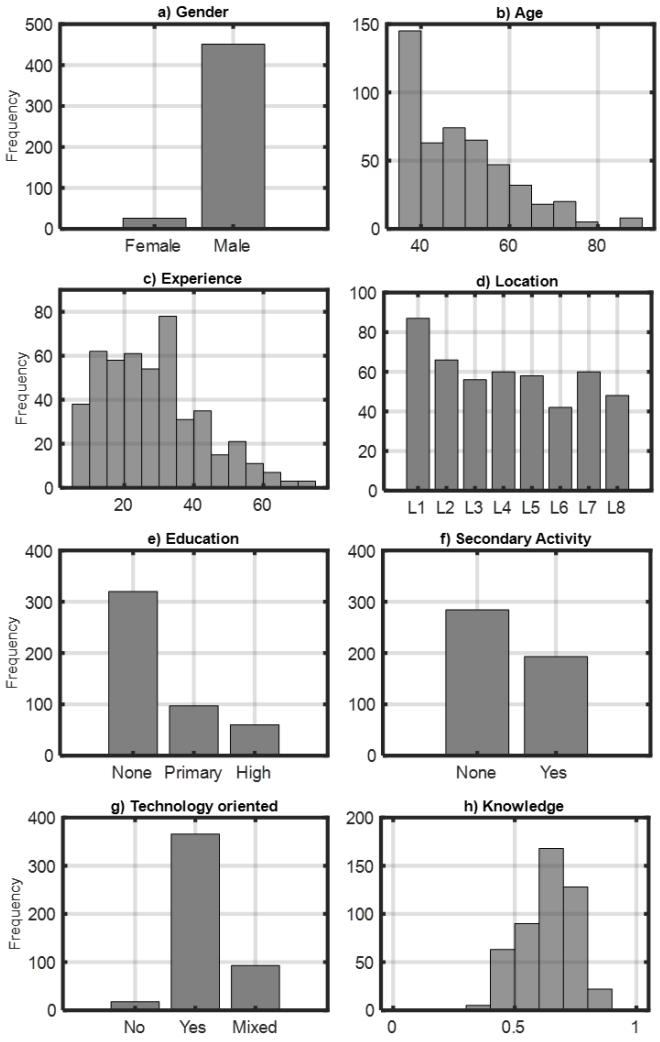

Figure 32: Distribution of the factors gender **(a)**, age **(b)**, farming experience **(c)**, location of the household **(d)**, level of education **(e)**, secondary activity besides farming **(f)**, technology/science-oriented view **(g)**, and knowledge score **(h)** of the 509 households surveyed.

6.1.3. Relationships between the variables surveyed

The Spearman correlation analysis shows that age and experience are positively correlated with the knowledge score, significant at the 5% level (**Erreur ! Source du renvoi introuvable.**). Hence, older and more experienced farmers tend to have more knowledge about hydroclimatic variability and climate change. However, the correlation coefficients are small, and age and experience can only explain a small part of the variation in knowledge.

Table 9: Spearman correlation coefficient between knowledge, age, and experience. P-values are given in brackets. All correlations are significant at the 5% level.

	Knowledge	**Age**	**Experience**
Knowledge	1	0.09 (0.04)	0.19 (<0.01)
Age	0.09 (0.04)	1	0.53 (<0.01)
Experience	0.19 (<0.01)	0.53 (<0.01)	1

The Mann-Whitney U test and the Kruskal-Wallis test found significant differences between the groups for the categorical factors of location and level of education (Figure *33*). The null hypothesis 'the medians of all groups are equal' can therefore be rejected for these two factors. The knowledge scores vary significantly between the municipalities. It ranges from the lowest knowledge score of 0.55 (median value) for L5 to the highest value of 0.75 for L2. The level of education has a slightly negative influence on knowledge, suggesting that higher formal education does not necessarily translate into greater indigenous knowledge in this context. The remaining categorical factors (gender, technology/science-oriented view, secondary work) have no statistically significant influence on the knowledge score, and p-values are larger than 10% (Figure *33*).

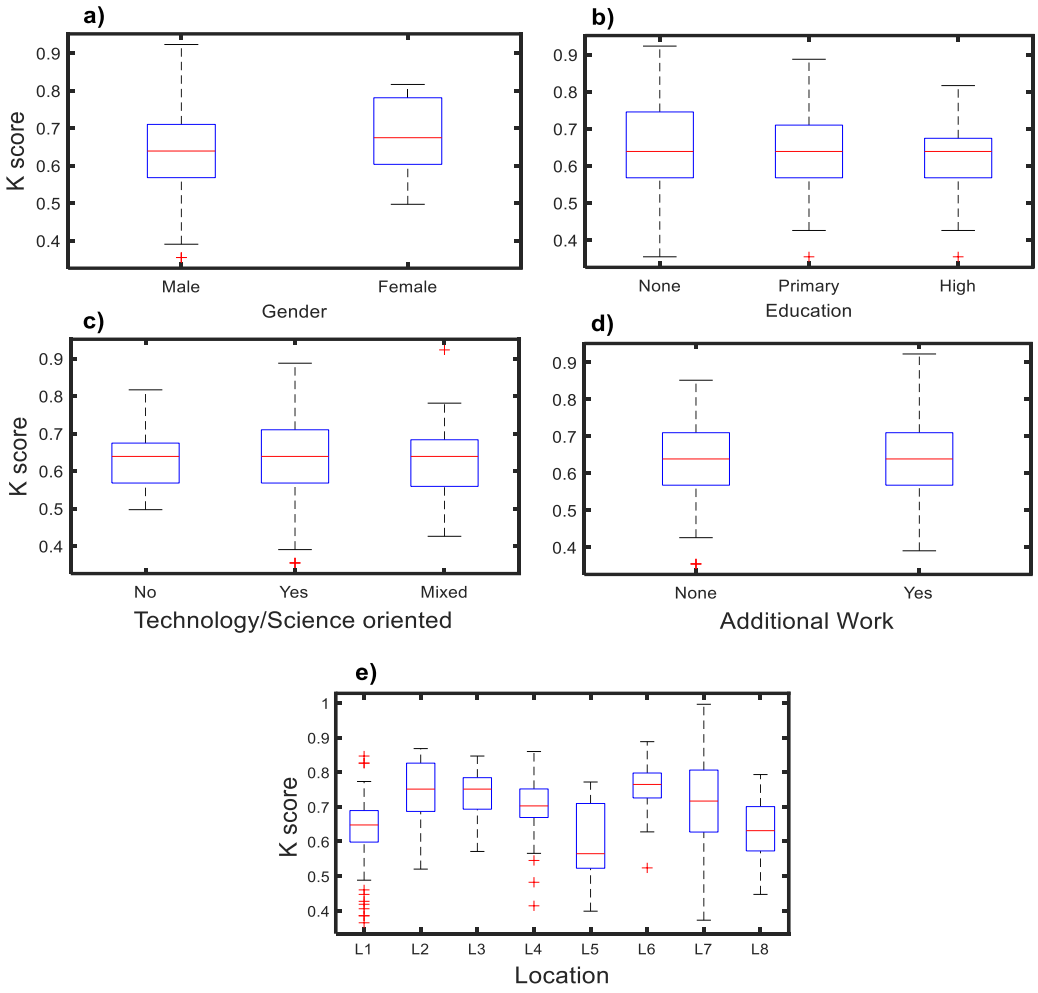

Figure 33: Boxplots of the knowledge score separated into different groups: **(a)** gender; p-value: 0.14, **(b)** level of education, p-value: 0.04, **(c)** Technology oriented view, p-value: 0.16, **(d)** secondary work, p-value: 0.15, and **(e)** location of household, P-value: <0.01.

P-values are calculated using the Mann-Whitney U test for the binary factors gender and secondary work, and the Kruskal-Wallis test is used for the remaining factors.

Besides the relationships between the different factors and the knowledge score, we also checked whether those factors, that show a significant influence on the knowledge score, are cross-correlated. A significant correlation of 0.53 between age and farming experience was found (Table 9). We also find statistically significant differences in the distribution of age and farming experience between the different municipalities (Figure 34). For instance, the municipality L2 with the highest average knowledge scores has also the highest values in age and farming experience.

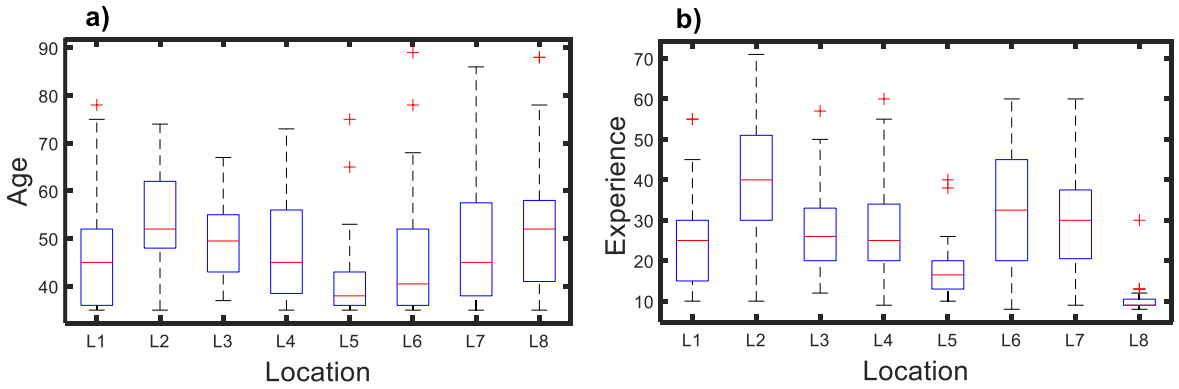

Figure 34: Boxplots of age (a) and farming experience (b) separated into the eight municipalities. Statistical significance (p-value for age: <0.01, p-Value for farming experience: 0.01) is calculated using the Kruskal-Wallis test.

6.1.4. Influences of the factors on the knowledge score

To assess the extent to which a non-linear, multi-dimensional model is able to explain the variation in knowledge scores, we built a random forest model with 300 trees. Using all seven factors as predictors for the knowledge in the random forest model, we obtain a modest R^2 value of 28% between the observed and simulated knowledge scores. We then applied the Accumulative Local Effect (ALE) method to understand and visualize how the different factors influence the knowledge score (Figure 35).

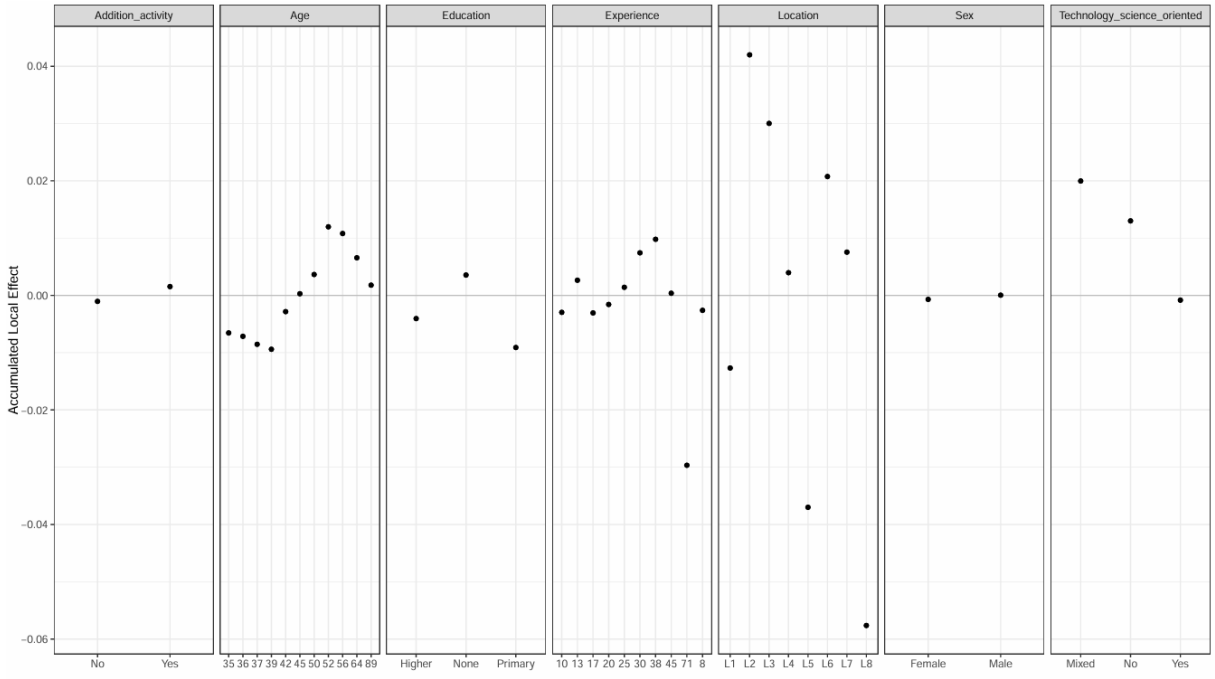

Figure 35: Accumulated local effects (ALE) of all seven factors.

The ALE plots illustrate how the model outcome, i.e., knowledge score, deviates from the mean prediction of the random forest model across the range of a predictor. Positive ALE values indicate a positive influence of the range of the predictor on the knowledge score. The ALE plots show that the non-linear random forest model identifies roughly the same factors as important predictors as were found when looking at the relationships between knowledge scores and the seven factors surveyed (section 6.2.3): Location is the dominant predictor, followed by age and experience and then, less important, level of education. In the ALE plot, the factor technology/science-oriented view features much higher compared to section 6.1.3. However, its distribution is very skewed (Figure 35-g), and most values fall into the class 'Yes'. This imbalance can lead to biased predictions (Siddiqui & Ali, 2016) . The factor age shows an interesting non-linear pattern: farmers from 35 to 42 years old have lower knowledge scores, then the knowledge scores increase with age until the age of 52 years, after which they decrease again. Experience shows a similar pattern.

6.2. Endogenous measures for adapting to hydroclimatic variability

In response to climate challenges, Northern Benin communities have developed various adaptation strategies rooted in traditional knowledge and external support. These strategies reflect a deep connection to local beliefs and practices and a gradual incorporation of new knowledge introduced by agricultural organizations. The main strategies include rituals to invoke weather changes and practical adjustments to agricultural practices to cope with varying rainfall patterns, drought, and temperature fluctuations. Key practices are as follows:

- During drought, elders perform sacrifices to appeal to the gods, while religious groups gather in mosques and churches to seek divine intervention. When sacred trees, used in rainmaking rites, are disturbed, ceremonies are held to restore rainfall (as per the village chief of Alibori-Gourou).

- ❖ Animal sacrifices at the base of sacred trees are conducted to call down rain. In times of excessive rainfall or flooding, communities similarly seek help from the gods.
- ❖ Farmers have adopted “staggered sowing and reseeding” and “early no-till sowing” to adapt to increased rainfall, building on past experiences and new climate knowledge.
- ❖ Due to rainfall disruptions, farmers now prioritize maize, a primary food crop, over cotton, which was traditionally sown first. This shift is driven by food insecurity resulting from shorter rainy seasons, erratic rainfall, and rising temperatures.
- ❖ Agro-pastoralists, facing persistent drought and scarce grazing land, now store crop residues (such as crop tops) to feed animals during the dry season, a practice rooted in traditional grazing habits.
- ❖ Not all strategies are purely traditional; external knowledge from local organizations (CeCPAs, NGOs) has contributed to adaptation practices, such as the use of agricultural inputs, which were initially taught by organizations (CeRPAs, CARDERs, ATDAs) and later modified to suit current climate conditions.

6.3. Limitations associated with endogenous measures in Northern Benin

- The oral nature of endogenous knowledge makes it difficult to pass on and is the basis for a variety of interpretations in the community.
- Elderly people who hold the knowledge and practices used by their ancestors disappear without bequeathing their knowledge. Young people's lack of interest in and respect for ancestral practices and the elderly justify their refusal to pass on their knowledge. The effectiveness of endogenous forms of management is now being questioned. In the past, ‘ritual impacts would be more palpable and immediate’. Today they are random.
- There are several reasons for these changes, according to the farmers: ‘more respect for people, God, ancestral customs and the rules of nature. The number of people has increased and there is no longer enough arable land, so we now even grow crops in groves and in places where they shouldn't be grown. Today's

‘old-timers’ don't know the true rules of our ancestors and nature. The rainmakers of today no longer know or follow the rules of our ancestors.

- Although there are coincidences in the facts that justify the effectiveness of popular practices, beliefs and attitudes, endogenous management does not offer a sufficient guarantee for the control of climatic hazards. In addition, cultural knowledge of climate change is not promoted.
- Farmers find the causes of these variations at village level to be amoral community behaviour and a failure to respect the rules of nature and the traditions of their ancestors. On a regional scale, these variations are due to the change from a humid tropical climate to a dry tropical or Sahelian climate.
- The reasons given by farmers for climate variations are largely similar to those given by scientists, i.e. environmental degradation, global warming, etc. The worsening climate puts farmers in a situation of almost total uncertainty. This forces them to grope their way through their activities and to seek palliatives through adjustments and adaptations.

Table 10: Proposed Strategies for Drought Management in North Benin

Themes	**Problems**	**Measure**	**Advantages**	**Responsible**
Crop production	Limited understanding of drought risks and crisis anticipation among stakeholders, especially at the grassroots level.	Adopt improved agricultural systems: 1) Increase access to drought-resistant crops; 2) Adopt better soil management practices. Raising farmer awareness to implement water conservation measures	Those measures enhance agricultural resilience, conserve water, improve soil health, and sustain crop yields during drought conditions	MAEP, ATDAs, AIC, NGOs, Local stakeholders
Water Resources	The hydrometeorological observation network is outdated, lacking modern equipment	Raise farmer awareness to adopt water conservation measures. Educate the public on efficient water use practices.	Those measures ensure efficient use, equitable distribution, and sustainable management,	Meteo-Benin DG-Eau PNE, NGOs

	• Conflict among water users. • Scarcity of water	Build capacity and enhance local Integrated Water Resources Management (IWRM) expertise.	reducing drought impacts on communities and ecosystems	Local stakeholders,
Forestry and Wildlife	Animal migration beyond the reserves is often due to a lack of water points during the drought period. Increase in frequency and intensity of Wild fires	Establish water points in ponds to support wildlife during drought episodes. Enforce bushburning regulations to ensure effective control of bushfires.	These measures preserve ecosystems, reduce wildfire risks, and maintain biodiversity during drought conditions.	Central government; District Office NGOs Research Institutes/Centers
Policy, legal framework and Institutional	Poor enforcement of existing legislation; Overlapping of sectoral policies; Obsolete policies and laws (a national drought management policy is largely absent; Weak institutional capacity.	Review existing policies and regulations to identify gaps. Sensitize policymakers about drought laws and the need for enforcement. Engage advocacy visits to relevant enforcement institutions. Create a special national agency to centralize data and tools for drought management	These measures collectively enhance forest resilience to drought, minimize wildfire risks, and maintain ecological balance.	Central government; Parliament's members NGOs MEDIA
Technology/ modern tools and AI contribution	Limited adoption of modern technologies in drought management	Provide training programs for stakeholders on the use of modern drought management and	These measures enhance early detection, improve resource allocation, and strengthen	Central government; NGOs

		communication technologies; Allocate funding for procuring and deploying advanced tools, such as remote sensing, GIS, and early warning systems	resilience to drought impacts.	Private sectors and tech companies

6.4. Discussion

Our survey highlights a number of challenges and opportunities for Benin's agricultural sector. The distribution of the households surveyed shows that women are severely under-represented in the agricultural labour force, with less than 10% of the farming population being female. Women tend to have fewer opportunities for income, decision-making roles, and access to resources such as land, credit, and training. This limits not only their economic empowerment but also their influence within their communities. Similar patterns across West Africa link this disparity to cultural norms and limited access to resources, restricting women's economic opportunities and affecting household food security (Doss, 2018). There also remains a significant educational challenge, as the majority of farmers have little formal education. More educated people tend to avoid agriculture, which could limit innovation. This gap could hinder the adoption of sustainable farming practices, as formal education often correlates with the ability to engage with modern technologies (Awojobi, 2018).

The survey results reveal that farmers in Northern Benin have overall a good knowledge of the region's hydro-climatology and its changes over time. While previous studies in West Africa, including Benin (Fadina & Barjolle, 2018; Loko et al., 2013; Tossa et al., 2016), Ghana (Fosu-Mensah et al., 2010; Hammond Antwi et al., 2018; Yaro, 2013), Niger (Ado et al., 2019), Nigeria (Oyerinde et al., 2015; Ozor, 2010) and South Africa (Thomas et al., 2007; Topp & Thesis, 2020), have documented farmers' intricate understanding of local climatic patterns based on long-term observations and experiences, there remains a gap in investigating the knowledge of the specific hydroclimatic changes in Northern Benin. This study addresses that gap, providing new

insights into the high consistency between farmers' perceptions and observed climatic data in this region.

However, the survey also reveals gaps in understanding hydroclimatic changes. Notably, the link between global climate change and regional temperature increases remains poorly understood. Nearly half of the respondents explained rising temperatures in the region over the recent past by divine will or other religious or cultural beliefs, while only 9% attributed it to global climate change. Such perspectives are often shaped by long-standing spiritual beliefs and traditional knowledge systems that differ from scientific explanations. The persistence of these beliefs can be attributed to limited access to climate science education and low scientific literacy, especially in rural areas. Moreover, religious and cultural worldviews can significantly influence how communities perceive environmental changes.

Our data suggests that, while farmers have a good understanding of climate, weather and the hydro-climatological general trends in their region, their knowledge of the underlying causes is very limited. This lack of knowledge might hinder their ability to implement effective long-term adaptation measures. Closing this knowledge gap is essential for preparing rural communities to address rising temperatures and shifting rainfall patterns.

It is important to understand why (some) farmers have less knowledge. Understanding which factors influence the level of knowledge can inform strategies to close existing knowledge gaps. However, analyzing the factors explaining variations in the knowledge between farmers found only relatively weak relationships. The strongest influence was location, followed by age and experience. Older and more experienced farmers tended to have better knowledge. This result points to the importance of long-term exposure to environmental changes in shaping farmers' understanding. Older farmers, with decades of experience, have likely observed multiple cycles of climate variability, allowing them to develop more intuitive knowledge of weather patterns, soil conditions, and seasonal shifts.

The result that location had the strongest impact on the knowledge score is partially explained by the age and experience, as those municipalities where the age and experience distribution showed higher values had higher knowledge scores. However, age and experience explained only a modest share of the variability in knowledge. Other

differences between the municipalities seem to play a role, which could not be investigated given the information in our survey. Variables such as access to training programs, farmer networks, and media exposure may significantly shape farmers' knowledge and merit further investigation.

A counterintuitive finding is that formal education had a weak or even a slightly negative impact on knowledge. Formal education, particularly in its traditional form, often emphasizes standardized, theoretical knowledge, which may not always align with the practical, context-specific understanding essential for hydroclimatic systems. This mismatch can create a negative relationship between formal education and hydroclimatic knowledge in specific contexts. According to Maldonado et al., (2016), formal education sometimes overlooks indigenous and local knowledge systems, which tend to be more attuned to local environmental realities. Consequently, individuals with higher formal education may possess knowledge that is less relevant or disconnected from local climate conditions.

However, Jain et al. (2024) and previous research (Belfer et al., 2017; Etchart, 2017; Makondo & Thomas, 2018) emphasize the complementary roles of indigenous knowledge and formal education in addressing climate challenges, particularly in combating desertification. They suggest that indigenous knowledge can enhance climate resilience, particularly in regions heavily dependent on natural resources. Jain et al., (2024) also acknowledge that formal education plays a critical role in bridging gaps in understanding and facilitating the application of new technologies and approaches. While indigenous knowledge offers practical, context-specific solutions, formal education helps scale these solutions and integrate them into broader climate policy frameworks. In comparison to earlier studies, for instance, Jain et al., (2024) emphasize the challenges faced by marginalized communities, who, despite their reliance on indigenous knowledge, often struggle to transform this knowledge into actionable policies due to limited resources, education, and infrastructure. This finding resonates with Maldonado et al. (2016), who highlight that communities with limited access to formal education are often the least adaptable to climate change and desertification.

The gaps between farmers' perceptions and scientific knowledge show that climate education needs to be more practical, accessible, and locally relevant. Providing simple explanations of climate drivers, using local languages, and linking forecasts to real farming decisions can help farmers better understand and use climate information. Combining scientific data with indigenous knowledge and using trusted community channels can also build confidence and improve early action against drought.

Our study highlights the multifaceted nature of knowledge acquisition and its dependence on various demographic and socio-cultural factors. By recognising and addressing these factors, it is possible to develop more effective and contextually relevant climate adaptation strategies that enhance the resilience of rural communities in West Africa. The vast experience of older farmers provides them with a deeper understanding of hydroclimatic variability. Programs that capitalize on the experience of older farmers could be particularly effective in transferring valuable indigenous knowledge to younger and less experienced farmers. Moreover, the slightly negative relation between formal education and hydroclimatic knowledge suggests that integrating indigenous knowledge systems into formal education curricula could be beneficial. In Kenya, indigenous farming practices are taught in schools through agriculture classes where students learn about traditional crop rotation, soil conservation, and native plants from local farmers. This hands-on approach connects students to sustainable practices rooted in their communities' heritage. The result that the causes of observed temperature increases were attributed to global warming by only a small fraction of households surveyed suggests the need for integrating scientific information with indigenous knowledge to address these knowledge gaps (Oyerinde et al., 2015). Based on our finding, Table 10 proposes some actionable strategies for integrating indigenous knowledge into education systems. This study is among the first of its kind in West Africa, offering a unique contribution by combining statistical and machine learning methods to analyze hydroclimatic knowledge among farmers. Previous studies in Africa have primarily focused on qualitative insights (Nyadzi et al., 2021) or farmer perceptions without advanced modeling (Kabore et al., 2023). By integrating machine learning, this study moves beyond basic correlations to identify key predictors of hydroclimatic knowledge,

aligning with recent calls for data-driven approaches to assess climate adaptation in sub-Saharan Africa (Mertz et al., 2011).

Table 11: Implications and actionable strategies for integrating indigenous knowledge into education systems.

Key Area	Implications	Actionable Strategy	Supporting References
Curriculum Development	Indigenous knowledge is often undervalued in formal education systems. Its integration can improve climate literacy.	Develop hybrid curricula that incorporate traditional climate indicators alongside scientific methods. Train educators on culturally relevant teaching approaches.	Jumba & Mwendwa Mwiti (2022), Petzold et al. (2020)
Community-Based Monitoring	Farmers rely on experiential knowledge, but hydrological data could improve decision-making.	Establish local hydrologic monitoring stations to validate traditional observations. Engage farmers in data collection and interpretation.	González (2019), Singhal et al. (2024)
Climate Risk Awareness	Farmers recognize hydroclimatic variability but often lack an understanding of global climate drivers.	Organize farmer extension workshops combining indigenous climate perceptions with climate science. Strengthen outreach programs.	del Pozo et al. (2019)
Policy and Decision-Making	Indigenous knowledge can complement scientific data in environmental planning and policy.	Advocate for policies that promote the integration of indigenous knowledge into national education strategies.	Wheeler & Root-Bernstein (2020)

Conclusion

The survey results indicate that farmers in Northern Benin generally possess a good understanding of the region's hydro-climatology, but that a significant gap exists in linking regional temperature increases to global climate change. This disconnect may limit their ability to adopt long-term adaptation strategies, underscoring the need for targeted interventions. The study also highlights that age and farming experience are key determinants of hydroclimatic knowledge, whereas formal education had little to no impact. This suggests that indigenous knowledge remains central to farming practices in North Benin. Older and more experienced farmers tend to possess better knowledge, while the level of formal education does not improve the knowledge. These results suggest that indigenous knowledge plays an important role in the daily life of farming households in Northern Benin. These insights emphasize the importance of demographic, socio-cultural, and experiential factors in shaping climate awareness. Strengthening context-specific education and integrating scientific and indigenous knowledge can enhance the climate resilience of rural communities in West Africa.

Our findings are based on data collected from a limited number of municipalities in Norther Benin, which may limit their generalizability to other regions of Benin or broader West Africa. Future research could include a more diverse set of locations to better capture regional differences. The strong variation in knowledge and the low value of R^2 found calls for a broader set of factors to be collected.

CHAPTER 7: GENERAL CONCLUSION, SUGGESTIONS AND PERSPECTIVES

This chapter concludes the study by summarizing the key findings and insights, while also presenting recommendations and perspectives for future research and actions. It highlights the overall outcomes of the analysis, identifies areas for improvement, and proposes pathways for addressing the identified challenges.

7.1. General conclusion

- **Hydroclimatic variability analysis**

The study reveals distinct temporal patterns of drought, with severe and prolonged events during the 1970s and 1980s followed by a recovery phase in the 1990s. Rainfall and mean streamflow during the rainy season exhibit high interannual variability, often showing a biannual zigzag pattern, as well as substantial decadal fluctuations. However, recent decades show an increasing trend in consecutive dry days (CDD) and streamflow droughts (SDI), indicating a growing persistence of dry conditions and intensifying water stress.

- **Improving drought predictability**

Wavelet coherence analysis reveals significant links between climate indices and rainfall across the three catchments, with a shift from lower-frequency coherence in earlier decades to higher-frequency coherence in recent decades. These patterns are less pronounced for streamflow, which responds more indirectly to teleconnections. The improved performance of predictors such as Niño indices, TASI, SAT, and SWIO demonstrates their effectiveness in capturing rainfall variability, highlighting the growing influence of ocean–atmosphere interactions on regional climate during the monsoon season. These results are instrumental in improving drought predictability, fostering better water resource management, and guiding agricultural and environmental policies.

- **Local perceptions and adaptation**

Importantly, the study also reveals gaps in farmers' understanding of the root causes of hydroclimatic changes, suggesting a need for targeted capacity-building initiatives to enhance resilience in rural communities. This research contributes to a growing body of

knowledge essential for addressing the challenges posed by climate variability in drought-prone West Africa, providing a foundation for more effective mitigation and adaptation strategies.

7.2. Suggestions

To better support agricultural producers in combating the effects of climate change, several targeted suggestions are proposed:

a) **Towards government, public authorities and Niger Basin Authority**
Time horizon: Short to long term

- Strategic decisions by public authorities, rural development agencies, research institutions, and local communities are essential for embedding effective adaptation measures into climate change mitigation efforts.
- Support the development and implementation of climate-resilient policies aligned with the National Drought Management Plan (NDMP) and ECOWAS frameworks.
- Reforestation initiatives can mitigate the effects of strong winds through the use of windbreaks, while agroforestry practices can enhance soil fertility and integrate agricultural and environmental benefits. These approaches not only protect the environment but also support sustainable farming practices.
- Creating an early warning system to inform farmers of potential climatic disturbances is crucial. By combining meteorological service data with indigenous climate knowledge, farmers can better anticipate and manage weather-related risks.
- To strengthen knowledge of water resource management, rural populations need to be informed of national laws and international health and hygiene standards;
- Awareness-raising is needed to help people understand the obstacles to the development of dispersed housing and the advantages of grouped housing, to encourage them to build in grouped housing from now on.

b) **For Public Intervention Structures (ATDAs, AICs) and NGOs**
Time horizon: Short to medium term

- Farmers increasingly rely on riverbanks and lowlands as part of their strategies to cope with climate change. While these areas are rich in resources, they present challenges for effective cultivation. Supervisory services should provide technical support to ensure optimal and sustainable use of these landscape units, while also considering the specific climatic challenges faced by producers.
- Support participatory approaches that involve local communities in designing adaptation strategies.
- Intervention structures must integrate climate-related challenges into their support strategies to better address the needs of farmers. This includes providing tools, resources, and guidance that enhance the resilience of agricultural practices to climate variability.
- To strengthen farmers' economic resilience, support should be provided for income diversification initiatives. This includes facilitating access to credit and financial services, enabling farmers to explore alternative income sources and reducing their vulnerability to climate-related shocks.

c) Towards farmers

Time horizon: Immediate to medium term

- Farmers should actively engage in open collaboration with stakeholders, including research institutions, public intervention structures, and NGOs, to ensure the successful implementation of climate adaptation measures.
- Better organization among farmers is crucial for effectively managing the support systems and resources provided.
- Farmers must actively contribute their indigenous knowledge and practical expertise to work collaboratively with research and support centers.
- Working collectively in organized groups will facilitate access to support and enable intervention structures to provide more effective assistance.

7.3. Perspectives

This thesis explored meteorological and hydrological droughts, emphasizing the interplay of hydroclimatic factors and effective management strategies.

- Future research should focus on integrating human activities into basin hydrology models, particularly simulating water abstraction for households, industries, , land use and land cover changes and livestock, to better understand the combined impacts of natural and anthropogenic drivers on drought.
- Future research should focus on refining predictive models by incorporating high-resolution data and expanding the range of teleconnection indices considered. Combining CHIRPS with additional gauge observations or reanalysis datasets would help reduce data uncertainties and strengthen model robustness.
- Fostering local adaptive capacities and integrating indigenous knowledge systems can strengthen resilience to the growing risks posed by hydroclimatic variability in the region.

8. References

Adam, S. K. , & Boko, M. (1993). Le climat du Bénin. Paris, Edicef, 2e édition, 93p, [Report].

Adechina, E. A., Halissou, Y., Aliou, M. D., Obada, E., Iboukoun, E. B., & Felicien, D. B. (2022). Historical and projected meteorological droughts in the Beninese Niger River Basin, Benin. International Journal of Water Resources and Environmental Engineering, 14(2), 39–54. https://doi.org/10.5897/ijwree2021.1026

Adjinacou C., & Onibon H. (2004). Etude multisectorielle pour le développement durable dans la portion béninoise du bassin du fleuve Niger : analyse des opportunités et des contraintes. Autorité du Bassin du fleuve Niger (ABN)/DG-Eau, 176p., [Report].

Ado, A. M., Leshan, J., Savadogo, P., Bo, L., & Shah, A. A. (2019). Farmers' awareness and perception of climate change impacts: case study of Aguie district in Niger. Environment, Development and Sustainability, 21(6), 2963–2977. https://doi.org/10.1007/s10668-018-0173-4

Afouda A., L. E. , et L. T. (2004). A stochastic Streamflow Model based on Minimum Energy Expenditure Concept. In Contempory Problems in Mathematical Physics: Proceeding 3rd Intern. Workshop. Word Scientific Publishing Co. Ltd , p 153-169.

Agblonon Houelome, T. , Agbohessi, T. , Adandedjan, D. , Nechifor, R. , Chikou, A. , Lazar, I. , & Laleye, P. (2022). Ecological quality of the Alibori River, northern Benin, using macroinvertebrate indicators. African Journal of Aquatic Science, 47(2), 173–184.

Ahokpossi, Y. (2018). Analysis of the rainfall variability and change in the Republic of Benin (West Africa). Hydrological Sciences Journal, 63(15–16), 2097–2123. https://doi.org/10.1080/02626667.2018.1554286

Aich, V., Liersch, S., Vetter, T., Andersson, J. C. M., Müller, E. N., & Hattermann, F. F. (2015). Climate or land use? - Attribution of changes in river flooding in the Sahel zone. Water (Switzerland), 7(6), 2796–2820. https://doi.org/10.3390/w7062796

Akinsanola, A. A., Zhou, W., Zhou, T., & Keenlyside, N. (2020). Amplification of synoptic to annual variability of West African summer monsoon rainfall under global warming. Npj Climate and Atmospheric Science, 3(1). https://doi.org/10.1038/s41612-020-0125-1

Alamou E. (2011). Application of the Least Action Principle to Rain-Flow Modeling. [Doctoral Thesis]. University of Abomey Calavi. 231p & Annexes.

Alamou, E. A., Obada, E., & Afouda, A. (2017). Assessment of future water resources availability under climate change scenarios in the Mékrou Basin, Benin. Hydrology, 4(4). https://doi.org/10.3390/hydrology4040051

Albergel, Jean, Valentin, & Christian. (1989). «Sahelisation» d'un petit bassin versant soudanien : Kognere-Boulsa au Burkina-Faso. ORSTM, 179-190p.

Almendra-Martín, L., Martínez-Fernández, J., González-Zamora, Á., Benito-Verdugo, P., & Herrero-Jiménez, C. M. (2021). Agricultural drought trends on the iberian peninsula: An analysis using modeled and reanalysis soil moisture products. Atmosphere, 12(2). https://doi.org/10.3390/atmos12020236

Alsafadi, K., Al-Ansari, N., Mokhtar, A., Mohammed, S., Elbeltagi, A., Sh Sammen, S., & Bi, S. (2022). An evapotranspiration deficit-based drought index to detect variability of terrestrial carbon productivity in the Middle East. Environmental Research Letters, 17(1). https://doi.org/10.1088/1748-9326/ac4765

Apley, D. W., & Zhu, J. (2020). Visualizing the effects of predictor variables in black box supervised learning models. J. R. Statist. Soc. B, 82. https://academic.oup.com/jrsssb/article/82/4/1059/7056085

Awojobi, O. (2018). Adaptation plans: building climate resilience in agriculture. International Journal of Agriculture and Environmental Research. Volume:04, Issue:01 "January-February 2018". 211-221p.

Bader, J., & Latif, M. (2011). The 1983 drought in the West Sahel: A case study. Climate Dynamics, 36(3), 463–472. https://doi.org/10.1007/s00382-009-0700-y

Badou. (2016). Multi-Model Evaluation of Blue and Green Water Availability under Climate Change in Four-Non Sahelian Basins of the Niger River Basin [These de Doctorat]. University of Abomey-Calavi (UAC). Institut National de l'Eau (INE), 155p.

Badou, D. F., Adango, A., Hounkpè, J., Bossa, A., Yira, Y., Biao, E. I., Adounkpè, J., Alamou, E., Sintondji, L. O. C., & Afouda, A. A. (2021). Heavy rainfall frequency analysis in the Benin section of the Niger and Volta Rivers basins: Is the Gumbel's distribution a one-size-fits-all model? Proceedings of the International Association of Hydrological Sciences, 384, 187–194. https://doi.org/10.5194/piahs-384-187-2021

Badou, D. F., Kapangaziwiri, E., Diekkrüger, B., Hounkpè, J., & Afouda, A. (2017). Evaluation of recent hydro-climatic changes in four tributaries of the Niger River Basin (West Africa). Hydrological Sciences Journal, 62(5), 715–728. https://doi.org/10.1080/02626667.2016.1250898

Balliet, R., Saley, M. B., Anowa Eba, E. L., Sorokoby, M. V., N'Guessan Bi, H. V., N'Dri, A. O., Djè, B. K., & Biémi, J. (2016). Évolution Des Extrêmes Pluviométriques Dans La Région Du Gôh (Centre-Ouest De La Côte d'Ivoire). European Scientific Journal, ESJ, 12(23), 74. https://doi.org/10.19044/esj.2016.v12n23p74

Bekoe, E. O., & Logah, F. Y. (2013). The Impact of Droughts and Climate Change on Electricity Generation in Ghana. In Environmental Sciences (Vol. 1, Issue 1). 13-24p. www.m-hikari.com.

Belfer, E., Ford, J. D., & Maillet, M. (2017). Representation of Indigenous peoples in climate change reporting. Climatic Change, 145(1–2), 57–70. https://doi.org/10.1007/s10584-017-2076-z

Biasutti, M. (2019a). Rainfall trends in the African Sahel: Characteristics, processes, and causes. In Wiley Interdisciplinary Reviews: Climate Change (Vol. 10, Issue 4). Wiley-Blackwell. https://doi.org/10.1002/wcc.591

Biasutti, M. (2019b). Rainfall trends in the African Sahel: Characteristics, processes, and causes. In Wiley Interdisciplinary Reviews: Climate Change (Vol. 10, Issue 4). Wiley-Blackwell. https://doi.org/10.1002/wcc.591

Breiman, L. (2001). Random Forests (Vol. 45). Kluwer Academic Publishers. Manufactured in the Neitherlands. Machine learning 45, 5-32p.

Brown, C., & Lall, U. (2006). Water and economic development: The role of variability and a framework for resilience. In Natural Resources Forum (Vol. 30, No. 4, pp. 306-317). Oxford, UK: Blackwell Publishing Ltd.

Brown, J. R., Moise, A. F., & Colman, R. A. (2017). Projected increases in daily to decadal variability of Asian-Australian monsoon rainfall. Geophysical Research Letters, 44(11), 5683–5690. https://doi.org/10.1002/2017GL073217

Camberlin, P., Janicot, S., & Poccard, I. (2001). Seasonality and atmospheric dynamics of the teleconnection between African rainfall and tropical sea-surface temperature: Atlantic vs. ENSO. International Journal of Climatology, 21(8), 973–1005. https://doi.org/10.1002/joc.673

Charlene G. (2015). An Ensemble Approach Modelling to Assess Water Resources in the Mékrou Basin, Benin. Hydrology, 3(2), 22. https://doi.org/10.11648/j.hyd.20150302.11

Dai, A. (2011). Characteristics and trends in various forms of the Palmer Drought Severity Index during 1900-2008. Journal of Geophysical Research Atmospheres, 116(12). https://doi.org/10.1029/2010JD015541

Dai, A., & Trenberth, K. E. (2004). A global dataset of Palmer Drought Severity Index for 1870-2002: Relationship with Soil Moisture and effects of surface warming. http://climate.envsci.rutgers.edu/soilmoisture/

del Pozo, A., Brunel-Saldias, N., Engler, A., Ortega-Farias, S., Acevedo-Opazo, C., Lobos, G. A., Jara-Rojas, R., & Molina-Montenegro, M. A. (2019). Climate change impacts and adaptation strategies of agriculture in Mediterranean-climate regions (MCRs). In Sustainability (Switzerland) (Vol. 11, Issue 10). MDPI. https://doi.org/10.3390/su11102769

Diatta, S., Diedhiou, C. W., Dione, D. M., & Sambou, S. (2020). Spatial variation and trend of extreme precipitation in west africa and teleconnections with remote indices. Atmosphere, 11(9). https://doi.org/10.3390/atmos11090999

Dieppois, B., Durand, A., Fournier, M., Diedhiou, A., Fontaine, B., Massei, N., Nouaceur, Z., & Sebag, D. (2015). Low-frequency variability and zonal contrast in Sahel rainfall and Atlantic sea surface temperature teleconnections during the last century. Theoretical and Applied Climatology, 121(1–2), 139–155. https://doi.org/10.1007/s00704-014-1229-5

Dobor, L., Barcza, Z., Hlásny, T., Árendás, T., Spitkó, T., & Fodor, N. (2016). Crop planting date matters: Estimation methods and effect on future yields. Agricultural and Forest Meteorology, 223, 103–115. https://doi.org/10.1016/j.agrformet.2016.03.023

Doss, C. R. (2018). Women and agricultural productivity: Reframing the Issues. Development Policy Review, 36(1), 35–50. https://doi.org/10.1111/dpr.12243

Dunning, C. M., Black, E., & Allan, R. P. (2018). Later Wet Seasons with More Intense Rainfall over Africa under Future Climate Change. https://doi.org/10.1175/JCLI

Ebi, K. L., & Bowen, K. (2016). Extreme events as sources of health vulnerability: Drought as an example. Weather and Climate Extremes, 11, 95–102. https://doi.org/10.1016/j.wace.2015.10.001

Etchart, L. (2017). The role of indigenous peoples in combating climate change. Palgrave Communications, 3(1). https://doi.org/10.1057/palcomms.2017.85

Fadina, A. M. R., & Barjolle, D. (2018). Farmers' adaptation strategies to climate change and their implications in the Zou department of South Benin. Environments - MDPI, 5(1), 1–17. https://doi.org/10.3390/environments5010015

Fang, G., Li, X., Xu, M., Wen, X., & Huang, X. (2021). Spatiotemporal variability of drought and its multi-scale linkages with climate indices in the huaihe river basin, central china and east China. Atmosphere, 12(11). https://doi.org/10.3390/atmos12111446

Fang, W., Huang, S., Huang, Q., Huang, G., Wang, H., Leng, G., & Wang, L. (2020). Identifying drought propagation by simultaneously considering linear and nonlinear dependence in the Wei River basin of the Loess Plateau, China. Journal of Hydrology, 591. https://doi.org/10.1016/j.jhydrol.2020.125287

Fleig, A. K. , Tallaksen, L. M. , Hisdal, H., & Hannah, D. M. (2011). Regional hydrological drought in north-western Europe: linking a new Regional Drought Area Index with weather types. Hydrol. Process., 25, 1163–1179.

Fontaine, B., & Bigot, S. (1993). West African rainfall deficits and sea surface temperatures. International Journal of Climatology, 13(3), 271–285. https://doi.org/10.1002/joc.3370130304

Fontaine, B., & Janicot, S. (1996). Sea surface temperature fields associated with West African rainfall anomaly types. Journal of Climate, 9(11), 2935–2940. https://doi.org/10.1175/1520-0442(1996)009<2935:SSTFAW>2.0.CO;2

Fosu-Mensah, B. Y., Vlek, P. L. G., & Manschadi, A. M. (2010). “World Food System-A Contribution from Europe Farmers’’ Perception and Adaptation to Climate Change; A Case Study of Sekyedumase District in Ghana”. ”Tropentag, September 14 - 16, 2010, Zurich “World Food System — A Contribution from Europe, 1-6p.

Fougou, H. K., & Lemoalle, J. (2022). Variability of Lake Chad. In Congo Basin Hydrology, Climate, and Biogeochemistry (eds R.M. Tshimanga, G.D.M. N’kaya and D. Alsdorf). Geophysical Monograph Series, 513–518.

Funk, C., Peterson, P., Landsfeld, M., Pedreros, D., Verdin, J., Shukla, S., Husak, G., Rowland, J., Harrison, L., Hoell, A., & Michaelsen, J. (2015). The climate hazards infrared precipitation with stations - A new environmental record for monitoring extremes. Scientific Data, 2. https://doi.org/10.1038/sdata.2015.66

Gaba C. (2015). An Ensemble Approach Modelling to Assess Water Resources in the Mékrou Basin, Benin. Hydrology, 3(2), 22. https://doi.org/10.11648/j.hyd.20150302.11

Gal L. (2016). Modélisation de l’évolution paradoxale de l’hydrologie sahélienne. Application au bassin d’Agoufou (Mali). Université Toulouse 3 Paul Sabatier (UT3 Paul Sabatier), 221p.

Giannini, A. (2010). Mechanisms of climate change in the semiarid African Sahel: The local view. Journal of Climate, 23(3), 743–756. https://doi.org/10.1175/2009JCLI3123.1

Giannini, A., & Kaplan, A. (2019). The role of aerosols and greenhouse gases in Sahel drought and recovery. Climatic Change, 152(3–4), 449–466. https://doi.org/10.1007/s10584-018-2341-9

Giannini, A., Saravanan, R., & Chang, P. (2003). Oceanic Forcing of Sahel Rainfall on Interannual to Interdecadal Time Scales. Science, 302(5647), 1027–1030. https://doi.org/10.1126/science.1089357

Gizaw, M. S., & Gan, T. Y. (2017). Impact of climate change and El Niño episodes on droughts in sub-Saharan Africa. Climate Dynamics, 49(1–2), 665–682. https://doi.org/10.1007/s00382-016-3366-2

Global Water Partnership &, & PNE-Bénin. (2015). Analyse de l’utilisation actuelle des ressources en eau et définition de la situation de référence sur la portion du territoire du Bénin se situant dans le bassin de la Mékrou.

Great Britain Meteorological Office. (1951). Drought in England: Reports on drought conditions in England and Wales in 1947 and 1949. London: HMSO, [Report].

Grinsted A., Moore J. C., & Jevrejeva S. (2004). “Application of the cross wavelet transform and wavelet coherence to geophysical times series,.” Nonlinear Processes in Geophysics, 11(5–6), 561–566.

Grinsted, A., Moore, J. C., & Jevrejeva, S. (2004). Nonlinear Processes in Geophysics Application of the cross wavelet transform and wavelet coherence to geophysical time series (Vol. 11). https://doi.org/https://doi.org/10.5194/npg-11-561-2004

Guttman2, N. B. (1999). American Water Resources Association. In Journal of the American Water Resources Association. *JAWRA Journal of the American Water Resources Association*, *35*(2), 311-322.

Haile, G. G., Tang, Q., Li, W., Liu, X., & Zhang, X. (2020). Drought: Progress in broadening its understanding. Wiley Interdisciplinary Reviews: Water, 7(2). https://doi.org/10.1002/WAT2.1407

Halissou, Y., Eric, A. A., Ezéchiel, O., & Eliézer, B. I. (2021). Extreme Temperature Trends in the Beninese Niger River Basin (Benin). American Journal of Climate Change, 10(04), 371–385. https://doi.org/10.4236/ajcc.2021.104018

Hamed, K. H., & Rao, A. R. (1998). Hydrology A modified Mann-Kendall trend test for autocorrelated data. In Journal of Hydrology, 204(1-4), 182-196.

Hammond Antwi, S., Sumaila Mohammed, A., & David, O. (2018). Evaluating Rural Farmers Knowledge, Perception, and Adaptation Strategies on Climate Change in Ghana: A case study of the Wa West District, Ghana. 8(10). www.iiste.org

Handmer, J., Y. Honda, Z.W. Kundzewicz, N. Arnell, G. Benito, J. Hatfield, I.F. Mohamed, P. Peduzzi, S. Wu, B. Sherstyukov, K. Takahashi, & Z. Yan. (2012). Changes in impacts of climate extremes: human systems and ecosystems. In: Managing the Risks of Extreme Events and Disasters to Advance Climate Change Adaptation [Field, C.B., V. Barros, T.F. Stocker, D. Qin, D.J. Dokken, K.L. Ebi, M.D. Mastrandrea, K.J. Mach, G.-K. Plattner, S.K. Allen, M. Tignor, and P.M. Midgley (eds.)]. A Special Report of Working Groups I and II of the Intergovernmental Panel on Climate Change (IPCC).

Hargreaves H. G., & Samani A. Z. (1985). Reference Crop Evapotranspiration from Temperature. Applied Engineering in Agriculture, 1(2), 96–99. https://doi.org/10.13031/2013.26773

Hawkins, E., & Sutton, R. (2011). The potential to narrow uncertainty in projections of regional precipitation change. Climate Dynamics, 37(1), 407–418. https://doi.org/10.1007/s00382-010-0810-6

He, C., & Li, T. (2019). Does global warming amplify interannual climate variability? Climate Dynamics, 52(5–6), 2667–2684. https://doi.org/10.1007/s00382-018-4286-0

Hothorn, T., Hornik, K., & Zeileis, A. (2006). Unbiased recursive partitioning: A conditional inference framework. Journal of Computational and Graphical Statistics, 15(3), 651–674. https://doi.org/10.1198/106186006X133933

Hothorn, T., Hornik, K., & Zeileis, A. (2015). party: A Laboratory for Recursive Partytioning. (R package version 1.2-10.), 1-18p.

Houngue, R., Lawin, A. E., Afouda, A., Prof, A., & Alamou, E. A. (2020). Climate change impacts on hydrodynamic functioning of Oueme Delta (Benin) [PhD Thesis]. University of Abomey-Calavi.

Hua, W., Zhou, L., Chen, H., Nicholson, S. E., Raghavendra, A., & Jiang, Y. (2016). Possible causes of the Central Equatorial African long-term drought. Environmental Research Letters, 11(12). https://doi.org/10.1088/1748-9326/11/12/124002

Huang, B., Thorne, P. W., Banzon, V. F., Boyer, T., Chepurin, G., Lawrimore, J. H., Menne, M. J., Smith, T. M., Vose, R. S., & Zhang, H. M. (2017). Extended reconstructed Sea surface temperature, Version 5 (ERSSTv5): Upgrades, validations, and intercomparisons. Journal of Climate, 30(20), 8179–8205. https://doi.org/10.1175/JCLI-D-16-0836.1

Hulme, M., Doherty, R., Ngara, T., New, M., & Lister, D. (2001). African climate change: 1900-2100. Climate Research, 17(2 SPECIAL 8), 145–168. https://doi.org/10.3354/cr017145

INSAE. (2016). Effectifs de la population des villages et quartiers de ville du Bénin. 83p, [Report].

Intergovernmental Panel on Climate Change (IPCC). (2023). Weather and Climate Extreme Events in a Changing Climate. In Climate Change 2021 – The Physical Science Basis (pp. 1513–1766). Cambridge University Press. https://doi.org/10.1017/9781009157896.013

IPCC. (2012). Managing the Risks of Extreme Events and Disasters to Advance Climate Change Adaptation. A Special Report of Working Groups I and II of the Intergovernmental Panel on Climate Change [Field, C.B., V. Barros, T.F. Stocker, D. Qin, D.J. Dokken, K.L. Ebi, M.D. Mastrandrea, K.J. Mach, G.-K. Plattner, S.K. Allen, M. Tignor, and P.M. Midgley (eds.)].

Jain, S., Srivastava, A., Khadke, L., Chatterjee, U., & Elbeltagi, A. (2024). Global-scale water security and desertification management amidst climate change. In Environmental Science and Pollution Research. Springer. https://doi.org/10.1007/s11356-024-34916-0

Janicot, S., Moron, V., Fontaine, B., & Fontaine Sahel, B. (1996). Sahel droughts and Enso dynamics. Geophysical Research Letters, 23(5), 515–518. https://doi.org/10.1029/96GL00246ï

Jellason, N. P., Conway, J. S., Baines, R. N., & Ogbaga, C. C. (2021). A review of farming challenges and resilience management in the Sudano-Sahelian drylands of Nigeria in an era of climate change. In Journal of Arid Environments (Vol. 186). Academic Press. https://doi.org/10.1016/j.jaridenv.2020.104398

Jumba, H. A., & Mwendwa Mwiti, F. (2022). Teachers' Perception on Integration of Indigenous Knowledge Systems in Competence Based Curriculum at Selected Primary Schools in Buuri East Sub-County. In International Journal of Professional Practice (IJPP (Vol. 10, Issue 1).

Kabore, P. N., Zon, A. O., Bambara, D., Koussoubé, S., & Ouedraogo, A. (2023). Farmers' Perception of Indigenous Seasonal Forecast Indicators in North Central Burkina Faso. Sustainable Agriculture Research, 13(1), 28. https://doi.org/10.5539/sar.v13n1p28

Kasei, R. , Diekkrüger, B., & Leemhuis, C. (2010). Drought Frequency in the Volta Basin of West Africa. Sustainability Science, 5, 89–97.

Katchele F., O., Ma, Z. G., Yang, Q., & Batebana, K. (2017). Comparison of trends and frequencies of drought in central North China and sub-Saharan Africa from 1901 to 2010. Atmospheric and Oceanic Science Letters, 10(6), 418–426. https://doi.org/10.1080/16742834.2017.1392825

Katz, R. W., & Brown, B. G. (1992). Extreme events in a changing climate: Variability is more important than averages. Climatic Change, 21(3), 289–302. https://doi.org/10.1007/BF00139728

Kohler, M. A. (1949). On the Use of Double-Mass Analysis for Testing the Consistency of Meteorological Records and for Making Required Adjustments. Bulletin of the American Meteorological Society, 30, 188–195.

Krishnan, V. U., Mirajkar, A., Nair, S., Mirajkar, A. B., & Nair, S. C. (2019). Comparative Study on Drought in Marathwada using SPI and SPEI Study of Glacial Dynamics and Sustainable Hydrological Resources in Arunachal Himalaya View project Drought Analysis in Marathwada Region View project Comparative Study on Drought in Marathwada using SPI and SPEI (Vol. 18, Issue 20). https://www.researchgate.net/publication/353481379

Le Barbé L., Alé, G. , Millet, G., Texier, H. , Borel, Y. , & Gualde, R. (1993). Surface waters resources of the Republic of Benin. *Monogr. Hydrol., Orstom, Paris(France)*, (11), 540.

Liaw, A., & Wiener, M. (2002). Classification and Regression by randomForest (Vol. 2, Issue 3). http://www.stat.berkeley.edu/. Accessed on July 9th, 2024

Lin, Y. C., & Weng, T. H. (2024). Development of wavelet-based machine learning models for predicting long-term rainfall from sunspots and ENSO. Applied Water Science, 14(1). https://doi.org/10.1007/s13201-023-02051-9

Linsley R. K. (1958). Correlation of rainfall intensity and topography in northern California. Eos Trans. AGU, 39(1), 15–118.

Lloyd-Hughes, B., & Saunders, M. A. (2002). A drought climatology for Europe. International Journal of Climatology, 22(13), 1571–1592. https://doi.org/10.1002/joc.846

Loko, Y., Dansi, A., Agre, A., Akpa, N., Dossou-Aminon, I., Assogba, P., Dansi, M., Akpagana, K., & Sanni, A. (2013). Perceptions paysannes et impacts des changements climatiques sur la production et la diversité variétale de l'igname dans la zone aride du nord-ouest du Bénin. International Journal of Biological and Chemical Sciences, 7(2). https://doi.org/10.4314/ijbcs.v7i2.23

Longobardi, A., Boulariah, O., & Villani, P. (2020). Assessment of centennial (1918-2019) drought features in the Campania region by historical in situ measurements (southern Italy). Natural Hazards and Earth System Sciences Discussions, 2021, 1-23.

Lorenzo-Lacruz, J., Moŕan-Tejeda, E., Vicente-Serrano, S. M., & Ĺopez-Moreno, J. I. (2013). Streamflow droughts in the Iberian Peninsula between 1945 and 2005: Spatial and temporal patterns. Hydrology and Earth System Sciences, 17(1), 119–134. https://doi.org/10.5194/hess-17-119-2013

Losada, T., Rodriguez-Fonseca, B., Mohino, E., Bader, J., Janicot, S., & Mechoso, C. R. (2012). Tropical SST and Sahel rainfall: A non-stationary relationship. Geophysical Research Letters, 39(12). https://doi.org/10.1029/2012GL052423

Luini, L., & Capsoni, C. (2012). The impact of space and time averaging on the spatial correlation of rainfall. Radio Science, 47(3). https://doi.org/10.1029/2011RS004915

Mahé, G., & Paturel, J. E. (2009). 1896-2006 Sahelian annual rainfall variability and runoff increase of Sahelian Rivers. Comptes Rendus - Geoscience, 341(7), 538–546. https://doi.org/10.1016/j.crte.2009.05.002

Makondo CC, & Thomas DS. (2018). Climate change adaptation: linking indigenous knowledge with western science for effective adap tation. Environ Sci Policy , 88, 83–91.

Maldonado J, Bennett TM, Chief K, Cochran P, Cozzetto K, Gough B, & ... Voggesser G. (2016). Engagement with indigenous peoples and honoring traditional knowledge systems. In The US National Climate Assessment. Springer, Cham, 111–126.

Maraun, D., & Kurths, J. (2004). Nonlinear Processes in Geophysics Cross wavelet analysis: significance testing and pitfalls. Nonlinear Processes in Geophysics, 11(4), 505-514.

Mascaro, G., White, D. D., Westerhoff, P., & Bliss, N. (2015). Performance of the CORDEX-Africa regional climate simulations in representing the hydrological cycle of the Niger river basin. Journal of Geophysical Research, 120(24), 12,425-12,444. https://doi.org/10.1002/2015JD023905

Mckee, T. B., Doesken, N. J., & Kleist, J. (1993). The relationship of drought frequency and duration to time scales. In *Proceedings of the 8th Conference on Applied Climatology* (Vol. 17, No. 22, pp. 179-183).

Mertz, O., Mbow, C., Reenberg, A., Genesio, L., Lambin, E. F., D'haen, S., Zorom, M., Rasmussen, K., Diallo, D., Barbier, B., Moussa, I. B., Diouf, A., Nielsen, J., & Sandholt, I. (2011). Adaptation strategies and climate vulnerability in the Sudano-Sahelian region of West Africa. Atmospheric Science Letters, 12(1), 104–108. https://doi.org/10.1002/asl.314

Ministry for the Environment and Sustainable Development (MCVDD). (2019). National Drought Plan. 171p, [Report].

Mishra, A. K., & Singh, V. P. (2010). A review of drought concepts. In Journal of Hydrology (Vol. 391, Issues 1–2, pp. 202–216). https://doi.org/10.1016/j.jhydrol.2010.07.012

Mohammed, S., Alsafadi, K., Enaruvbe, G. O., Bashir, B., Elbeltagi, A., Széles, A., Alsalman, A., & Harsanyi, E. (2022). Assessing the impacts of agricultural drought (SPI/SPEI) on maize and wheat yields across Hungary. Scientific Reports, 12(1). https://doi.org/10.1038/s41598-022-12799-w

Möller González, N. (2019). Indigenous Media and Political Imaginaries in Contemporary Bolivia. Journal of Latin American & Caribbean Anthropology, 24(3), p765.

Molnar, C. (2021). Interpretable Machine Learning A Guide for Making Black Box Models Explainable. https://christophm.github.io/. Accessed on November 22nd, 2023.

Nalbantis I. et Tsakiris G. (2008). Assessment of hydrological drought revisited. Water Resources Management, 23(5), 881–897.

National Drought Mitigation Center (NDMC). (2006). Understanding your risk and impacts of drought. https://drought.unl.edu/Publications.aspx.Accessed on September 18th, 2022

Ndehedehe, C. E., Agutu, N. O., Ferreira, V. G., & Getirana, A. (2020). Evolutionary drought patterns over the Sahel and their teleconnections with low frequency climate oscillations. Atmospheric Research, 233. https://doi.org/10.1016/j.atmosres.2019.104700

Ndehedehe, C. E., Awange, J. L., Corner, R. J., Kuhn, M., & Okwuashi, O. (2016). On the potentials of multiple climate variables in assessing the spatio-temporal characteristics of hydrological droughts over the Volta Basin. Science of the Total Environment, 557–558, 819–837. https://doi.org/10.1016/j.scitotenv.2016.03.004

New, M., Hewitson, B., Stephenson, D. B., Tsiga, A., Kruger, A., Manhique, A., Gomez, B., Coelho, C. A. S., Masisi, D. N., Kululanga, E., Mbambalala, E., Adesina, F., Saleh, H., Kanyanga, J., Adosi, J., Bulane, L., Fortunata, L., Mdoka, M. L., & Lajoie, R. (2006). Evidence of trends in daily climate extremes over southern and west Africa. Journal of Geophysical Research Atmospheres, 111(14). https://doi.org/10.1029/2005JD006289

Nicholson, S. (2005). On the question of the “recovery” of the rains in the West African Sahel. Journal of Arid Environments, 63(3), 615–641. https://doi.org/10.1016/j.jaridenv.2005.03.004

Nicholson, S. E. (2013). The West African Sahel: A Review of Recent Studies on the Rainfall Regime and Its Interannual Variability. ISRN Meteorology, 2013, 1–32. https://doi.org/10.1155/2013/453521

Nicholson, & Selato. (2000). The influence of la Nina on African rainfall. In *International Journal of Climatology: A Journal of the Royal Meteorological Society*, *20*(14), 1761-1776.

Nyadzi, E., Ajayi, O. C., & Ludwig, F. (2021). Indigenous knowledge and climate change adaptation in Africa: a systematic review. In CAB Reviews: Perspectives in Agriculture,

Veterinary Science, Nutrition and Natural Resources (Vol. 16, Issue 29). CABI International. https://doi.org/10.1079/PAVSNNR202116029

Obada, E. (2016). On the Use of Simple Scaling Stochastic (SSS) Framework to the Daily Hydroclimatic Time Series in the Context of Climate Change. Hydrology, 4(4), 35. https://doi.org/10.11648/j.hyd.20160404.11

Obada, E., Alamou, E. A., Biao, E. I., & Zandagba, E. B. J. (2021). Interannual variability and trends of extreme rainfall indices over benin. Climate, 9(11). https://doi.org/10.3390/cli9110160

Obarein, O. A., & Lee, C. C. (2022). Differential signal of change among multiple components of West African rainfall. Theoretical and Applied Climatology, 149(1–2), 379–399. https://doi.org/10.1007/s00704-022-04052-1

Ogunrinde, A. T., Emmanuel, I., Olasehinde, D. A., Faloye, O. T., Babalola, T., & Animashaun, I. M. (2024). Impact of climate teleconnections on hydrological drought in the Sahel Region of Nigeria (SRN). Meteorology and Atmospheric Physics, 136(3). https://doi.org/10.1007/s00703-024-01016-0

Okonkwo, C. (2014). An Advanced Review of the Relationships between Sahel Precipitation and Climate Indices: A Wavelet Approach. International Journal of Atmospheric Sciences, 2014, 1–11. https://doi.org/10.1155/2014/759067

Ouedraogo, I., Runge, J., Eisenberg, J., Barron, J., & Sawadogo Kaboré, S. (2014). The re-greening of the Sahel: Natural cyclicity or human-induced change? Land, 3(3), 1075–1090. https://doi.org/10.3390/land3031075

Oyerinde, G. T., Hountondji, F. C. C., Wisser, D., Diekkrüger, B., Lawin, A. E., Odofin, A. J., & Afouda, A. (2015). Hydro-climatic changes in the Niger basin and consistency of local perceptions. Regional Environmental Change, 15(8), 1627–1637. https://doi.org/10.1007/s10113-014-0716-7

Ozer P, Hountondji Y., Niang A., Karimoune S., Laminou Manzo O, & Salmon M. (2010). Désertification au sahel : historique et perspectives. BSGLg, 16, 69–84.

Ozor, N. (2010). Barriers to Climate Change Adaptation Among Farming Households of Southern Nigeria. In Journal of Agricultural Extension. Journal of Agricultural Extension, 14(1).

P. Frich, L. V. Alexander, P. Della-Marta, B. Gleason, M. Haylock, A. M. G. Klein Tank, & T. Peterson. (2002). Observed coherent changes in climatic extremes during the second half of the twentieth century. https://doi.org/10.3354/cr019193

Pan, S., He, Z., Gu, X., Xu, M., Chen, L., Yang, S., & Tan, H. (2024). Agricultural drought-driven mechanism of coupled climate and human activities in the karst basin of southern China. Scientific Reports, 14(1). https://doi.org/10.1038/s41598-024-62027-w

Pendergrass, A. G., Knutti, R., Lehner, F., Deser, C., & Sanderson, B. M. (2017). Precipitation variability increases in a warmer climate. Scientific Reports, 7(1). https://doi.org/10.1038/s41598-017-17966-y

Petzold, J., Andrews, N., Ford, J. D., Hedemann, C., & Postigo, J. C. (2020). Indigenous knowledge on climate change adaptation: A global evidence map of academic literature. In Environmental Research Letters (Vol. 15, Issue 11). IOP Publishing Ltd. https://doi.org/10.1088/1748-9326/abb330

Pomposi, C., Giannini, A., Kushnir, Y., & Lee, D. E. (2016). Understanding Pacific Ocean influence on interannual precipitation variability in the Sahel. Geophysical Research Letters, 43(17), 9234–9242. https://doi.org/10.1002/2016GL069980

Quenum, G. M. L. D., Klutse, N. A. B., Dieng, D., Laux, P., Arnault, J., Kodja, J. D., & Oguntunde, P. G. (2019). Identification of Potential Drought Areas in West Africa Under Climate Change and Variability. In Earth Systems and Environment (Vol. 3, Issue 3, pp. 429–444). Springer. https://doi.org/10.1007/s41748-019-00133-w

Rind, D., Goldberg, R., & Ruedy, R. (1989). Change in climate variability in the 21st century. *Climatic change*, *14*(1), 5-37.

Robette, N. (2020). Moreparty: A Toolbox for conditional inference random forests. (R package version (0.2.0) [Dataset]. Retrieved from https:// CRAN.R-project.org/package=moreparty).

Rodríguez-Fonseca, B., Janicot, S., Mohino, E., Losada, T., Bader, J., Caminade, C., Chauvin, F., Fontaine, B., García-Serrano, J., Gervois, S., Joly, M., Polo, I., Ruti, P., Roucou, P., & Voldoire, A. (2011). Interannual and decadal SST-forced responses of the West African monsoon. In Atmospheric Science Letters (Vol. 12, Issue 1, pp. 67–74). https://doi.org/10.1002/asl.308

Rowhani, P., Lobell, D. B., Linderman, M., & Ramankutty, N. (2011). Climate variability and crop production in Tanzania. Agricultural and Forest Meteorology, 151(4), 449–460. https://doi.org/10.1016/j.agrformet.2010.12.002

Salack, S., Klein, C., Giannini, A., Sarr, B., Worou, O. N., Belko, N., Bliefernicht, J., & Kunstman, H. (2016). Global warming induced hybrid rainy seasons in the Sahel. Environmental Research Letters, 11(10). https://doi.org/10.1088/1748-9326/11/10/104008

Sambieni, K. S., Hountondji, F. C. C., Sintondji, L. O., & Fohrer, N. (2023). Spatial distribution of water reservoirs in the Sota catchment (Benin, West Africa) and implications for local development. Heliyon, 9(3). https://doi.org/10.1016/j.heliyon.2023.e14458

Sambieni, K. S., Hountondji, F. C. C., Sintondji, L. O., Fohrer, N., Biaou, S., & Sossa, C. L. G. (2024). Climate and Land Use/Land Cover Changes within the Sota Catchment (Benin, West Africa). Hydrology, 11(3). https://doi.org/10.3390/hydrology11030030

Sanogo, S., Fink, A. H., Omotosho, J. A., Ba, A., Redl, R., & Ermert, V. (2015). Spatio-temporal characteristics of the recent rainfall recovery in West Africa. International Journal of Climatology, 35(15), 4589–4605. https://doi.org/10.1002/joc.4309

Schubert, S. D., Suarez, M. J., Pegion, P. J., Koster, R. D., & Bacmeister, J. T. (2004). 485 Causes of Long-Term Drought in the U.S. Great Plains. Journal of Climate, 17(3), 485-503.

Schubert, S. D., Wang, H., Koster, R. D., Suarez, M. J., & Groisman, P. Y. (2014). Northern Eurasian heat waves and droughts. Journal of Climate, 27(9), 3169–3207. https://doi.org/10.1175/JCLI-D-13-00360.1

Shikwambana, S., Malaza, N., & Shale, K. (2021). Impacts of rainfall and temperature changes on smallholder agriculture in the limpopo province, south africa. Water (Switzerland), 13(20). https://doi.org/10.3390/w13202872

Siddiqui, F., & Ali, Q. M. (2016). Performance of non-parametric classifiers on highly skewed data. In Global Journal of Pure and Applied Mathematics. *Glob. J. Pure Appl. Math*, *12*(2), 1547-1565.

Singhal, A. , Jaseem, M., Divya, Sarker, S., Prajapati, P. , Singh, A. , & Jha, S. K. (2024). Identifying Potential Locations of Hydrologic Monitoring Stations Based on Topographical and Hydrological Information. Water Resources Management, 38(1), 369–384.

Smith, S. C., & Ubilava, D. (2017). The El Niño Southern Oscillation and economic growth in the developing world. Global Environmental Change, 45, 151–164. https://doi.org/10.1016/J.GLOENVCHA.2017.05.007

Sun, J., Bi, S., Bashir, B., Ge, Z., Wu, K., Alsalman, A., Ayugi, B. O., & Alsafadi, K. (2023). Historical trends and characteristics of meteorological drought based on SPI and SPEI over the past 70 years in China (1951-2020). https://doi.org/10.20944/preprints202306.2042.v1

Tall, M., Sylla, M. B., Dajuma, A., Almazroui, M., Houteta, D. K., Klutse, N. A. B., Dosio, A., Lennard, C., Driouech, F., Diedhiou, A., & Giorgi, F. (2023). Drought variability, changes and hot spots across the African continent during the historical period (1928–2017). International Journal of Climatology, 43(16), 7795–7818. https://doi.org/10.1002/joc.8293

Tambo, J. A., & Abdoulaye, T. (2013). Smallholder farmers' perceptions of and adaptations to climate change in the Nigerian savanna. Regional Environmental Change, 13(2), 375–388. https://doi.org/10.1007/s10113-012-0351-0

Thomas, D. S. G., Twyman, C., Osbahr, H., & Hewitson, B. (2007). Adaptation to climate change and variability: Farmer responses to intra-seasonal precipitation trends in South Africa. Climatic Change, 83(3), 301–322. https://doi.org/10.1007/s10584-006-9205-4

Thompson, D. W. J., Barnes, E. A., Deser, C., Foust, W. E., & Phillips, A. S. (2015). Quantifying the role of internal climate variability in future climate trends. Journal of Climate, 28(16), 6443–6456. https://doi.org/10.1175/JCLI-D-14-00830.1

Thompson, H. E., Berrang-Ford, L., & Ford, J. D. (2010). Climate change and food security in Sub-Saharan Africa: A systematic literature review. In Sustainability (Vol. 2, Issue 8, pp. 2719–2733). MDPI. https://doi.org/10.3390/su2082719

Topp, E. N., & Thesis, P. (2020). Butterfly diversity and land manager decision-making in critically endangered South African renosterveld. PhD dissertation, Georg-August University Göttingen, 188p.

Torrence C, & Compo G P. (1998). A Practical Guide to Wavelet Analysis. American Meteorological Society. Bulletin of the American Meteorological society, 79(1), 61-78.

Tossa, J., Fangnon, B., Babadjide, C., & Ogouwale, E. (2016). Catastrophes hydroclimatiques : impacts agricoles et stratégies d'adaptation dans la commune des Aguégués au Bénin. In Rev. Ivoir. Sci. Technol (Vol. 27). http://www.revist.ci

Van Lanen, H. A. J., Wanders, N., Tallaksen, L. M., & Van Loon, A. F. (2013). Hydrological drought across the world: Impact of climate and physical catchment structure. Hydrology and Earth System Sciences, 17(5), 1715–1732. https://doi.org/10.5194/hess-17-1715-2013

Vicente-Serrano, S. M., Beguería, S., & López-Moreno, J. I. (2010). A multiscalar drought index sensitive to global warming: The standardized precipitation evapotranspiration index. Journal of Climate, 23(7), 1696–1718. https://doi.org/10.1175/2009JCLI2909.1

Vissin. (2007). Impact de la Variabilité climatique et de la dynamique des états de surface sur les écoulements du bassin béninois du fleuve Niger [Thèse de Doctorat, Universite de Bourgogne]. https://tel.archives-ouvertes.fr/tel-00456097

Vogel, R. M., Lall, U., Cai, X., Rajagopalan, B., Weiskel, P. K., Hooper, R. P., & Matalas, N. C. (2015). Hydrology: The interdisciplinary science of water. Water Resources Research, 51(6), 4409–4430. https://doi.org/10.1002/2015WR017049

Wang, F., Wang, Z., Yang, H., & Zhao, Y. (2018). Study of the temporal and spatial patterns of drought in the Yellow River basin based on SPEI. Science China Earth Sciences, 61(8), 1098–1111. https://doi.org/10.1007/s11430-017-9198-2

Waongo, M., Laux, P., & Kunstmann, H. (2015). Adaptation to climate change: The impacts of optimized planting dates on attainable maize yields under rainfed conditions in Burkina Faso. Agricultural and Forest Meteorology, 205, 23–39. https://doi.org/10.1016/j.agrformet.2015.02.006

West, C. T., Roncoli, C., & Ouattara, F. (2008). Local perceptions and regional climate trends on the Central Plateau of Burkina Faso. Land Degradation and Development, 19(3), 289–304. https://doi.org/10.1002/ldr.842

Wheeler, H. C., & Root-Bernstein, M. (2020). Informing decision-making with Indigenous and local knowledge and science. In Journal of Applied Ecology (Vol. 57, Issue 9, pp. 1634–1643). Blackwell Publishing Ltd. https://doi.org/10.1111/1365-2664.13734

Wilhite, D. A., Glantz, M. H., & And Glantz, M. H. (1985). Understanding the Drought Phenomenon: The Role of Definitions. http://digitalcommons.unl.edu/droughtfacpubhttp://digitalcommons.unl.edu/droughtfacpub/20. Accessed on June 12th, 2022.

WMO, & GWP. (2016). World Meteorological Organization (WMO) and Global Water Partnership (GWP). In Drought Indicators and Indices Integrated Drought Management Programme (IDMP), Integrated Drought Management Tools and Guidelines Series 2. Geneva, issue 1173, 24p.

Worou, K., Goosse, H., Fichefet, T., Guichard, F., & Diakhate, M. (2020). Interannual variability of rainfall in the Guinean Coast region and its links with sea surface temperature changes over the twentieth century for the different seasons. Climate Dynamics, 55(3–4), 449–470. https://doi.org/10.1007/s00382-020-05276-5

Yaro, J. A. (2013). The perception of and adaptation to climate variability/change in Ghana by small-scale and commercial farmers. Regional Environmental Change, 13(6), 1259–1272. https://doi.org/10.1007/s10113-013-0443-5

Yeh, S. W., Cai, W., Min, S. K., McPhaden, M. J., Dommenget, D., Dewitte, B., Collins, M., Ashok, K., An, S. Il, Yim, B. Y., & Kug, J. S. (2018). ENSO Atmospheric Teleconnections and Their Response to Greenhouse Gas Forcing. Reviews of Geophysics, 56(1), 185–206. https://doi.org/10.1002/2017RG000568

Zeng. (2003). Drought in the Sahel. Atmospheric Science, VOL 302, 999–1000. https://www.scirp.org/reference/referencespapers?referenceid=1564294. Accessed on October 3rd , 2022.

Zhang, W., Furtado, K., Wu, P., Zhou, T., Chadwick, R., Marzin, C., Rostron, J., & Sexton, D. (2021). Increasing precipitation variability on daily-to-multiyear time scales in a warmer world. In Sci. Adv (Vol. 7). https://www.science.org

9. Annex

Annex 1: Publications and Conferences

- Published papers

Ganni Mampo, O. M., Guedje, K. F., Merz, B., Obada, E., Guntu, R. K., Yarou, H., Alamou, A. E., & Hounkpe, J. (2025). Rainfall and streamflow variability in North Benin, West Africa, and its multiscale association with climate teleconnections. Journal of Hydrology: Regional Studies, 59, 102319. https://doi.org/10.1016/j.ejrh.2025.102319

Ganni Mampo OM, Guedje KF, Merz B, Yarou H, Macdonald E and Alamou AE (2025) Farmers' perceptions of hydroclimatic variability and climate change: survey-based insights in Northern Benin, West Africa. Front. Water 7:1530395. doi: 10.3389/frwa.2025.1530395

- Co-authored papers

Kouyaté F., Guédjé F. K, Ndiaye A., **Ganni Mampo O. M**. Spatial and Temporal Variability of Extreme Hydroclimatic Events in the Bani River Basin. *Hydrology*. 2025; 12(1):5. https://doi.org/10.3390/hydrology12010005

Bodjrènou R., Azian D., Sintondji L. O., Bossa A. Y., Amou M., Sessou F., **Ganni Mampo O. M.**, Comandan F., Sohindji S. F. (2024). Bias adjustment of hourly rainfall distributions in WFDE5 reanalysis for hydrological impact studies in Benin (West Africa). Theoretical and Applied Climatology (2024) 155:7361–7376 https://doi.org/10.1007/s00704-024-05078-3

Yarou H, Obada E, Alfari A. A.,**Ganni Mampo O. M.**, Tore D. B., Alamou E. A. Rainfall Variability and Cotton Production in Kouandé in the Atacora Department of Benin (West Africa). Applied Sciences Research Periodicals – ISSN 3033-330X. December 2024, Vol. 2, No. 10 pp. 42-52. http://dx.doi.org/10.63002/asrp.210.719

- Conferences attended
  - Oral presentation during the World PhD Students and Postdoctoral Research Summit on Climate Change, Humburg/Germany in 2024 (online)
  - Oral presentations at UNSTIM in Abomey in 2024 (In-person)
  - Oral presentations at UNSTIM in Abomey in 2023 (In-person)
  - Attending the 8th Colloquium on Science, Culture and Technology at the University of Abomey-Calavi in 2023 (In-person)

Annex 2

Domains of the selected climate teleconnections

Figure 36: Domains of the selected climate indices Nino 3.4, AMO and DMI

Station data used

Table 12: Rainfall and streamflow stations used

Station Rainfall (P)	Country	Longitude (°)	Latitude (°)	Annual Rainfall [mm]	Rainfall Apr-Oct [mm]
Alfakoara (P1)	Benin	3.07	11.45	908	901
Banikoara (P2)	Benin	2.43	11.3	974	964
Bembereke (P3)	Benin	2.67	10.2	1084	1060
Djougou (P4)	Benin	1.67	9.7	1179	1128
Fada Ngourma (P5)	Burkina Faso	0.37	12.05	800	789
Gaya (P6)	Niger	3.45	11.88	820	817
Ina (P7)	Benin	2.73	9.97	1094	1055
Kalale (P8)	Benin	3.38	10.3	1087	1065
Kandi (P9)	Benin	2.93	11.13	1039	988
Karimama (P10)	Benin	3.18	12.07	696	691
Kouande (P11)	Benin	1.68	10.33	1170	1131
Malanville (P12)	Benin	3.4	11.87	806	797
Natitingou (P13)	Benin	1.38	10.32	1194	1158
Niamey (P14)	Niger	2.1	13.52	530	528
Nikki (P15)	Benin	3.2	9.93	1052	1008
Parakou (P16)	Benin	2.6	9.35	1162	1102
Segbana (P17)	Benin	3.7	10.93	1008	996

Tanguieta (P18)	Benin	1.27	10.62	1030	1002

Streamflow (D)	Country	Longitude (°)	Latitude (°)	Mean streamflow [m^3/s]
Couberi (D1)	Benin	3.35	11.75	39.4
Yankin (D2)	Benin	2.65	11.15	33.3
Kompongou (D3)	Benin	2.20	11.40	28.7

Filling of data gaps in the streamflow time series

We used the hydrological model ModHyPMA to fill the data gaps in streamflow observations for the three catchments. ModHyPMA consists of a production function and a transfer function (Afouda A., 2004; Alamou E., 2011). The catchment response is controlled by two parameters, a non-linearity parameter and the basin drying coefficient. The model has been calibrated and validated for both wet and dry periods, demonstrating its ability to accurately distinguish between these two hydrological conditions. For all three catchments, a good model performance has been found with R^2 (coefficient of determination) and NSE (Nash Sutcliff Efficiency) values in the range of 0.56–0.73 and 0.56–0.60, respectively, for the validation periods (Table 13).

Table 13: Performance of the ModHyPMA model for calibration and validation periods.

Catchment	Period	R^2	NSE	Period	R^2	NSE
	Calibration			Validation		
B1	**1986-1989**	0.78	0.74	**2003-2007**	0.73	0.56
B2	**1984-1987**	0.64	0.63	**2005-2008**	0.66	0.60
B3	**1971-1974**	0.84	0.83	**2007-2010**	0.56	0.59

Table 14: MMK test result of SPI

Stations	Tau value			Sen's slope			P_Value			Significancy		
	SPI3	SPI6	SPI12	SPI3	SPI6	SPI12	SPI3	SPI6	SPI12	SPI3	SPI6	SPI12
Alfakoara	0.067	0.074	9.20E-02	4.90E-04	6.25E-04	8.13E-04	0.263	1.12E-01	1.02E-01	*	*	*
Banikoara	0.033	0.052	9.08E-02	1.90E-04	4.53E-04	8.29E-04	0.567	2.85E-01	2.18E-01	*	*	*
Bembereke	0.065	0.091	1.25E-01	4.47E-04	7.23E-04	1.02E-03	0.105	8.55E-02	1.21E-01	*	**	*
Djougou	0.089	0.110	1.13E-01	7.05E-04	1.00E-03	1.09E-03	0.053	8.91E-02	1.47E-01	*	**	**
Fada	0.029	0.042	5.25E-02	1.45E-04	3.45E-04	4.09E-04	0.590	3.00E-01	3.65E-01	*	*	*
Gaya	0.086	0.113	1.28E-01	6.74E-04	1.00E-03	1.16E-03	0.102	3.78E-03	2.17E-03	*	**	**
Ina	0.088	0.126	1.79E-01	6.79E-04	1.10E-03	1.52E-03	0.045	1.78E-02	3.59E-03	**	**	**
Kalale	0.007	0.0035	2.56E-02	0.00E+00	2.62E-05	2.41E-04	0.909	9.25E-01	6.31E-01	*	*	*
Kandi	0.054	0.091	1.36E-01	3.61E-04	8.05E-04	1.17E-03	0.359	4.88E-02	7.47E-02	*	**	*
Karimama	-0.049	-0.043	-5.02E-03	-2.84E-04	-3.54E-04	-3.13E-05	0.512	5.13E-01	9.57E-01	*	*	*
Kouande	0.092	0.134	1.74E-01	7.05E-04	1.13E-03	1.46E-03	0.005	4.39E-04	4.25E-06	**	**	**
Malanville	0.096	0.133	1.90E-01	6.84E-04	1.04E-03	1.26E-03	0.075	6.73E-05	2.27E-07	*	**	**
Natitingou	0.014	-0.001	-1.82E-02	1.01E-04	0.00E+00	-1.60E-04	0.692	9.81E-01	8.12E-01	*	*	*
Niamey	0.074	0.103	1.39E-01	5.08E-04	8.64E-04	1.22E-03	0.142	5.30E-03	5.95E-03	*	**	**
Nikki	-0.006	-0.022	-2.95E-02	0.00E+00	-1.84E-04	-2.47E-04	0.855	5.96E-01	4.84E-01	*	*	*
Parakou	0.062	0.065	5.34E-02	5.11E-04	5.59E-04	4.81E-04	0.040	2.83E-03	3.27E-01	**	**	*
Segbana	-0.028	0.012	5.06E-02	-1.06E-04	1.04E-04	4.17E-04	0.486	7.93E-01	4.76E-01	*	*	*
Tanguieta	-0.032	-0.034	-1.25E-02	-2.04E-04	-2.96E-04	-9.69E-05	0.481	5.86E-01	9.04E-01	*	*	*

The result of the MMK test show a significant trend at 7 over 18 stations. This significant trend is decreasing at 5 stations (Bembereke, Ina, Kalale, Nikki and Parakou stations) and increasing at the remaining 2 stations (Gaya and Niamey stations).

Table 15: The Modified Mann-Kendall test SDI for time scales of 3, 6 and 12 months for each station

SDI types	Stations	Tau Value	Sen's slope	P_Value	Significancy
SDI-3	Gbasse	0.191	0.0016	3.83E-03	**
	Couberi	0.130	0.0011	5.03E-02	*
	Yankin	0.212	0.0017	3.41E-03	**
	Kompongou	0.143	0.0011	8.89E-02	*
SDI-6	Gbasse	0.287	0.0024	3.33E-08	**
	Couberi	0.214	0.0018	9.55E-04	**
	Yankin	0.199	0.0017	8.82E-03	**
	Kompongou	0.184	0.0015	3.74E-02	**
SDI-12	Gbasse	0.380	0.0033	2.93E-16	**
	Couberi	0.306	0.0026	2.20E-05	**
	Yankin	0.174	0.0016	7.35E-02	*
	Kompongou	0.209	0.0016	1.01E-02	**
SDI-24	Gbasse	0.492	0.0044	7.69E-11	**
	Couberi	0.398	0.0034	3.03E-05	**
	Yankin	0.264	0.0025	3.60E-02	**
	Kompongou	0.277	0.0020	6.72E-03	**

* No trend, ** Significant trend

Trends analysis of Standardized Precipitation Evapotranspiration Index

The result of the MMK test shows a significant trend at 7 over 18 stations. This significant trend is decreasing at 5 stations (Bembereke, Ina, Kalale, Nikki and Parakou stations) and increasing at the remaining 2 stations (Gaya and Niamey stations).

Table 16: Result of the Modified Mann-Kendall (MMK) test of SPEI for time scales of 3, 6 and 12 months for each station

Stations	Tau value			Sen's slope			P_Value			Significance		
	SPEI3	SPEI6	SPIE12	SPEI3	SPEI6	SPIE12	SPEI3	SPEI6	SPIE12	SPEI3	SPEI6	SPIE12
Alfakoara	3.42E-02	7.44E-02	1.47E-01	4.34E-04	9.19E-04	1.82E-03	5.57E-01	2.92E-01	6.96E-02	*	*	*
Banikoara	-4.38E-02	-1.01E-02	-3.19E-03	-5.56E-04	-1.34E-04	-4.25E-05	3.89E-01	8.47E-01	9.63E-01	*	*	*
Bembereke	-5.05E-01	-5.21E-01	-5.07E-01	-5.71E-03	-5.66E-03	-5.13E-03	1.48E-14	9.16E-18	1.33E-07	**	**	**
Djougou	4.38E-02	5.20E-02	7.11E-02	5.53E-04	6.81E-04	9.81E-04	5.71E-01	5.10E-01	3.42E-01	*	**	**
Fada	5.91E-02	7.50E-02	2.11E-01	5.90E-04	7.42E-04	1.99E-03	1.41E-01	9.16E-02	1.29E-01	*	*	*
Gaya	2.13E-01	2.62E-01	3.39E-01	2.62E-03	3.36E-03	4.27E-03	8.43E-06	4.50E-06	1.66E-05	**	**	**
Ina	-3.91E-01	-3.79E-01	-3.77E-01	-4.36E-03	-3.88E-03	-3.13E-03	1.04E-05	1.72E-05	6.89E-04	**	**	**
Kalale	-4.54E-01	-4.60E-01	-4.17E-01	-5.34E-03	-5.16E-03	-4.67E-03	1.66E-08	2.17E-06	2.33E-04	**	**	**
Kandi	7.29E-02	1.49E-01	2.18E-01	9.24E-04	1.87E-03	2.87E-03	1.49E-01	1.07E-02	4.97E-03	*	**	**
Karimama	4.82E-03	5.31E-02	9.52E-02	5.78E-05	6.78E-04	1.19E-03	9.35E-01	3.66E-01	2.27E-01	*	*	*
Kouande	2.78E-03	1.70E-02	2.27E-02	2.95E-05	2.20E-04	2.83E-04	9.67E-01	8.30E-01	7.76E-01	**	**	**
Malanville	-2.62E-02	5.27E-03	4.39E-03	-3.19E-04	5.28E-05	5.21E-05	5.72E-01	9.00E-01	9.46E-01	*	**	**
Natitingou	-7.57E-02	-9.62E-02	-1.25E-01	-9.84E-04	-1.25E-03	-1.60E-03	3.50E-01	2.64E-01	1.72E-01	*	*	*
Niamey	1.41E-01	1.72E-01	2.92E-01	1.56E-03	1.64E-03	2.28E-03	1.07E-02	1.67E-04	7.40E-06	**	**	**
Nikki	-4.48E-01	-4.80E-01	-4.56E-01	-5.19E-03	-5.36E-03	-5.08E-03	2.98E-07	2.49E-10	3.57E-09	**	**	**
Parakou	-4.33E-01	-4.28E-01	-4.33E-01	-5.03E-03	-4.73E-03	-4.48E-03	2.99E-09	3.88E-06	4.20E-04	**	**	**
Segbana	2.93E-02	8.46E-02	1.69E-01	3.84E-04	1.07E-03	2.09E-03	6.12E-01	2.86E-01	3.31E-02	*	*	**
Tanguieta	-8.19E-02	-1.06E-01	-1.58E-01	-9.73E-04	-1.27E-03	-2.05E-03	1.79E-01	1.22E-01	5.40E-02	*	*	*

* No trend, ** Significant trend

Trends analysis of CDD

Table 17: Result of the Modified Mann-Kendall test of CDD per station

Stations	Mean_CDD	Tau	Decennial changes/variation	Sen's slope	P_Value	Significancy
Alfakoara	164.02	0.132	1.32	0.3333	0.252	*
Banikoara	161.51	0.125	1.25	0.4000	0.199	*
Bembereke	134.24	-0.111	-1.11	-0.1106	0.255	*
Djougou	119.71	0.090	0.9	0.3529	0.528	*
Fada	153.22	0.015	0.15	0.0526	0.900	*
Gaya	169.24	-0.106	-1.06	-0.3571	0.276	*
Ina	125.27	-0.074	-0.74	-0.2083	0.450	*
Kalale	145.71	0.117	1.17	0.3158	0.232	*
Kandi	155.55	0.045	0.45	0.1429	0.649	*
Karimama	173.06	0.086	0.86	0.3846	0.656	*
Kouande	122.55	0.027	0.27	0.0698	0.789	*
Malanville	171.69	-0.140	-1.4	-0.4444	0.150	*
Natitingou	116.49	0.028	0.28	0.08	0.776	*
Niamey	196.00	-0.113	-1.13	-0.3182	0.249	*
Nikki	132.59	-0.106	-1.06	-0.3810	0.280	*
Parakou	103.25	0.008	0.08	0.04	0.942	*
Segbana	145.63	0.176	1.76	0.6957	0.071	*
Tanguieta	135.55	0.292	2.92	0.8889	0.0002	**

* No trend, ** Significant trend

The result of the MMK test on the CDD shows a significant trend at only Tanguieta station. This significant trend is increasing, as shown on Table 14.

Table 18: Result of the Modified Mann-Kendall test of CDD in rainy season per station

Stations	Mean_CDDin	Tau	Decennial changes/variation	Sen's slope	P_Value	Significancy
Alfakoara	12.94	0.147	1.467	0.050	0.129	*
Banikoara	11.53	-0.071	-0.714	0.000	0.461	*
Bembereke	10.78	-0.044	-0.439	0.000	0.652	*
Djougou	8.53	0.024	0.243	0.000	0.805	*
Fada	12.04	0.153	1.529	0.050	0.113	*
Gaya	12.57	-0.011	-0.109	0.000	0.915	*
Ina	10.08	-0.007	-0.071	0.000	0.948	*
Kalale	10.92	0.201	2.008	0.057	0.019	**
Kandi	10.49	-0.055	-0.549	0.000	0.570	*
Karimama	17.37	0.166	1.663	0.143	0.222	*
Kouande	8.76	0.087	0.871	0.000	0.368	*
Malanville	14.59	-0.135	-1.349	-0.067	0.043	*
Natitingou	8.14	-0.010	-0.102	0.000	0.921	*
Niamey	20.57	-0.005	-0.047	0.000	0.968	*
Nikki	11.06	0.112	1.122	0.029	0.322	*
Parakou	9.92	0.038	0.376	0.000	0.481	*
Segbana	10.10	0.033	0.329	0.000	0.737	*
Tanguieta	9.90	0.120	1.200	0.030	0.213	*

Wavelet analysis for catchment rainfall, streamflow and climate indices

Figure 36 shows the wavelet analysis for rainfall, discharge and climate indices of annual time series. The left panels show the Wavelet Power Spectrum with the color scale indicating the magnitude of the wavelet power. Warmer colors represent higher magnitudes of power. The V-shaped black line outlines the cone of influence, which indicates the region beyond which the results are less reliable due to boundary-edge effects. The thick black contour highlights regions where the wavelet power is statistically significant. This contour delineates areas where the wavelet transform is robust and exceeds at 95% significance threshold, indicating real periodicities or signals in the data. The right panels show the Global Wavelet Spectrum corresponding to each time series. The peaks in these spectra highlight the dominant periodicities in the data. The red dashed line represents the significance threshold at the 95% confidence level. Periods where the global wavelet spectrum curve (blue) exceeds the dashed line (red) are considered statistically significant at this confidence level.

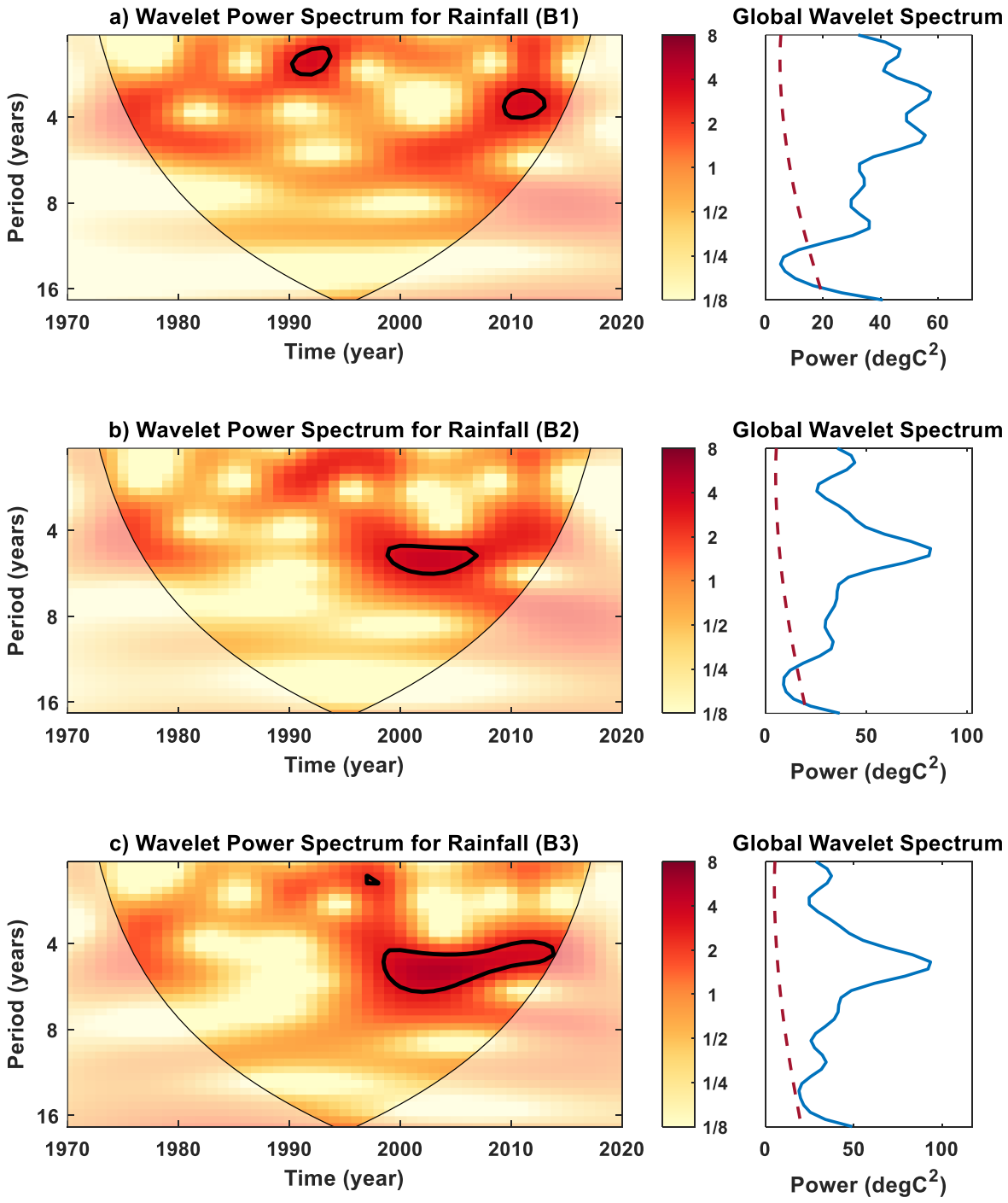
a) Wavelet Power Spectrum for Rainfall (B1)
Global Wavelet Spectrum
Period (years)
4
8
16
1970
1980
1990
2000
2010
2020
Time (year)
8
4
2
1
1/2
1/4
1/8
0
20
40
60
Power (degC^2)
b) Wavelet Power Spectrum for Rainfall (B2)
Global Wavelet Spectrum
Period (years)
4
8
16
1970
1980
1990
2000
2010
2020
Time (year)
8
4
2
1
1/2
1/4
1/8
0
50
100
Power (degC^2)
c) Wavelet Power Spectrum for Rainfall (B3)
Global Wavelet Spectrum
Period (years)
4
8
16
1970
1980
1990
2000
2010
2020
Time (year)
8
4
2
1
1/2
1/4
1/8
0
50
100
Power (degC^2)

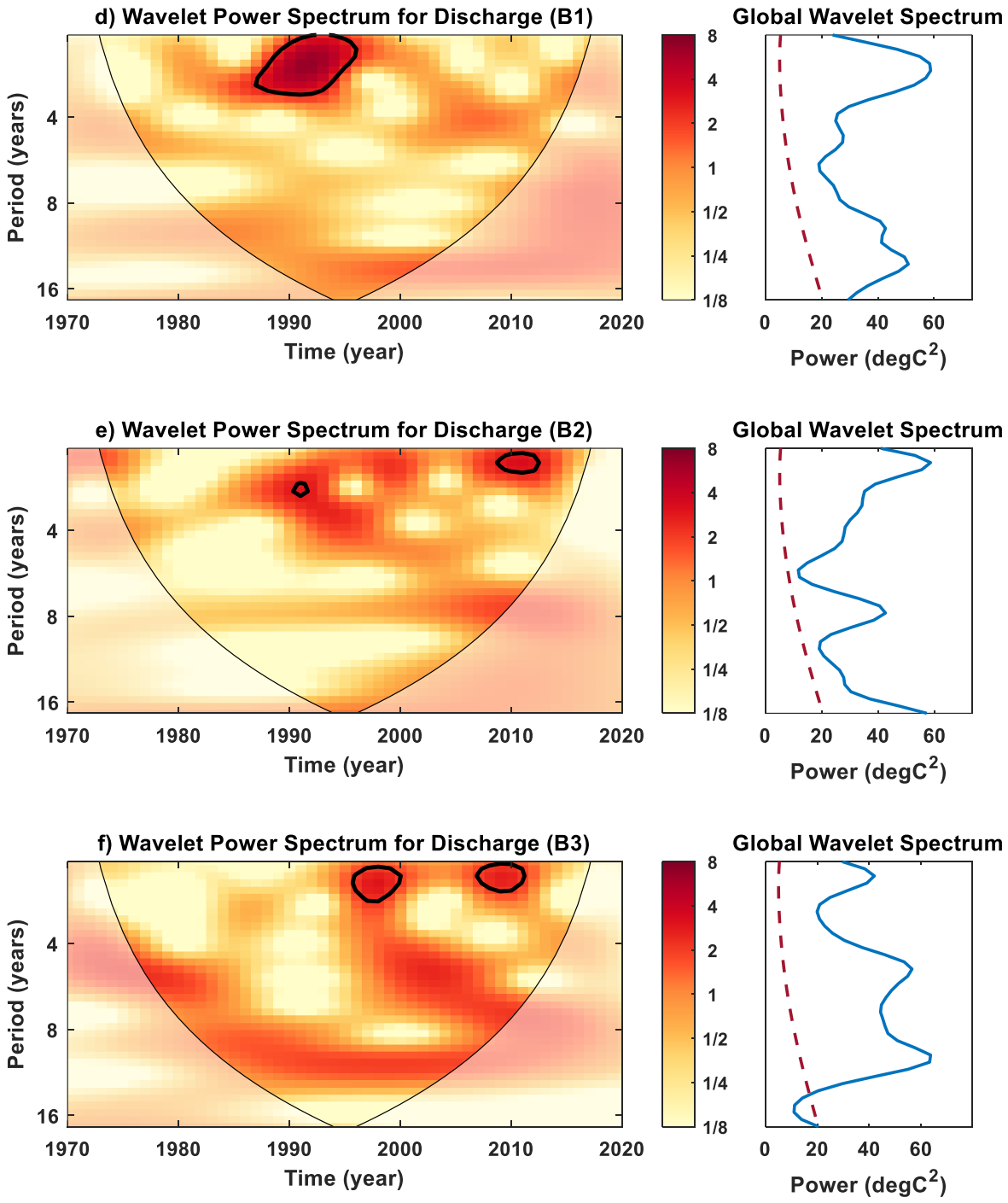
d) Wavelet Power Spectrum for Discharge (B1)
Global Wavelet Spectrum
Period (years)
4
8
16
1970
1980
1990
2000
2010
2020
Time (year)
8
4
2
1
1/2
1/4
1/8
0
20
40
60
Power (degC^2)
e) Wavelet Power Spectrum for Discharge (B2)
Global Wavelet Spectrum
Period (years)
4
8
16
1970
1980
1990
2000
2010
2020
Time (year)
8
4
2
1
1/2
1/4
1/8
0
20
40
60
Power (degC^2)
f) Wavelet Power Spectrum for Discharge (B3)
Global Wavelet Spectrum
Period (years)
4
8
16
1970
1980
1990
2000
2010
2020
Time (year)
8
4
2
1
1/2
1/4
1/8
0
20
40
60
Power (degC^2)

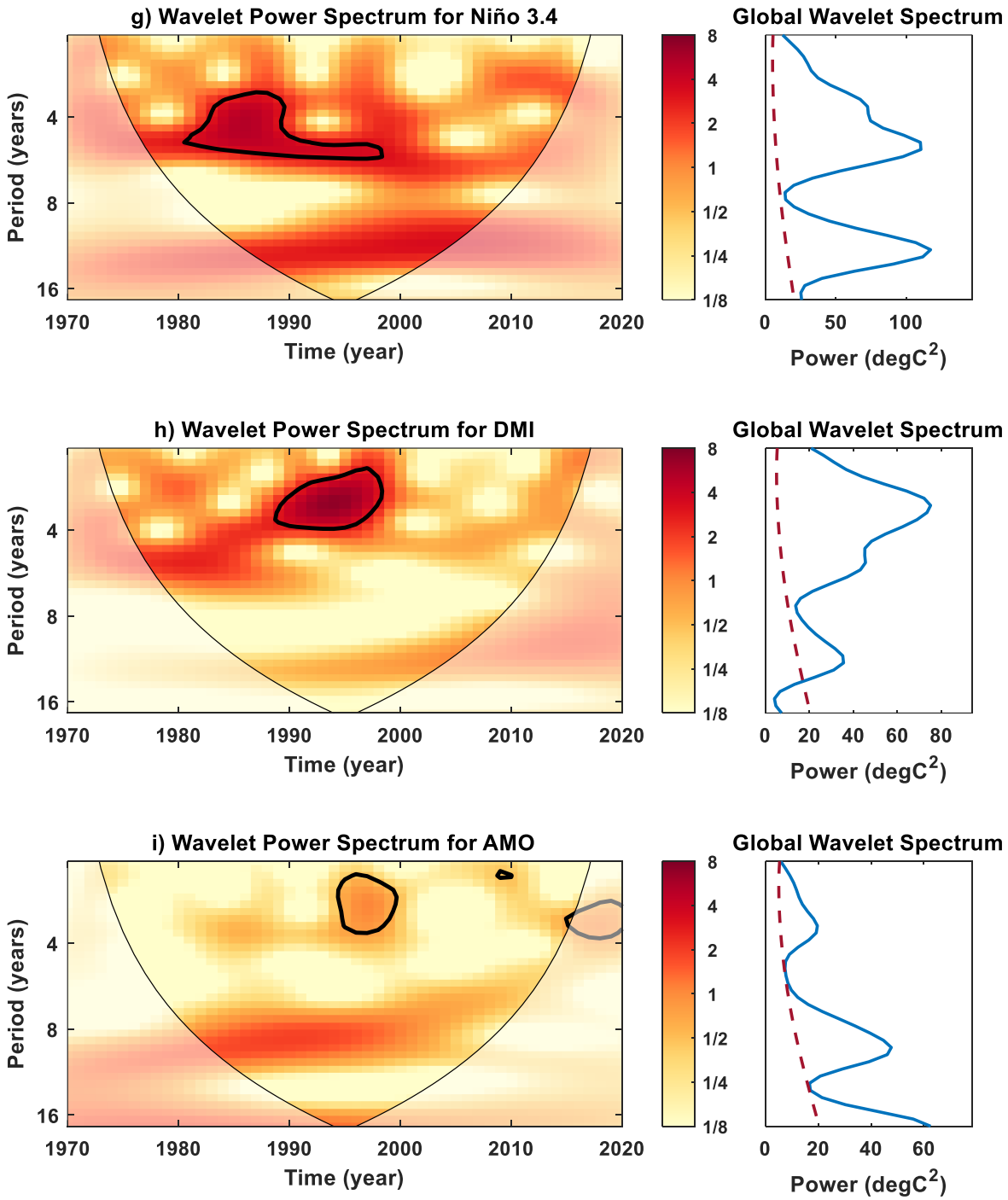

Figure 37: Wavelet Power Spectrum (left) and Global Wavelet Spectrum (right) of (a-c) catchment rainfall for catchments B1, B2, and B3, (d-f) streamflow for catchments B1, B2, and B3, and (g-i) climate indices Niño 3.4, AMO, and DMI for 1970–to 2020.

SURVEY QUESTIONNAIRE

This questionnaire is part of the thesis project entitled: **"Hydro-meteorological droughts understanding and predictability across the Beninese Part of the Niger River Basin (West Africa)".**

File number: .....

First name and surname of interviewer: .....

Date of survey: ____/____/ /____/____/ /____/____/

Time: start: ..... End : .....

Name of the municipality: .....

Name of district: ..... Neighbourhood/village: .....

House: .....

I. IDENTIFICATION OF THE RESPONDENT

N°	Questions	Responses	Code
Q101	I.1. Full name		
Q102	I.2.Sex	M F	0 1
Q103	I.3. Age		
Q104	I.4. What is your level of education?	None..... Koranic school..... Primary ..... Secondary/equivalent..... Higher education/equivalent.....	0 1 2 3 4
Q105	I.5. How long have you been farming?		
Q106	I.6. Do you have any other economic activity apart from farming?		

II. FARMERS' PERCEPTIONS OF CLIMATE CHANGE

Q201	II.1. How many rainy seasons do you have in your area?	A single season Two seasons Other (please specify)	1 2 96
Q202	II.2. In which month do the rains start in your locality?	April May June	1 2 3
Q203	II.3. In which month do the rains stop in your area?	September October November	9 10 11
Q204	II.4. How many months does the rainy season last?	3 months 4 months 5 months 6 months other	1 2 5 6 96
Q205	II.5. Have the start dates of the rainy seasons changed?	Yes No	1 0

Q206	II.6. During the rainy season, are there days when it doesn't rain?	Yes No	1 0
Q207	II.7. If so, what is the average number of days without rain?	3 days 4 days …… …… 10 days >10 days	1 2 … …. 5
Q208	II.8. How many months does the drought last?	5 months 6 months 7 months 8 months Other	1 2 3 4 96
Q209	II.9 In which month does the drought begin in your locality?	September October November	1 2 3
Q210	II.10. In exactly which month does the drought end in your area?	April May June	1 2 3
Q211	II.11. How is the drought affecting your locality?	Drainage of rivers and streams Drying up of wells/boreholes Other (please specify)	1 2 3
Q212	II.12. Do you think it is warmer than it used to be?	Yes…… No…… Other (please specify)……	1 0 96
Q213	II.13. If yes, what is the cause of the increase in heat?		
Q214	II.14. If so, how often?	A year out 10 years 2 years out 10 years 3 years out of 10 years 4 years out of 10 years 5 years out of 10 years Other	1 2 3 4 5 96
Q215	II.15. Which major rivers are close to your locality?	Quote them ……	
Q216	II.16. Has the average level of these rivers fallen or risen compared with 30 years ago?	declined…….. Increased…… Other (please specify) ……	1 2 3
Q217	II.17. What are the reasons for these changes?	Precipitation... ..... Human activities	1 2
Q218	II.18. If changes in river levels are due to human activities, please specify these activities.	…… …… ……	
Q219	II.19. Do rivers dry up during the dry season?	Yes…… No…… Other (please specify) ……	1 0 96
Q220	II.20. If the answer to the previous question is yes, give	Every year..... Every two years..... Every five years	1 2 4

	the frequency with which the watercourses dry up.	other (please specify)	96
Q221	II.21. 30 years ago, did rivers dry up with the same frequency?	Yes…… No…… other (please specify)	1 0 96
Q222	II.22. Do you know of any rivers that existed 30 years ago but have completely disappeared today?	Yes…… No…… other (please specify)	1 0 96
Q223	II.23. If so, what caused this disappearance?	The decline in precipitation..... Human activities .... Other (please specify)	1 2 96
Q224	II.24. If the disappearance of rivers is due to human activities, name these activities		
Q225	II.25. What are the key indicators of drought in your locality?	Animals Vegetables/plants Autre	
Q226	II.26. What difficulties do you currently face in using these indicators?	a) Disappearance b) Rarity c) Behavioural changes d) Other (please specify) ……	Oui Non 1 0 1 0 1 0

III. THE IMPACTS OF CLIMATE CHANGE ON AGRICULTURE AND FARMERS' ENDOGENOUS ADAPTATION STRATEGIES

Q301	III.1. What economic activities are carried out during the rainy season in your locality?	a) Agriculture b) Trade c) Fishing d) Hunting e) Other (please specify) _____	Oui Non 1 0 1 0 1 0 1 0
Q302	III.2What economic activities are carried out in your locality during the dry season?	a) Agriculture b) Trade c) Fishing d) Hunting e) Other (please specify) _____	Oui Non 1 0 1 0 1 0 1 0
Q303	III.3. What is the state of your agricultural production yields?	Very low..... low..... high..... other (please specify)	1 2 3 96
Q304	III.4. What are the causes of the state of these yields?	Soil degradation..... Insufficient rainfall..... Irregular rainfall..... Other (please specify)	1 2 3 96

Q305	III.5. What new farming practices are you using to improve production?	…… ……	
Q306	III.6. How did you learn about these practices?	Ancient practices..... Continuation of a training course..... Training organisation..... Other (please specify)	1 2 3 96
Q307	III.7. Do these practices enable you to improve yields?	Yes No	1 0
Q308	III.8. How and when is the endogenous knowledge transmitted in your household?		
Q309	III.9. Are there any religious rites to pray for the success of economic activities in your locality?	Oui Non	1 0
Q310	III.10. If yes, please list them	---------- ---------- ---------- ------	
Q311	III.11. When and how often will it be organised?	a) Annually b) Other (please specify)	1 96

Q312 — III.12. What adaptation strategies have been developed to deal with the risks of drought?

Before	During	After

Q313 — III.13. What measures have you taken to deal with seasonal changes in your work in the fields?

Measures taken	Yes	No
Changes to the cropping calendar	1	0
Increase in area sown	1	0
Use of fertilisers	1	0
Rotations des cultures	1	0
Combining crops	1	0
Mutual aid	1	0
Adoption of new varieties	1	0
Off-season cultivation	1	0
Other (please specify)		

Mr. Orou Moctar Ganni Mampo was born on January 1, 1995, in Brignamaro (Kerou) in the Atacora region of Benin. He obtained his baccalaureate in the Science (Series D) with distinction. In 2016, he earned a bachelor's degree in Quantitative Hydrology from the National Institute of Water at the University of Abomey-Calavi. Following his undergraduate studies, he pursued a master's degree in Hydrology at the same university, where he successfully defended his thesis, titled "Contribution of GIS and Remote Sensing in Flood Management in the Oueme Delta," with great honors. Mr. Ganni Mampo is the recipient of a prestigious WASCAL scholarship, enabling him to pursue a PhD in Climate Change and Water. He has demonstrated his academic prowess during his doctoral studies by publishing two articles, one submission and co-authoring three papers in international peer-reviewed journals.

Abstract**:** Understanding hydroclimatic variability and climate teleconnections in a warming world is crucial for drought-prone regions like West Africa, where economies heavily depend on rain-fed agriculture. This study investigates the spatiotemporal dynamics of hydrological and meteorological droughts and their links to climate teleconnections in the Beninese Part of the Niger River Basin (BPNRB). Using the Standardized Precipitation Index (SPI), the Standardized Precipitation Evapotranspiration Index (SPEI), the Consecutive Dry Days Index (CDD), and the Streamflow Drought Index (SDI), the study assessed drought variability on 3- and 12-month timescales. Statistical and wavelet coherence analyses were employed to explore the connections between drought patterns and global climate drivers. Using a questionnaire administered to 509 households across 96 villages in eight municipalities, we collected and analyzed qualitative and quantitative data through statistical and machine-learning methods. The findings reveal a recovery phase in the 1990s following severe droughts in the 1970s and 1980s. Significant trends include increased CDD values during the rainy season, with an average of 18 dry spell days, and a pronounced upward trend in SDI, indicating intensifying hydrological droughts. The application of wavelet transform coherence reveals that rainfall and streamflow variability are modulated by the climate teleconnections El Niño-Southern Oscillation (ENSO), Atlantic Multidecadal Oscillation (AMO), and Dipole Mode Index (DMI). In relation to rainfall, we find a tendency for a shift from lower-frequency coherence (around 4–10 years) in earlier decades to higher-frequency coherence (1–3 years) in recent decades. These patterns are less pronounced for streamflow which is more indirectly influenced by climate teleconnections. The survey results reveal that while most farmers possess a good knowledge of local hydroclimatic variability, gaps remain in their understanding of the underlying causes. Only 9% attributed recent increases in temperature to global climate change. Key factors influencing knowledge levels include age and farming experience, with older and more experienced farmers demonstrating better understanding, whereas formal education showed a weak effect. These insights support policymakers in designing more effective climate adaptation policies, and drought monitoring in Northern Benin and inform policies on agriculture and water management.

Key words: Niger River Basin; West Africa; rainfall; streamflow; teleconnection; drought.

PhD

OROU MOCTAR GANNI MAMPO

Hydro-meteorological drought understanding and predictability across the Beninese Part of Niger River Basin, West Africa

GRP/CCWR/WASCAL – UAC NOVEMBER, 2025